Mechanistic Insights into Unusual Reactions by High -Valent Iron Intermediates

A Thesis Submitted in Partial Fulfillment of the
Requirements for the degree of

DOCTOR OF PHILOSOPHY

Submitted By

V. Anil Kumar

(Roll No. 08612223)

Department of Chemistry

Indian Institute of Technology Guwahati, India

Guwahati-781039

Assam, India

5th November , 2013

Dedicated to

Maa Kamakhya

&

My Family

Contents

Statement

I hereby declare that the matter embodied in this thesis is result of investigations carried out by me in the Department of Chemistry, Indian Institute of Technology Guwahati, India under the guidance of Dr. Chivukula V. Sastri. In keeping with the general practice of reporting scientific observations, due acknowledgements have been made wherever the work described is based on the findings of other investigators.

V. ANIL KUMAR

Certificate

This is to certify that V. ANIL KUMAR has been working under my supervision since January 2009 as a regular registered Ph. D. student. I am forwarding his thesis entitled **"Mechanistic Insights into Unusual Reactions by High Valent Iron Intermediates"** for being submitted for the Ph. D. (Science) degree of this institute. I certify that he has fulfilled all the requirements according to the rules of this institute regarding the investigations embodied in his thesis and this work has not been submitted elsewhere for a degree.

5th November, 2013.

Dr. Chivukula V. Sastri

Supervisor

Department of Chemistry

Indian Insitute of Technology Guwahati

Ackowledgements

First and foremost, I feel it as a great privilege in expressing my deepest and most sincere gratitude to my supervisor Dr. Chivukula V. Sastri, for his excellent guidance throughout my study. My heart full thanks to you sir for the unlimited support and patience shown to me. He has also created an indispensable environment for me to conduct my project work. I would particularly like to thank him for all his help in patiently and carefully correcting all my manuscripts. I could not have imagined having a better advisor and mentor for my Ph.D study.

I am also very thankful to my doctoral committee chairman and members Prof. Gopal Das, Prof. P. K. Iyer and Dr. M. Qureshi for sparing their precious time to evaluate the progress of my work. I would also like to thank the Head of the Department, Dr. Boomi Shankar and the other faculty members for their kind help in carrying out this work. I am also grateful to all the members of the research and technical staff of the department without whose help I could not have completed this thesis.

I would like to thank IIT Guwahati for financial support and all the facilities that were made available to me. I thank CIF, IIT Guwahati for providing the facility of LC-MS, Mr. K. Singh for their help.

I must thank my lab mate Prasenjit Barman (special thanks), for the support and pleasant environment in the laboratory also my sincere thanks to my seniors, friends and other research scholars in the department, especially Mr. Laxminarayana, Bheem Raju, Aswini Kakita, Dr. Ziyauddin Khan, Dr. Mohan lal, Dr. Himanshu Sekhar Jena, Dr. Babulal Das, Arvind Kumar Gupta and other departments friends Ch. Nagesh (ECE), Santhosh (Physics).

My special thanks to chemistry teachers Dr. Ramachary, Dr. J.P sir, Dr. Ramesh , my close friends Rathnakar, Manda Srinivas, Niranjan, Komal, Uppal Suresh and my uncle-aunt Janardhan-Vani.

Most importantly, last, but not the least, to my parents Lakshmi-Prakash, my wife Srujana, my brothers Shiva Kumar, Arun Kumar, sister Madhavi, brother-in-law S. Anil Kumar and our chotus Vikranth Somnath, Suhas Kartikeya for their endless moral support and motivation especially at difficult times. My Ph.D endeavors would not have been completed without their blessings. I express my sincere gratitude to them. I would like to thank all others who are associated with my work directly or indirectly at IIT Guwahati for their help.

V. ANIL KUMAR

Abstract

High-valent non-heme iron(III)-hydroperoxo and iron(IV)-oxo units are proposed as key oxidizing intermediates in many biological iron dependent oxygenases. The oxidant, iron(IV)-oxo species were proposed as active oxidant in several catalytic cycles. In recent years, emphasis on the evaluation of the kinetic and mechanistic insights into the reactivity of iron(IV)-oxo, iron(III)-hydroperoxo and other high-valent isolabal intermediates have increased.

In the present work, the reactivity studies towards halide oxidation, S-oxidation, C-H activation with high-valent iron(III)-hydroperoxo, iron(IV)-oxo and iron(IV)-imido species supported by penta-dentate ligands have been evaluated. These reactivity studies provide remarkable insights into the mechanistic pathway of these intermediates.

Iron(III)-hydroproxo and iron(IV)-oxo complexes were compared in halide oxidation and observed that iron(III)-hydroproxo were efficient oxidizing species. In comparison of Iron(IV)-oxo and iron(IV)-imido complexes towards S-oxidation and C-H activation, a conflicting results were observed. For S-oxidation reactions, iron(IV)-imido complexes were a better oxidants as compared to iron(IV)-oxo. On the contrary, for C-H activation a complete reversal of the reactivity was observed where in iron(IV)-oxo species were more reaction than iron(IV)-imido complexes. Finally, the reactivity of iron(IV)-oxo complexes were evaluated for the oxidation of one of the most difficult pollutant (dibenzothiophene) and its thermodynamic parameters were evaluated.

List of Tables

List of Figures and Schemes

Abbreviations

α-KG	α-ketoglutarate
BLM	Bleomycin
Bn-Tpen	N-benzyl-N,N',N'-tris(2-pyridylmethyl)-1,2-diaminoethane
CAN	Cerium (IV) ammonium nitrate
CHD	1,4-cyclohexadiene
DAP	2,3-diaminophenazine
DBT	Dibenzothiophene
DHA	9,10-dihydroanthracene
DMSO	Dimethyl sulphoxide
$EDTA^{4-}$	Ethylenediaminetetraacetate
ESI-MS	Electrospray ionization mass spectrometry
EXAFS	Extended x-ray absorption fine structure
KIE	Kinetic isotope effect
LMCT	Ligand to metal charge transfer
m-CPBA	meta chloro per benzoicacid
MeCN	Acetonitrile
MeOH	Methanol
NADH	Nicotinamide adenine dinucleotide Hydride
N4Py	N-bis(2-pyridylmethyl)-N-bis(2-pyridyl)methylamine
NMR	Nuclear magnetic resonance

OPD	*o*-Phenylenediamine
OTf	Triflate
PCET	Proton coupled electron transfer
PhIO	Iodosylbenzene
PhINTs	[N-(p-tolylsulfonyl)-imino)]phenyliodinane
PPh_3	Triphenylphosphine
TAML	tetraamidomacrocyclic ligand
TauD	taurine/α-KG dioxygenase
TBABr	Tetrabutylammonium bromide
TBACl	Tetrabutylammonium chloride
TBAF	Tetrabutylammonium fluoride
TBAI	Tetrabutylammonium iodide
TMC	Tetramethylcyclam
TMG_3tren	1,1,1-tris{2-[N^2-(1,1,3,3-tetramethylguanidino)]ethyl}amine
TPA	tris(2-pyridylmethyl)amine

Compounds Abbreviations by Chapter

Chapter 3

1a	$[Fe^{III}(OOH)(N4Py)]^{2+}$
1b	$[Fe^{IV}(O)(N4Py)]^{2+}$
2a	$[Fe^{III}(OOH)(Bn\text{-}Tpen)]^{2+}$
2b	$[Fe^{IV}(O)(\ Bn\text{-}Tpen)]^{2+}$

Chapter 4

1a	$[Fe^{III}(OOH)(N4Py)]^{2+}$
1b	$[Fe^{IV}(O)(N4Py)]^{2+}$
2a	$[Fe^{III}(OOH)(Bn\text{-}Tpen)]^{2+}$
2b	$[Fe^{IV}(O)(Bn\text{-}Tpen)]^{2+}$

Chapter 5

1c	$[Fe^{IV}(NTs)(N4Py)]^{2+}$
1b	$[Fe^{IV}(O)(N4Py)]^{2+}$

Chapter 6

1b	$[Fe^{IV}(O)(N4Py)]^{2+}$
2b	$[Fe^{IV}(O)(Bn\text{-}Tpen)]^{2+}$

Synopsis

The thesis entitled **"Mechanistic Insights into Unusual Reactions by High-Valent Iron Intermediates"** deals with exploring novel reactivities of high-valent iron intermediates towards various substrates that incorporate well characterized pentadentate ligands viz. N4Py and Bn-Tpen (N4Py = N,N-bis(2-pyridylmethyl)-N-bis(2-pyridyl)methylamine) (Bn-Tpen = N-benzyl-N,N',N'-tris(2-pyridylmethyl)ethane-1,2-diamine).

Enzymes plays key role in most of the biological functions. Nature has taken advantage of the special properties of the metal ions and tuned them by encapsulation with different protein matrices to perform a large variety of specific functions associated with life processes. More than 30% of all proteins and over 40% of all enzymes contain one or more metals to perform various functions. Metals play roles in approximately one-third of the known enzymes. Metals may be a co-factor or they may be incorporated into the molecule, and these are known as metalloenzymes.

Biologically relevant metals like Mn, Fe, Co, Ni, Cu and Zn are the obvious working examples for biomimetic chemistry. Iron is one of the most essential elements for life, found in the active site of many proteins and enzymes and plays key roles in many biological processes. The iron containing proteins are broadly classified into two categories: heme and non-heme. The metalloproteins bearing a porpyrin submit are classified as heme systems and the rest of the metalloproteins having non-porphyrin subunits are classified as non-heme proteins.

Oxygen-containing mononuclear iron species iron(III)–peroxo, iron(III)–hydroperoxo and iron(IV)–oxo are key intermediates in the catalytic activation of dioxygen by iron-containing metalloenzymes. Many non-heme iron enzymes act

by catalyzing the activation of dioxygen (O_2) in many metabolically important functions. Oxygen-coordinating metal intermediates, such as metal super-oxo, peroxo, hydroperoxo, and oxo species, play central roles in many biological and catalytic processes. In all the iron catalyzed biochemical reactions the suspected intermediates are iron(III)-peroxo, iron(III)-hydroperoxo, iron(IV)-oxo and iron(IV)-imido Figure 1.

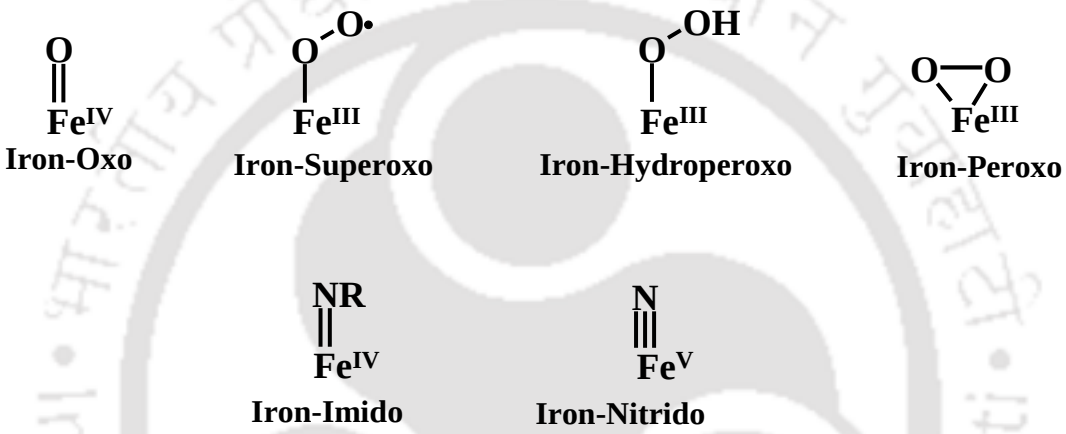

Figure 1. Plausible high-valent intermediates of iron with Oxygen and Nitrogen.

The work embodied in this thesis has been divided into six Chapters. A brief, Chapter-wise account of the results is presented below.

Chapter-1. Introduction

In this Chapter, recent literature related to iron(IV)-oxo, iron(III)-hydroperoxo, iron(III)-peroxo and iron(IV)-imido complexes and their reactivity studies have been reviewed as function of their spectroscopic and structural information, kinetics, reactivity trends and mechanisms insights. Recent developments taken place by high-valent non-heme iron complexes are also discussed.

Chapter-2. Material and Methods

A general description of the synthesis of various precursor compounds and high-valent non-heme iron complexes as well as the spectroscopic, ESI-MS and GC techniques employed during the research work is presented in this Chapter.

Chapter-3. Non-Heme Ferric Hydroperoxo Intermediates are Efficient Oxidants of Bromide Oxidation

The non-heme iron chemistry of biomimetic systems and enzymes led to the characterization of a number of high-valent iron(IV)-oxo intermediates in electrophilic and nucleophilic oxygenation reactions. However, the reactivity patterns of the corresponding non-heme iron(III)-hydroperoxo intermediates are not well understood. The non-heme complexes bearing pentadentate ligands and their corresponding iron(IV)-oxo complexes have been shown to give efficient electrophilic reactivity patterns with substrates including hydrogen atom abstraction mechanisms. Earlier studies on the reactivity of iron(III)-hydroperoxo intermediates were found to be inactive towards the oxidation reactions of thioanisole and cyclohexene when compared with their corresponding iron(IV)-oxo complexes. This chapter aims to present a better insights into the reactivity patterns of non-heme iron(III)-hydroperoxo intermediates in electrophilic reaction mechanisms. The results of the investigation in bromide oxidation by $[Fe^{III}(OOH)(N4Py)]^{2+}$ (**1a**) and $[Fe^{III}(OOH)(Bn\text{-}Tpen)]^{2+}$ (**2a**) are presented in this chapter. The oxidation rates of the iron(III)-hydroperoxo intermediates were compared with their respective iron(IV)-oxo complexes viz: $[Fe^{IV}(O)(N4Py)]^{2+}$ (**1b**) and $[Fe^{IV}(O)(Bn\text{-}Tpen)]^{2+}$ (**2b**).

Bromide oxidation reactions were studied upon addition of excess amount of tetrabutylammonium bromide (TBABr) to iron(III)-hydroperoxo and oxo(IV)-oxo complexes. The reactions were monitored by the changes in the absorption peak of these intermediates. Addition of TBABr to solution of **1a** at 253 K, resulted in a rapid decay (within 300s) of the characteristic 548 nm peak in the UV-vis spectra. The second order rate constants for this reaction was evaluated for **1a**, **2a**, **1b** and **2b** towards bromide oxidation and found that iron(III)-hydroperoxo complexes are more efficient than corresponding iron(IV)-oxo complexes. The reactivity of **1a** and **2a** towards bromide oxidation was further confirmed by catalytic bromination of phenol-red to phenol-blue.

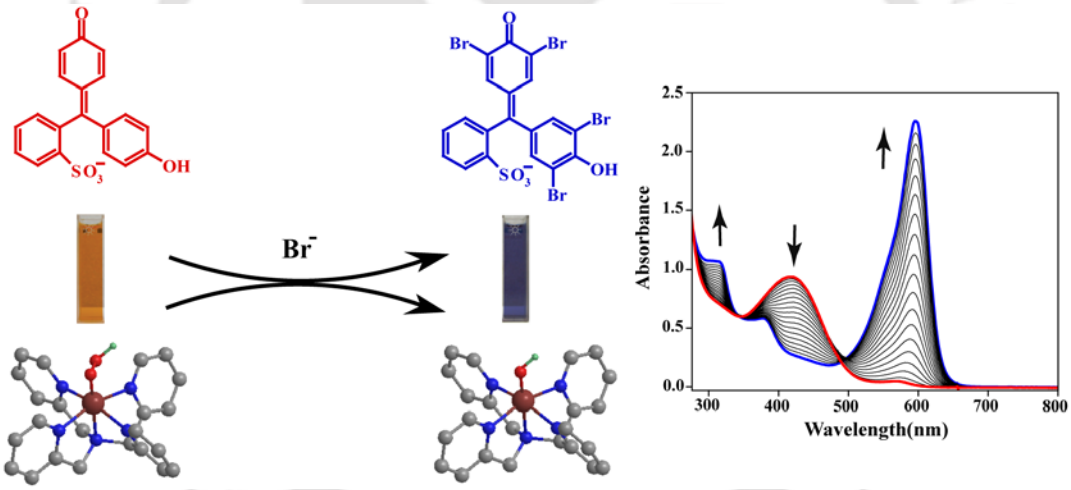

In conclusion, this results discussed in this chapter presents one of the early examples of electrophilic character of iron(III)-hydroperoxo complexes. The reactivity of iron(III)-hydroperoxo was superior to iron(IV)-oxo complexes for bromide oxidation. The DFT work carried out in collaboration has attributed the enchanced reactivity of iron(III)-hydroperoxo intermediates to its BDE_{O-H} values which are proportional to H-abstraction rate constants. The larger BDE_{O-H} values correspond to faster reactions rates. This chapter provides and experimental evidence to the fact that iron(III)-hydroperoxo species **1a** was more reactive towards bromide oxidation than **2a**, where as in iron(IV)-oxo intermediates **2b**>**1b**.

Chapter-4. Mechanistic Insight into Halide Oxidation by Non-Heme Iron Complexes. Haloperoxidase versus Halogenase Activity

Halogens are an abundant component of the Earth`s bio-sphere, so it is of little surprise that nature produces a copious number of organo halogens. Nature has developed an exquisite array of methods to introduce halogen atoms into organic compounds. In nature, halogenation is strategy used to increase the biological activity of secondary metabolites, compounds that are often effective as drugs. However halides are not particularly reactive unless they are activated, typically by oxidation.

Halogenating enzymes are divided into H_2O_2 required haloperoxidases (heme systems) and oxygen dependent halogenases (non-heme systems). Iron catalyzed biological halogenation occurs with heme haloperoxidases and the recently discovered and characterized •-ketoglutarate dependent non-heme halogenases. Haloperoxidases are a class of enzymes that catalyse the oxidation of halide ions with subsequent halogenation of organic substrates, equn. 1. These

processes, which play a major role in global organohalogen production, are thought to be important components of the chemical defense of organisms that produce them. In addition, these halogenated natural products are of pharmacologiacal interst due to their antifungal, antibacterial, antineoplastiic, antiviral and anti-inflammatory activities.

$$RH + X^{-} + H^{+} + H_2O_2 \xrightarrow{\textbf{Haloperoxidase}} RX + 2H_2O \qquad \text{----- (equn. 1)}$$

(RH = substrate, X = Cl^{-}, Br^{-} and I^{-} but not F^{-})

For the catalysis of halogenation reactions, haloperoxidases require hydrogen peroxide (H_2O_2) and halide ions (Cl^{-}, Br^{-} and I^{-} but not F^{-})

The results from Chapter 3 has motivated to evaluate the mechanistic pathway for halide oxidation reaction by Fe(III)-hydroperoxo intermediates and compare them with iron(IV)-oxo complexes. This chapter discusses the results of the halide oxidation reactions (X^{-} = F^{-}, Cl^{-}, Br^{-} and I^{-}) by $[Fe^{III}(OOH)(N4Py)]^{2+}$ (**1a**) and $[Fe^{III}(OOH)(Bn\text{-}Tpen)]^{2+}$ (**2a**) and compare the kinetics with the corresponding iron(IV)-oxo complexes, viz: $[Fe^{IV}(O)(N4Py)]^{2+}$ (**1b**) and $[Fe^{IV}(O)(Bn\text{-}Tpen)]^{2+}$ (**2b**).

Addition of tetrabutylammonium halides (TBA-X; X = Cl^{-}, Br^{-}, I^{-}) to **1a** under the conditions as discussed in Chapter 3, led to decay of the characteristic 548 nm peak in the UV-vis spectra. The second order rate constants extracted from these experiments showed a difference of as large as a factor of 8, and the reactivity decreased in the order of I^{-} > Br^{-} > Cl^{-}. Surprisingly, the observed trend does not correlate with the electron affinities of these halides. Moreover, when TBA-F was added to **1a** no oxidation reaction of F^{-} was observed. Similar trends were observed for the halide oxidation reaction with **1b** albeit the difference was in the order of ~10^7 interestingly, the second order rate constants

determined and conformed that a reversal of the trend was observed in the presence of I^- when compare **1a**, **1b** and also **2a**, **2b**.

The details of the mechanistic pathway were postulated based on the slopes obtained from the plot of second order rate constants {log(k_2)}against the one electron oxidation potential (E^0_{ox}) of these halides. A linear correlation was observed with a slope of –0.88 and –6.62 for **1a** and **1b** respectively. Further confirmation of the difference the reaction pathway of iron(III)-hydroperoxo and iron(IV)-oxo complexes were obtained during catalytic halogenation of anisole. The difference in the product distribution confirms different reaction pathways

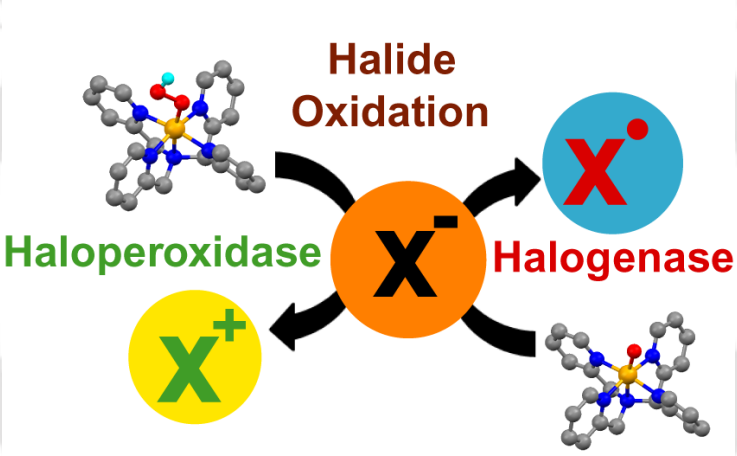

This chapter presents a comparative study of the reactivity of non-heme iron(III)-hydroperoxo versus iron(IV)-oxo in halide oxidation reactions. Here identify dramatic differences in the electron transfer processes for the two reactions, whereby iron(IV)-oxo reacts via a one-electron transfer and iron(III)-hydroperoxo by group transfer.

Chapter-5. Comparison of the Reactivity of Non-Heme Iron(IV)-Oxo versus Iron(IV)-Imido Complexes

The results obtained and discussed in Chapters 3 & 4 reveal novel reactions that could be explored to understand the reaction mechanism of high-valent iron intermediates. By contrast to iron(IV)-oxo complexes, which have been extensively studied over the years, only few studies have been reported on its closely related iron(V)-nitrido species (Fe^{V}• N) or the iron(IV)-imido (Fe^{IV}=NR) species. In principle, these high-valent metal-nitrido/imido complexes should have strong oxidative power and capable to catalyze isolobal amination reactions. During the past decade, the chemistry of metal-catalyzed aziridination of alkenes and aminidation of aliphatic C–H bonds using iminoiodane reagents has been studied by several groups. In recent years, the putative metal-nitrogen multiple bonded species have been isolated and spectroscopically characterized, which led to significant progress on the understanding of its fundamental chemical properties. However, details on its potential as nitrogen atom transfer agent are lacking and little knowledge exists in its relative reactivity with respect to the well-known iron(IV)-oxo species.

In non-heme iron chemistry, the aromatic amination of ligands by an iron-nitrido complex was reported by several groups, and recently, the spectroscopic characterization of the iron(IV)-tosylimido (tosylimido^{2-} = NTs) complex with pentadentate N4Py ligand (N4Py = *N*,*N*-bis(2-pyridylmethyl)-*N*-bis(2-pyridyl) methylamine), $[Fe^{IV}(NTs)(N4Py)]^{2+}$, was described. As this species was shown to have a relatively long lifetime, it makes it highly suitable for reactivity studies, especially since the iron(IV)-oxo analogue can be studied in tandem. In this chapter reactivity study of $[Fe^{IV}(NTs)(N4Py)]^{2+}$ (**1c**) and $[Fe^{IV}(O)(N4Py)]^{2+}$ (**1b**) towards S-oxidation and C-H activation reactions were evaluated.

In pursuit of mechanistic pathway for Fe^{IV}=NR species in the presence of organic substrates, a comparative reactivity study of $[Fe^{IV}(NTs)(N4Py)]^{2+}$ (**1c**) and $[Fe^{IV}(O)(N4Py)]^{2+}$ (**1b**) were carried out. For the two electron oxidation reactions (thioanisole oxidation), 1c was found to be a better oxidant with a second order rate constant higher by a magnitude of five times. A detailed investigation into the mechanistic pathway using substituted thioanisoles showed for sulphoxidation reactions with **1c** proceed via step wise electron transfer process which is contrary to a group transfer oxidation pathway by **1b**.

In oxidation of activation hydrocarbons via hydrogen atom abstraction (HAT) reaction, **1b** was found to be a better oxidant over **1c** by approximately 6 times. Detailed KIE studies along with hydrocarbons having variable BDE_{C-H} were also evaluated to conclude the mechanistic pathway for HAT reactions.

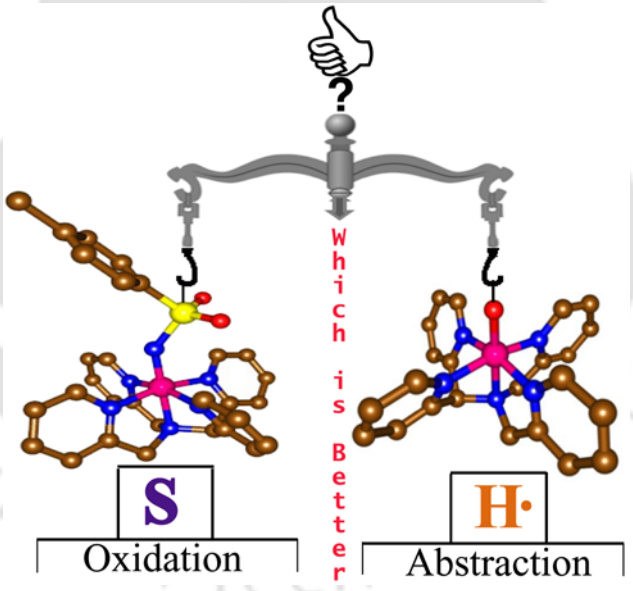

In summary, this chapter present here the first comparative study on the reactivity patterns of nonheme iron(IV)-oxo versus iron(IV)-imido. This chapter explained that due to the larger electron affinity of the oxidant the iron(IV)-imido

is a better oxidant of sulfoxidation reactions than iron(IV)-oxo. By contrast, these trends are reversed for stepwise one-electron transfer reactions, such as, hydrogen atom abstraction reactions where stereochemical interactions upon substrate approach determine the relative rate constants.

Chapter-6. Oxidation of Dibenzothiophene by Mononuclear Non-Heme Iron Complexes

Sulphur is a natural constituent of hydrocarbon fuels, such as coal and crude oil. The presence of sulphur in these fuels causes poisoning of catalysts, corrosion of surfaces, and air pollution. Consequently, sulphur-containing compounds must be removed from coal in order to attain high energy values and satisfactory environmental standards. The conventional process of sulphur removal in fuels is known as hydrodesulphurization (HDS). Oxidative desulphurization (ODS) provides a deep desulphurization process alternative to traditional HDS, because it can be conducted in liquid phase under mild conditions. In oxidation, the divalent sulphur of dibenzothiophenes (DBTs), which are the most unreactive sulphur compounds during HDS, can be oxidized by the electrophilic addition reaction of oxygen atoms to the hexavalent of sulfones. The oxy-desulfurization process involves S-oxidation mainly by hydrogen peroxide and either using a homogeneous catalyst, such as acetic acid, formic acid or using different heterogeneous catalysts. This chemical process involves the removal of organic sulphur from coal via oxidation of dibenzothiphene to its S-oxide and then to its S-dioxide (sulfone) (Scheme 1).

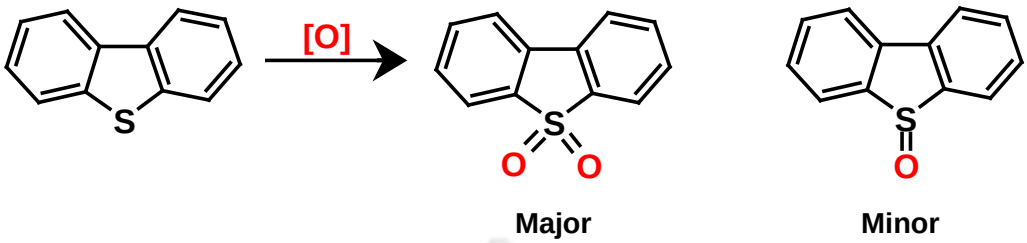

Scheme 1. Oxidation reaction of dibenzothiophene

Dibenzothiophene is a widely accepted model compound for organic sulphur in coal. This substance possesses low reactivity since the electron density is delocalized by benzene rings; hence, it is difficult to transform by chemical methods. Metallo-peroxidases are also known to participate in the oxidative metabolism of organosulfur compounds. The oxygenation of benzyl methyl sulfide, thioanisole, and thiobenzamide to the respective sulfoxides has been found to be catalyzed by chloroperoxidase, lactoperoxidase, and horseradish peroxidase. It has been demonstrated that nonheme iron(IV)-oxo complexes are capable of oxygenating various organic substrates such as PPh_3, sulphides, olefins, and alkanes.

This chapter deals with exploring the reactivity of such intermediates to oxidize DBT to the corresponding S-oxide and/or sulfone. The rationale behind this transformation is as follows: oxidation of dibenzothiophene should improve its solubility in water, thereby facilitating the subsequent aqueous extraction from coal; and oxidized species of dibenzothiophene are more amenable to the subsequent biological or chemical degradation than the parent compound. This chapter presents the biomimetic approach for the oxidation of dibenzothiophene by mononuclear non-heme iron(IV)-oxo complexes $[Fe^{IV}(O)(N4Py)]^{2+}$ (**1b**) and $[Fe^{IV}(O)(Bn\text{-}Tpen)]^{2+}$ (**2b**) bearing pentadentate ligands. The detailed kinetic and

thermodynamic parameters for DBT oxidation have been evaluated and compared with those of simple sulphur oxidation (thioanisole).

The oxidation reactions of DBT and thioanisole were followed by monitoring the change in absorption spectrum of the intermediates using UV-vis. spectroscopy. The second order rate constants were determined by varying the concentration of DBT, thioanisole and evaluated second order rate constants and thermodynamic parameters.

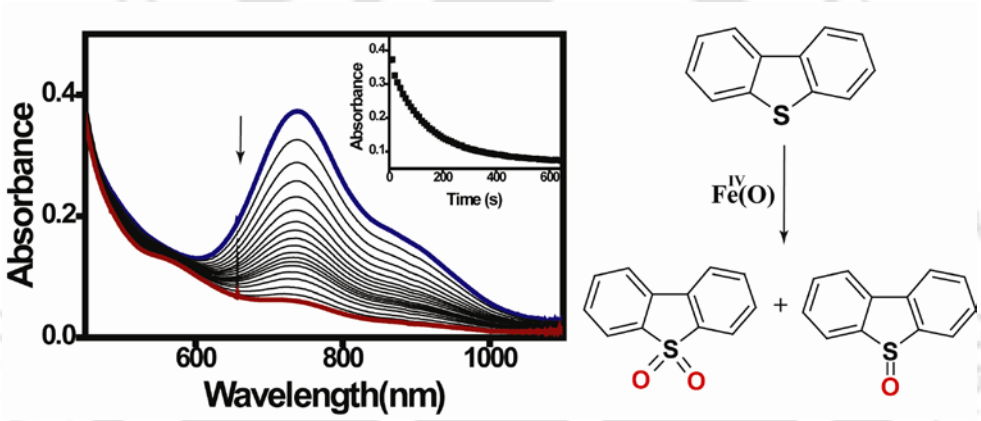

The S-oxidation reaction rates of DBT have been compared with that of thioanaisole to highlight the challenges present for the oxidation of deactivated sulphur. The results also highlight the use of environmentally benign oxidant like H_2O_2 with appropriate non-heme catalysts as a feasible technique for deep desulfurization of commercial fuels. It should be stressed that DBT and some similar sulphur compounds present in fuel can be effectively removed, after oxidation, using ethanol. Efforts are currently underway to design more effective catalysts for DBT oxidation by tuning the ligand architechture.

List of publications

1. **Anil Kumar, V.**, Prasenjit, B.; Sastri, C. V.; Devesh, K.; Sam P, D. V. Mechanisitic Insights to Halide Oxidation by Non-Heme Iron Complexes. Haloperoxidase versus Halogenase. *Chem. Commun.*, 2013, **49**, 10926-10928.
2. **Anil Kumar, V**.; Prasenjit, B.; Sastri, C. V.; Devesh, K.; Sam P, D. V. Comparison of the Reactivity of Nonheme Iron(IV)-Oxo versus Iron(IV)-Imido Complexes: Which is the Better Oxidant? *Angew. Chem. Int. Ed.* 2013, **52**, 12288-12292.
3. **Anil Kumar, V**.; Sastri, C. V.; Devesh, K.; Sam P, D. V. Nonheme ferric hydroperoxo intermediates are efficient oxidants of bromide oxidation. *Chem. Commun.*, 2011, **47**, 11044-11046.
4. **Anil Kumar, V**.; Subhajit, S.; Sastri, C. V. Oxidation of Dibenzothiophene by Mononuclear Non-Heme Iron Complexes: A Biomimetic Approach for Oxidative Desulphurization. *Indian J. Chem., Sect A.*, 2011, **50A**, 427-431.

CHAPTER-I

Introduction

1.1 Introduction

Metallo-enzymes plays key role in most of the biological functions. Nature has taken advantage of the special properties of the metal ions and tuned them by encapsulation with different protein matrices to perform a large variety of specific functions associated with life processes. More than 30% of all proteins and over 40% of all enzymes contain one or more metals to perform various functions. Metals play roles in approximately one-third of the known enzymes. Metals may be a co-factor or they may be incorporated into the molecule, and these are known as metalloenzymes.

Biologically relevant metals like Mn, Fe, Co, Ni, Cu and Zn are the obvious working examples for biomimetic chemistry. Iron is one of the most essential elements for life, found in the active site of many proteins and enzymes and plays key roles in many biological processes. The iron containing proteins are broadly classified into two categories: heme and non-heme proteins. A hemoprotein, or heme protein, is a metalloprotein containing a heme (porphyrin) prosthetic group while others are classified as non-heme proteins (non-porphyrin prosthetic group).

A large, functionally and mechanistically diverse family of enzymes utilize similar, mononuclear non-heme metal centers to couple the activation of oxygen to the oxidation of substrates.[1-5] In most cases, oxygen is inserted into inactivated C-H bond of the substrate (hydroxylation), but many other outcomes, including halogenations, desulphurization, cyclization, epoxidation, and decarboxylation are known. Enzymes, such as Cytochrome P450 family have evolved into what are in effect nature's fenton reagents, with additional levels of sophistication leading to impressive regio and chemo selectivity. But enzymatic oxidation catalysis is different from fenton chemistry. The key difference between fenton chemistry and enzymatic oxidation catalysis is: In enzymatic

oxidation catalysis, it is shown the utilization of the terrestrial pool of dioxygen while in Fenton chemistry deals with the reduced form of the enzyme.[6, 7]

Oxygen-containing mononuclear iron species iron(III)–peroxo, iron(III)–hydroperoxo and iron(IV)–oxo are key intermediates in the catalytic activation of dioxygen by iron-containing metalloenzymes.[8-14] Many non-heme iron enzymes act by catalyzing the activation of dioxygen (O_2) in many metabolically important functions.[15-19] Oxygen-coordinating metal intermediates, such as metal super-oxo, peroxo, hydroperoxo, and oxo species, play central roles in many biological and catalytic processes.[20] In all the iron catalyzed biochemical reactions the suspected intermediates are iron(III)-peroxo, iron(III)-hydroperoxo and iron(IV)-oxo, (Figure 1.1).[21,22]

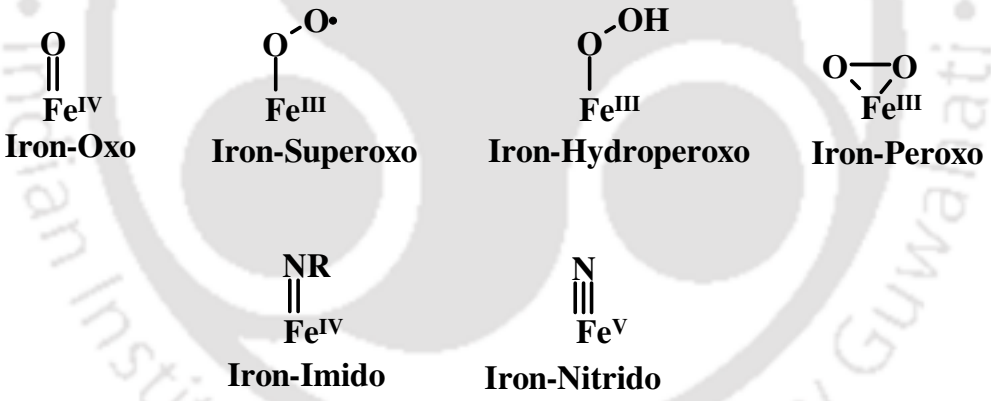

Figure 1.1. Plausible high-valent intermediates of iron with Oxygen and Nitrogen.

Understanding of the catalytic reactions of the enzymes, especially the nature of active oxidizing species, has improved recently with intensive mechanistic studies of the enzymes and their model compounds. One example is the catalytic cycle of dioxygen activation and oxygen atom transfer by α-KG-dependent oxygenases (TauD), Figure 1.2.[23,24] High-valent non-heme iron–oxo intermediates have been proposed for decades as the key intermediates in numerous biological oxidation reactions.

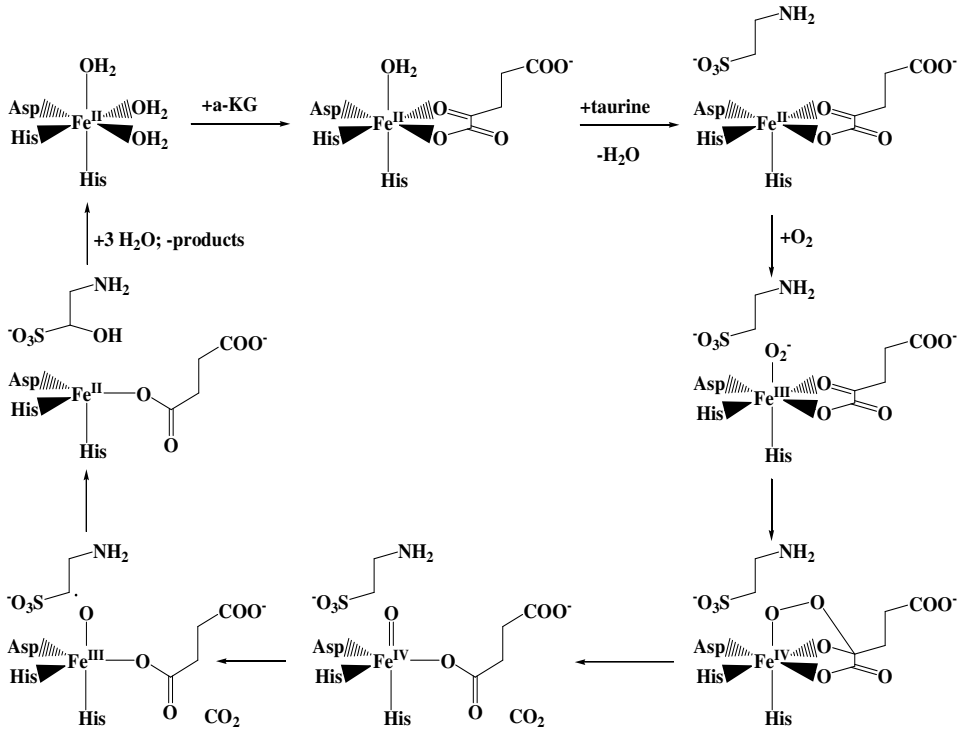

Figure 1.2. Proposed mechanism of TauD

It was only recently that the first direct characterization of such intermediates has been provided by studies of several α-ketoglutarate-dependent (α-KG) oxygenases (TauD) that catalyze either hydroxylation or halogenation of their substrates.[25]

1.2.1 Synthetic non-heme iron(IV)-oxo systems (Mimics)

Non-heme high-valent iron(IV)-oxo compond was first reported and characterized by Prof. Karl Weighardt in the year of 2000.[26] This species supported by the cyclam-acetate ligand. This iron(IV)-oxo complex was generated using the $[Fe^{III}(\text{cyclam-acetate})(CF_3SO_3)]^+$ complex on ozonolysis in a water/acetone solvent mixture to give rise to a green complex (λ_{max} = 676 nm) at -40°C or -80°C that was persisted for less than one hour. This green species was identified as an iron(IV) center by its Mössbauer spectrum, giving values of δ = 0.01 mm/s and ΔE_Q = 1.37 mm/s, parameters consistent with those found for heme iron(IV)-oxo species. The low yields (< 25%), of this initially iron(IV)-oxo species hampered further characterization.

Subsequently, the research groups of Prof(s). Nam and Que reported the first high yield route to a non-heme iron(IV)-oxo unit using the macrocyclic ligand TMC (TMC = 1,4,8,11-tetramethyl-1,4,8,11-tetraazacyclotetradecane). $[Fe^{IV}(O)(TMC)(CH_3CN)]^{2+}$ was generated at -40 °C in CH_3CN by treatment of the iron(II) precursor with either PhIO or H_2O_2, which resulted in a green solution with absorption in the near-IR region at 820 nm (ε = 400 M^{-1} cm^{-1}). The green species was identified as an iron(IV) center based on its Mössbauer parameters of δ = 0.17mm/s and ΔE_Q = 1.24 mm/s. These values were consistent with an S = 1 iron(IV) species, and the spin state assignment was confirmed by high-field measurements.[27] The X-ray quality crystals of $[Fe^{IV}(O)(TMC)(CH_3CN)]^{2+}$, provided the first example of a crystallographically

characterized mononuclear iron(IV)-oxo unit.[27] The most important feature of this structure was the short Fe-O bond length of 1.646(3) Å, a bond length that shows an appropriate shortening from the 1.813(3) Å distance from an earlier reported iron(III)-oxo species.[28] The high stability of $[Fe^{IV}(O)(TMC)(CH_3CN)]^{2+}$ fated low reactivity of this intermediate. Soon later, the same group has reported another family of iron(IV)-oxo intermediates bearing tripodal ligands, $[Fe^{IV}(O)TPA]^{2+}$ (TPA = Tris(2-pyridylmethyl)amine).[29] This intermediate was formed in nearly quantitative yield from the stoichiometric reaction of its iron(II) precursor with a peracid and is a more reactive species. Its greater oxygen-atom transfer capabilities toward substrates like thioanisole and cyclooctene emphasize the important role that ligand structure can play in modulating the reactivity of the iron(IV)-oxo unit.

Over the past decade, subsequent to the first reports of $[Fe^{IV}(O)(TMC)(CH_3CN)]^{2+}$ and $[Fe^{IV}(O)(TPA)(CH_3CN)]^{2+}$, there has been a surge in the formation and spectral / structural characterization of several non-heme mononuclear iron(IV)-oxo complexes bearing varying ligand architectures, Figure 1.3.[30-36] Among those reports, numerous were typically generated in organic solvent and all are in low spin state S=1. Some of the exceptional being a high spin S=2 non-heme iron(IV)-oxo complex $[Fe^{IV}(O)(H_2O)_5]^{2+}$, which was generated in water and water mixtures, first reported by Bakac and co-workers. The high spin state would be expected with iron ligated by five weak field water ligands.[33, 37-38] Recently Prof. Que and Prof. Münck were reported another high spin S = 2 iron(IV)-oxo complex $[Fe^{IV}(O)(TMG_3tren)](CF_3SO_3)_2$, with a half-life ($t_{1/2}$ = 4.3 h) at –30°C.[39] The first report of iron(V)-oxo species was by Collins and co-workers with a tetraamido macrocyclic ligand architechture. It was generated insitu upon the treatment of $[Fe^{III}(TAML)]^-$ with *m*-CPBA.[40]

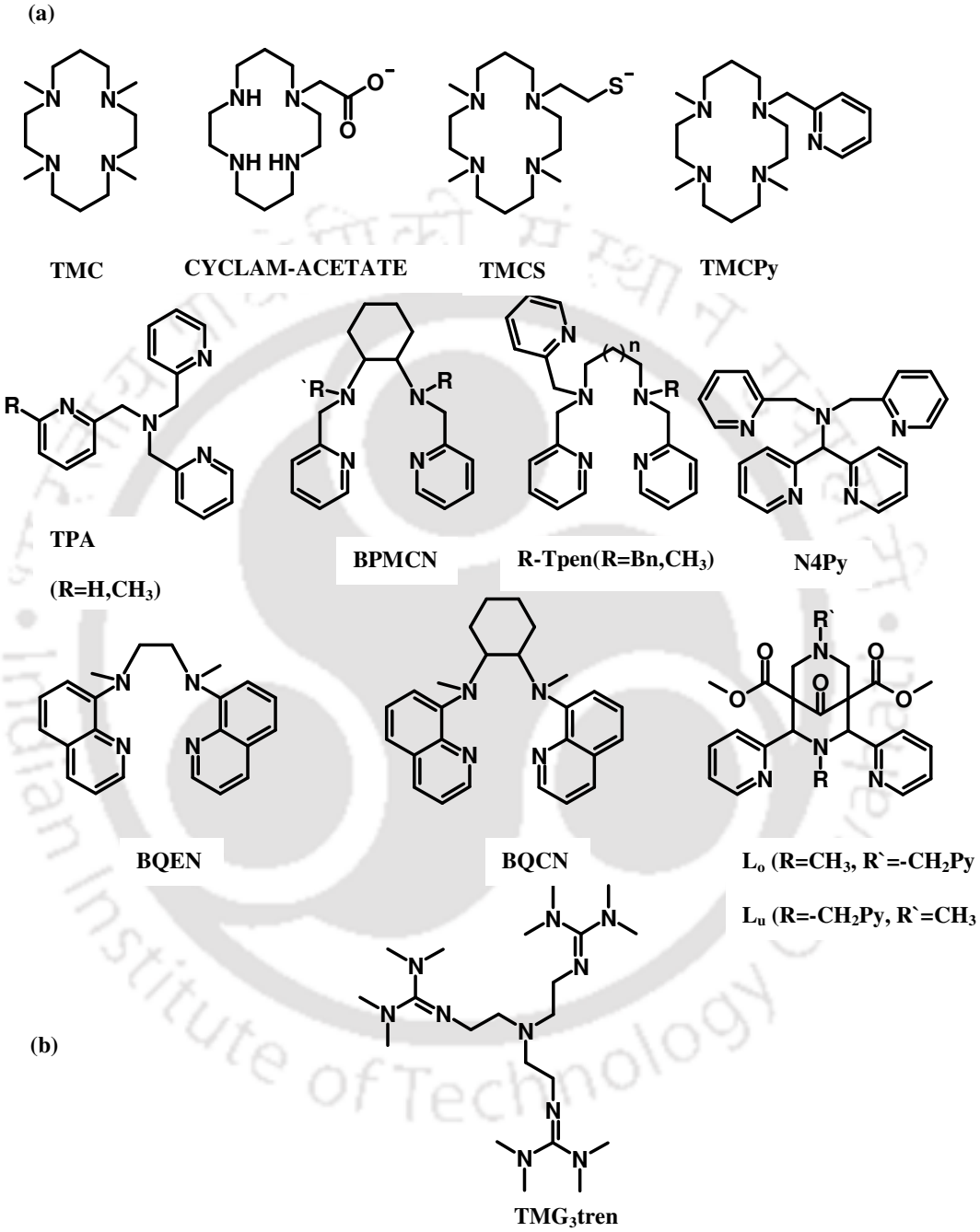

Figure 1.3. Ligands capable of supporting (a) low-spin (*S* = 1) (b) high-spin (*S* = 2) iron(IV)-oxo center.

1.2.2 Oxidants used in the generation of high-valent iron intermediates

In literature reports so far, non-heme iron(IV)-oxo complexes were generated using various "O" transfer oxidants like PhIO, H_2O_2 or peracids (peracetic acid, m-chloroperbenzoic acid etc). The first report of iron(IV)-oxo was generated by ozonolysis of iron cyclam-acetate.[26] Alternatively, high-valent iron(IV)-oxo intermediates have been produced by two-electron oxidation of the metal complexes with water as an oxygen source. A strong one-electron oxidant [e.g., cerium(IV) ammonium nitrate] is usually employed for the generation of iron(IV)-oxo intermediates.[41] Alternatively, a combination of a photosensitizer in the presence of a weak one electron oxidant can also be employed to generate oxoiron(IV) intermediates using water as a source of oxidant. Que and co-workers reported an indirect route for the generation iron(IV)-oxo intermediates wherein, $Fe^{(III)}$-OOR complex was converted into iron(IV)-oxo complex in the presence of pyridine-N-oxides by hemolytic O-O cleavage.[42] An electrochemical generation of iron(IV)-oxo species in the presence of water has also been reported by Que and Co-workers.[43] More recently, it has been shown that treating iron(III)-peroxo complexes with Sc^{+3} leads to the formation of iron(IV)-oxo intermediates.[44] Dioxygen activation of iron(II) complexes in the presence of proton is also known to generate iron(IV)-oxo intermediates. [45, 46]

1.2.3 Reactions of non-heme iron(IV)-oxo

Synthetic non-heme iron(IV)-oxo complexes are known to react with a wide range of organic substrates. Some of the most studies oxidation reactions involving iron(IV)-oxo species have been suphoxidation, phosphorous oxidation, alkene epoxidation, alcohol oxidation, aliphatic and aromatic hydroxylation, hydride transfer, hydrogen atom abstraction, electron transfer, halide oxidation, N-dealkylation, ligand exchange and water exchange reactions, (Figure 1.4).

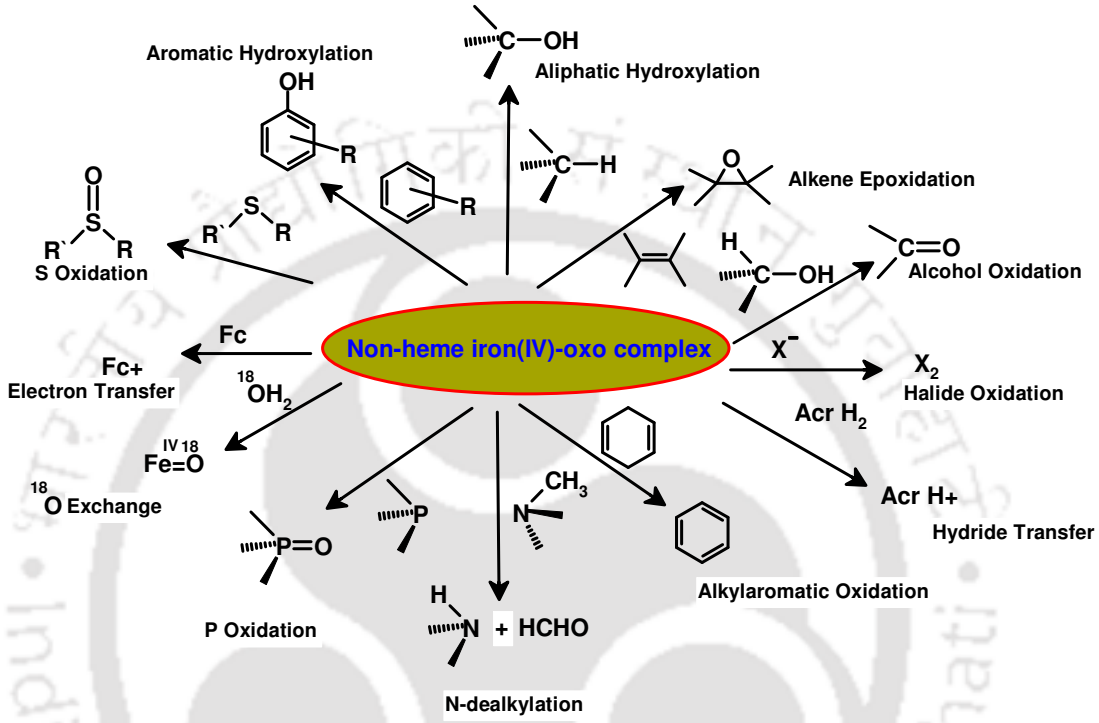

Figure 1.4. Reactions carried out by synthetic non-heme iron(IV)-oxo complexes.

Some of the important reactions involving iron(IV)-oxo complexes pertaining to this thesis include oxidation reactions involving thioanisole(s) and triphenyl phosphine. These are the commonly used substrates to demonstrate "Oxygen Atom Transfer" (OAT) reactions. These are two electron oxidation reactions (of S- and P-) where in the oxygen atom is being transferred from iron(IV)-oxo to the substrate. The mechanistic insights of OAT reactions have been confirmed by using ^{18}O labeled experiments.[27, 47]

Organic substrates like xanthene, 9,10-dihydroanthracene (DHA), 1,4-cyclohexadiene (CHD), fluorene, indene, triphenylmethane are commonly

employed to evaluate Hydrogen Atom Transfer (HAT) reactions. The HAT mechanism involved consecutive two one electron reactions involving iron(IV)-oxo interemdiates. The mechanistic conclusion usually comes from the observed KIE values. Both OAT and HAT have been the key reactions to understand the factors influencing the reactivity of iron(IV)-oxo complexes. It has been shown that by changing the axial ligand on the iron(IV) center in $[Fe^{IV}(O)(TMC)X]$ (where X = $NCCH_3$, N_3, $OOCCF_3$, S) one can actually tune the electrophilic character of iron(IV)-oxo intermediates. The electron rich anionic ligands favoured HAT reactions while neutral $NCCH_3$ favoured OAT reactions.[48, 49]

Electron transfer reaction of iron(IV)-oxo are another important class of reactions which are well studied. Substrates like ferrocene and/or its derivatives are commonly employed to evaluate the one electron reduction of Fe^{IV} to Fe^{III}.[50,51] At times, one can tune the two electron reactivity of iron(IV)-oxo complexes by changing the ligand environment. For example, thioanisole undergoes two electron oxidation by $[Fe(O)N4py]^{2+}$ via OAT. The reaction mechanism changes to electron transfer in the presence of Sc^{3+}.[52] In other words, depending on the ligand architecture and steric factors involved in substrate approaching the electrophilic iron center, it is possible to tune the reactivity from OAT to electron transfer.

1.3 Non-heme iron(III)-peroxo history

Unlike iron(IV)-oxo complexes which have been generated using different pathways, iron(III)-peroxo complexes are usually generated using excess of H_2O_2 as an oxidant in the presence of a base (Et_3N). $[Fe^{III}(O_2)(EDTA)]$ is one of the earliest examples of well characterized ferric peroxo complexes.[53-55] The iron(III) peroxo complexes are usually characterized by their distinct low intensity peroxo-to-iron(III) charge transfer LMCT band in absorption spectra.

The main contrasting feature in iron(III)-peroxo complexes is their spin state. While most of the iron(IV)-oxo and iron(III)-hydroperoxo species are of low spin, iron(III)-peroxo complexes are usually of high spin.

Over the past decade, several groups have reported the generation and spectral characterization of iron(III)-peroxo intermediates bearing tetra- and penta-dentate ligands.[56-59] Inspite of one of the well documented literature of the peroxo complexes, the first structural characterization was reported very recently.[58] The reactivity of iron(III)-peroxo complexes is striking different from that of iron(IV)-oxo complexes. The iron center in the peroxo complexes is neucleophilic in nature. The reactivity studies involving iron(III)-peroxo complexes have been deformylation reactions of aldehydes. Evidence for the ferric-peroxo species behaving as a nucleophile and attacking an aldehyde carbon has been obtained from mechanistic studies using isotopically labeled $H_2{}^{18}O_2$.[59]

1.4 Non-heme iron(III)-hydroperoxo history

In heme systems, iron(III)-hydroperoxo species (Fe^{III}-OOH), has always been proposed as a "second electrophilic oxidant" in a variety of oxygenation reactions including alkane hydroxylation and olefin epoxidation reactions,[60-68] In addition, a lowspin Fe^{III}-OOH species has been well characterized as an active oxidant for "activated bleomycin", which is the last detectable intermediate in the reaction cycle of bleomycin (BLM) and a plausible oxidant responsible for DNA cleavage reaction and the oxygenation of hydrocarbons.[69-71]

In non-heme chemistry iron(III)-peroxo complexes are usually generated using tetra- and penta-dentate as ligand architecture bearing pyridine subunits to support the system.[72-87] The iron(III)-peroxo complexes can be easily generated upon addition of H_2O_2 (usually in excess) in methanolic (or acetone) solution at lower temperatures, except for the ligand Ph_4DBA^{2-} which gives dinuclear iron

complexes.[80] The hydroperoxo complexes of iron are usually characterized by the presence of a high intensity LMCT band in their absorption spectra.

The reactivity studies of iron(II)-hydroperoxo complexes have always been debatable. Under catalytic conditions, hydroperoxo species have also been often proposed as reactive intermediates in the oxygenation of olefins and alkanes by non-heme iron catalysts and H_2O_2.[76,83] However there is no direct evidence that such Fe^{III}-OOH species are active intermediate. Some reports in litterature we found that it does catalytical epoxidation by group transfer mechanism but in single turnover experiments itwas a sluggish oxidant.[84] This ambiguty in the reactivity details of iron(III)-hydroperoxo complexes has insprired several groups to closely at the intracacies of the reactivity. The first experimental and theoritical evidence for the enchanced reactivity of Fe^{III}-OOH over Fe^{IV}=O species was provided in halide oxidation reaction.[85,86] The mechanistic insights revealed Fe^{III}-OOH complexes to be electrophilic in character.[86] Subsequently, Nam and co-workers have reported a high-spin iron(III)-hydroperoxo complexes bearing TMC ligand.[58,87] This intermediate showed a borderline reactivity both in terms of electrophilic sulphoxidation as well as nucleophilic aldehyde deformylation reactions.

1.5 Non-heme iron isolobal intermediates

Though there are several reports of high-valent iron-oxygen adducts, the reports on their isolobal analogs have been very limited. Iron complexes with terminal nitrides are some of the few well studies systems. The nitride ligand is known to stabilize iron in variable oxidation states of +4, +5 and +6.[88-90] The first report of iron(V)-nitrido was reported by Weighardt and co-workers.[26,89] This was prepared by photolysis of iron-azide complex. Subsequently the same group has also reported iron(VI)-nitrido complex bearing trimethycyclam acetate as

ligand core. generated by laser irradiation of the electrochemically generated iron(IV)-azide which again led to photo-oxidation.[90] In the non-heme iron(IV) category, the isolobal nitrido complexes were reported bearing tris-(phosphino)borate ligands.[88,91] These species were generated in two steps , in first step iron(I) precursor treated with a nitrene transfer reagent Li(dbabh) to form iron(III)-imide intermediate, then in second step the high-valent nitride species during warming of iron(III)-imide and loss of anthracene.

The iron centers bound to a terminal imido or nitrido ligand are called as iron-imido or iron-nitrido complexes, and these are comparable to the correponding Fe^{IV}=O systems.[92,93] Mononuclear non-heme iron nitrides and imides have recently appeared and are fewer in reports than the oxo analogues. Iron(IV)-imido complex [Fe4(μ_3-N^{t}Bu)$_4$] was first reported by Lee and co-workers.[94] It has a cubane like structure with iron(IV) center as one corner in cubane. The bridged iron centers were bound to a terminal chloride anion and the fourth iron center was ligated to a terminal t-butyl imide. The subsequent reports of iron(IV)-imido compound were reported in high yields using different ligand architectures.[96-105]

The high-valent metal-nitrido/imido complexes have strong oxidative power and capable to catalyze isolobal amination reactions. During the past decade, the chemistry of metal-catalyzed aziridination of alkenes and aminidation of aliphatic C–H bonds using iminoiodane reagents have been studied by several groups.[96-103] However, details on its potential as nitrogen atom transfer agent are lacking and little knowledge exists in its relative reactivity with respect to the well-known iron(IV)-oxo species.[104]

1.6 Scope and aim of the thesis

Over the recent decade, mechanistic insights into the reactivity of high-valent metal intermediates towards oxidations reactions have gained immense importance in bio-inorganic chemistry. The reactivity studies of iron(III)-hydroperoxo complexes were very limited. Though the reactivity of iron(IV)-oxo complexes were well explored, the reports of their potential towards industrial application are very limited. A comparative study on the reactivity and mechanism of Fe^{IV}=O and Fe^{IV}=NR towards *S*-oxidation and C-H activation were none. The work described in this thesis explores the unusual chemistry of high-valent iron complexes. Chapter 2 discusses the synthesis and characterization of a family of iron(III)-hydroperoxo, iron(IV)-oxo and iron(IV)-imido compounds supported by penta-dentate ligands. Chapter 3 give a thorough discussion on the reactivity of the iron(III)-hydroperoxo in comparison with iron(IV)-oxo complexes towards bromide oxidation. It was observed that the iron(III)-hydroperoxo complexes are efficient oxidants than the corresponding iron(IV)-oxo complexes for bromide oxidation reactions. Chapter 4 includes detailed mechanistic analysis of halide oxidation by iron(III)-hydroperoxo and iron(IV)-oxo complexes. Chapter 5 explores the comparative reactivity studies of high-valent iron(IV)-oxo and iron(IV)-imido compounds towards S-oxidation and C-H activation. It was observed that for two electron oxidation of thioanisole, iron(IV)-imido complexes are more reactive than iron(IV)-oxo complexes. A complete reversal of trend was observed for H-atom abstraction reactions. Finally, Chapter 6 deals with the oxidation of organic pollutant dibenzothiophene by iron(IV)-oxo complexes.

1.7 References.

1. *Cytochrome P450: Structure, Mechanism and Biochemistry, ed.*P. R. Ortiz de Montellano, 3rd edn, Kluwer Academic/Plenum Publ., New York, 2005.
2. I. G. Denisov, T. M. Makris, S. G. Siligar, I.Schlichting, *Chem. Rev.,* 2005**, 105**, 2253-2277.
3. B. Meunier, S. P. de Visser, S. Shaik, *Chem. Rev.,* 2004**, 104**, 3947-3980.
4. M. M.Abu-Omar, A. Loaiza, N. Hontzeas, *Chem. Rev.,*2005, **105**, 2227-2252.
5. M. Costas, M. P. Mehn, M. P. Jensen, L. Que Jr. *Chem. Rev.,*2004**, 104**, 939-986.
6. T. K. Matthew, G. R.Charle, *Acc. Chem. Res.,* 2007**, 40**, 618-625.
7. P. Hlavica, *Eur. J. Bio-chem.,* 2004**, 271**, 4335-4360.
8. E. I. Solomon, *Chem. Rev*., 2000, **100**, 235–350.
9. E. G. Kovaleva J. D. Lipscomb, *Nature Chem. Biol.,* 2008, **4**, 186–193.
10. L. C. Blasiak, F. H. Vaillancourt, C. T. Walsh, C. L. Drennan, *Nature*, 2006,**440**, 368–371.
11. J. Rittle, M. T. Green, *Science,* 2010, **330**, 933–937.
12. E. G. Kovaleva, J. D. Lipscomb, *Science*, 2007, **316**, 453–457.
13. A. Karlsson, *Science*, 2003, **299**, 1039–1042.
14. R. M.Cicchillo, *Nature*, 2009, **459**, 871–874.
15. E. I.Solomon, T. C. Brunold, M. I. Davis, J. N. Kemsley, S. –K. Lee,N. Lehnert, F. Neese, A. J.Skulan, Y. –S. Yang, J. Zhou, Chem. Rev., 2000, **100**, 235–349.
16. M. Costas, M. P. Mehn, M. P.Jensen, L. Que Jr, *Chem. Rev.,*2004**, 104**, 939-986.
17. R. P. Hausinger, *Crit. Rev. Biochem. Mol. Biol*., 2004, **39**, 21–68.

18. E. G. Kovaleva, J. D. Lipscomb, *Nat. Chem. Biol*., 2008, **4**, 186–193.
19. C. Loenarz , C. J. Schofield, *Nat. Chem. Biol*., 2008, **4**, 152–156.
20. W. Nam, *Acc. Chem. Res*., 2007, **40**, 522–531.
21. M. J. Park, J. Lee, Y.Suh, J. Kim, W. Nam, *J. Am. Chem. Soc.,*2006**, 128**, 2630-2634.
22. W. Nam, *Acc. Chem. Res.,* 2007**, 40**, 522-531.
23. J. M. Bollinger Jr, J. C. Price, L. M. Hoffart, E. W. Barr, C. Krebs, *Eur. J. Inorg. Chem.,* 2005, 4245-4254.
24. C. Krebs, J. C. Price, J. Baldwin, L. Saleh, M. T. Green, J. M. Bollinger Jr, *Inorg. Chem.,* 2005, **44**, 742-757.
25. J. C. Price, E. W. Barr, B. Tirupati, J. M. Bollinger Jr, C. Krebs, *Biochemistry,* 2003, **42**, 7497-7508.
26. C. A. Grapperhaus, B. Mienert, E. Bill, T. Weyhermüller, K. Wieghardt, *Inorg.Chem.,* 2000, **39**, 5306-5317.
27. J. –U. Rohde, J. –H. In, M. –H. Lim, W. W. Brennessel, M. R. Bukowski, A. Stubna, E. Münck, W. Nam, L.Que. Jr., *Science* 2003, **229**, 1037-1039.
28. C. E. MacBeth, A. P. Golombek, V. G. YoungJr, C. Yang, K.Kuczera, M. P. Hendrich, A. S. Borovik,*Science*, 2000, **289**, 938-941.
29. M. H. Lim, J. –U. Rohde, A. Stubna, M. R.Bukowski, M. Costas, R. Y. N. Ho, E. Münck, W. Nam, L. Que. Jr., *Proc. Natl. Acad. Sci. U. S. A.,* 2003, **100**, 3665-3670.
30. M. R. Bukowski, K. D. Koehntop, A. Stubna, E. L. Bominaar, J. A. Halfen, E. Münck, W. Nam, L. Que. Jr, *Science*, 2005, **310**, 1000-1002.
31. J. Kaizer, M. Costas, L. Que. Jr., *‚Angew. Chem. Int. Ed.,* 2003, **42**, 3671-3673.

32. J. Kaizer, E. J. Klinker, N. Y. Oh, J. –U. Rohde, W. J. Song, A. Stubna, J. Kim, E. Münck, W. Nam, L. Que. Jr.,, *J. Am. Chem. Soc.*, 2004, **126**, 472-473.
33. O. Pestovsky, S.Stoian, E.Bominaar, X. Shan, E.Munck, L. Que. Jr. A. Bakac, *Angew. Chem. Int. Ed.,* 2005, **44**, 6871-6874.
34. V. Ball, M. –F. Charlot, F. Banse,J. –J. Girerd, T. A. Mattioli, E. Bill, J. –F. Bartoli, P. Battioni, D. Mansuy, *Eur. J. Inorg. Chem.,* 2004, 301-308.
35. M. Martinho, F. Banse, J. –F.Bartoli, T. A. Mattioli, P.Battioni, O. Horner, S. Bourcier, J. –J. Girerd, *Inorg. Chem.,* 2005, **44**, 9592-9596.
36. T. K. Paine, M. Costas, J. Kaizer, L. Que. Jr., *J. Biol. Inorg. Chem.,* 2006, **11**, 272-276.
37. C. V. Sastri, M. S. Seo, M. J. Park, K. M. Kim, W. Nam, *Chem. Commun.* , 2005, 1405-1407.
38. J. Bautz, M. R. Bukowski, M. Kerscher, A. Stubna, P.Comba, A.Lienke, E. Münck, L. Que. Jr., *Angew. Chem. Int. Ed.* 2006, **45**, 5681-5684.
39. J. Engl, Y. Guo, E. R. Farquhar, V. G. Young Jr., E. Munck L. Que. Jr., *J. Am. Chem. Soc.,* 2010, **132**, 8635-8644.
40. F. Tiago de Oliveira, A. Chanda, D. Banerjee, X. Shan, S. Mondal, L. Que. Jr., E. Bominaar, E. Münck, T. J. Collins, *Science,* 2007, **315**, 835-838.
41. Y. M. Lee, S. N. Dhuri, S. C. Sawant, J. Cho, M. Kubo, T. Ogura, S.Fukuzumi, W. Nam, *Angew. Chem. Int. Ed.*, 2009, **48**, 1803-1806.
42. J. Kaizer, M. Costas, L. Que, Jr.*Angew. Chem. Int. Ed.*, 2003, **42**, 3671-3673.
43. M. J. Collins, K. Ray, L. Que. Jr., *J. Am. Chem. Soc.,* 2006, **45**, 8009-8011.

44. F. Li, K. M. V. Heuvelen, K. K. Meier, E. Munck L. Que. Jr., *J. Am. Chem. Soc.,* 2013, **135**, 10198-10201.
45. S. O. Kim, C. V.Sastri, M. S.Seo, J. Kim, W. Nam, *J. Am. Chem. Soc.*, 2005, **127**, 4178-4179.
46. Y. -M. Lee, S. Hong, Y. Morimoto, W. Shin, S. Fukuzumi, W. Nam, *J. Am. Chem. Soc.,*2010, **132**, 10668–10670.
47. M. J. Park, J. Lee, Y. Suh, J. Kim, W. Nam, *J. Am. Chem. Soc.,* 2006, **128**, 2630-2634.
48. J. –U. Rohde, L. Que, Jr., *Angew. Chem. Int. Ed.,* 2005, **44**, 2255–2258.
49. C. V. Sastri, J. Lee, K. Oh, Y. J. Lee, J. Lee, T. A. Jackson, K. Ray , H. Hirao, W. Shin, J. A. Halfen, J. Kim, L. Que, Jr., S. Shaik, W. Nam, *Proc. Natl. Acad. Sci. USA*. 2007, **104**, 19181–19186.
50. Y. -M. Lee, H. Kotani, T. Suenobu, W. Nam, S. Fukuzumi, *J. Am. Chem. Soc.,* 2008, **130**, 434–435.
51. P. Comba, S. Fukuzumi, H. Kotani, S. Wunderlich, *Angew. Chem. Int. Ed.,* 2010, **49**, 2622–2625.
52. S. Fukuzumi, H. Kotani, Y. –M. Lee, W. Nam, *J. Am. Chem. Soc.,* 2008, **130**, 15134-15142.
53. C. Walling, M. Kurz, H. J. Schugar, *Inorg. Chem.,* 1970, **9**, 931–937.
54. S. Ahmad, J. D. McCallum , A. K. Shiemke , E. H. Appelman, T. M. Loehr, J. S. –Loehr, *Inorg. Chem.,* 1988, **27**, 2230–2233.
55. F. Neese, E. I. Solomon, *J. Am. Chem. Soc.,* 1998, **120**, 12829–12848.
56. A. J. Simaan, F. Banse, P. Mialane, A. Boussac, S. Un, T. K. -Grisel, G. Bouchoux, J. –J.Girerd, *Eur. J. Inorg. Chem.,* 1999, 993–996.
57. K. B. Jensen, C. J. McKenzie, L. P. Nielsen, J. Z. Pedersen, H. M. Svendsen, *Chem. Commun.,* 1999, 1313-1314.

58. J. Cho, S. Jeon, S. A. Wilson, L. V. Liu, E. A. Kang, J. J. Braymer, M. H. Lim, B. Hedman, K. O. Hodgson, J. S. Valentine, E, I. Solomon, W. Nam, *Nature*, 2011, **478**, 502-505.
59. J. Annaraj, Y. Suh, M. –S. Seo, S. O. Kim, W. Nam, *Chem. Commun.,* 2005, 4529-4531.
60. P. Hlavica, *Eur. J. Biochem*., 2004, **271**, 4335-4360.
61. S. Jin, T. A. Bryson, J. H. Dawson, *J. Biol. Inorg. Chem*., 2004, **9**, 644-653.
62. W. Nam, Y. O. Ryu, W. J. Song, *J. Biol. Inorg. Chem*., 2004, **9**, 654-660.
63. S. Shaik, S. P. de Visser, D. Kumar, *J. Biol. Inorg. Chem*., 2004, **9**, 661-668.
64. M. Newcomb, P. F. Hollenberg, M. J. Coon, *Biochem. Biophys*., **2003**, *409*, 72-79.
65. W. J. Song, Y. O. Ryu, R. Song, W. Nam, *J. Biol. Inorg. Chem*., **2005**, **10**, 294-304 and references therein.
66. M. Newcomb, R. Shen, S. –Y. Choi, P. H. Toy, P. F. Hollenberg, A. D. N. Vaz, M. J. Coon, *J.Am. Chem. Soc*., 2000, **122**, 2677-2686.
67. P. H. Toy, M. Newcomb, M. J. Coon, A. D. N. Vaz, *J. Am. Chem. Soc*., 1998, **120**, 9718-9719.
68. A. D. N. Vaz, D. F. McGinnity, M. J. Coon, *Proc. Natl. Acad. Sci. U.S.A*., 1998, **95**, 3555-3560.
69. N. Lehnert, F. Neese, R. Y. N. Ho, L. Que Jr., E. I. Solomon, *J.Am. Chem. Soc.,* 2002, **124**, 10810-10822.
70. J. W. Sam, X. –J. Tang, J. Peisach, *J. Am. Chem. Soc.,* 1994, **116**, 5250-5256.
71. N. Murugesan, S. M. Hecht, *J. Am. Chem. Soc.,* 1985, **107**, 493-500.

72. A. J. Simaan, S. Dopner, F. Banse, S. Bourcier, G. Bouchoux, A. Boussac, P. Hildebrandt, J. –J. Girerd, *Eur. J. Inorg. Chem.,* 2000, **7**, 1627-1633.
73. I. Bernal, I. M. Jensen, K. B. Jensen, C. J. McKenzie, H. Toftlund, J. –P. Tuchagues, *J. Chem. Soc., Dalton Trans.,*1995, 3667-3675
74. P. Mialane , A. Nivorojkine , G. Pratviel , L. Azéma , M. Slany , F. Godde, A. Simaan, F. Banse,, T. K. -Grisel , G. Bouchoux , J. Sainton, O. Horner, J. Guilhem, L. Tchertanova, B. Meunier J. –J. G. Laborat, *Inorg. Chem.,* 1999, **38**, 1085–1092.
75. K. B. Jensen, C. J. McKenzie, L. P. Nielsen, J. Z. Pedersen, H. M. Svendsen. *Chem.Commun.,* 1999, 1313-1314.
76. M. Lubben, A. Meetsma, E. C. Wilkinson, B. Feringa, L. Que Jr., ,*Angew. Chem. Int. Ed.,* 1995, **34**, 1512–15146.
77. R. Y. N. Ho , G.Roelfes, B. L. Feringa, L. Que Jr., *J. Am. Chem. Soc.,*1999, **121**, 264–265.
78. G. Roelfes , M. Lubben , K. Chen , R. Y. N. Ho , A. Meetsma , S. Genseberger, R. M. Hermant , R. Hage , S. K. Mandal , V. G. Young Jr, Y. Zang , H. Kooijman , A. L. Spek , L. Que Jr., B. L. Feringa, *Inorg. Chem.,* 1999, 38, 1929–1936.
79. M. E. de Vries, R. M. La Crois, G. Roelfes, H. Kooijman, A. L. Spek, R.Hage, B. L. Feringa, *Chem. Commun.,*1997, 1549-1550.
80. T. J. Mizoguchi, S. J. Lippard. *J. Am. Chem. Soc.,* 1998, **120**, 11022–11023.
81. J. W. Sam, X. –J. Tang, J. Peisach. *J. Am. Chem. Soc.,* 1994, **116**, 5250–5256.
82. R. M. Burger, S. B. Horwitz, J. Peisach, J. B. Wittenberg. *J. Biol. Chem.,* 1979, **254**, 12299-12302.

83. W. Nam, R. Ho, J. S. Valentine. *J. Am. Chem. Soc.,* 1991, **113**, 7052–7054.
84. M. J. Park, J. Lee, Y. Suh, J. Kim, W. Nam. *J. Am. Chem. Soc.,* **2006**, **128**, 2630–2634.
85. A. K. Vardhaman, C. V. Sastri, D. Kumar, S. P. de visser. *Chem. Commun.,* 2011, 47, 11044-11046.
86. A. K. Vardhaman, P. Barman, S. Kumar, C. V. Sastri, D. Kumar, S. P. de visser. *Chem. Commun.,* 2013, 49, 10926-10928.
87. Y. M. Kim, K. –B. Cho, B. Wang, C. Li, S. Shaik, W. Nam. *J. Am. Chem. Soc.,* 2013, **135**, 8838–8841.
88. T. A. Betley, J. C. Peters. *J. Am. Chem. Soc.,* 2004, **126**, 6252–6254.
89. N. Aliaga-Alcalde, S. D. George, B. Mienert, E. Bill, K. Wieghardt, F. Neese. *Angew. Chem. Int. Ed.,* 2005, **44**, 2908–2912.
90. J. F. Berry, E. Bill, E. Bothe, S. D. George, B. Mienert, F. Neese, K. Wieghardt, *Science*, 2006, **312**, 1937-1941.
91. J. –U. Rohde, T. A. Betley, T. A. Jackson, C. T. Saouma, J. C. Peters L. Que Jr., *Inorg. Chem.,* 1999, **38**, 1929–1936.
92. M. P. Jensen, M. P. Mehn, L. Que Jr., *Angew. Chem. Int. Ed.,* 2003, **42**, 4357–4360.
93. R. L. Lucas, D. R. Powell, A. S. Borovik, *J. Am. Chem. Soc.,* 2005, **127**, 11596–11597.
94. A. K. Verma, T. N. Nazif, C. Achim, S. C. Lee, *J. Am. Chem. Soc.,* 2000, **122**, 11013–11014.
95. C. M. Thomas, N. P. Mankad, J. C. Peters, *J. Am. Chem. Soc.,* 2006, **128**, 4956–4957.
96. J. F. Berry, E. Bill, E. Bothe, S. D. George, B. Mienert, F. Neese, K. Wieghardt, *Science,*2006, **312**, 1937–1941.

97. P. Comba, C. Lang, C. Lopez de Laorden, A. Muruganatham, G. Rajaraman, H. Wadepohl, M. Zajaczkowski, *Chem. Eur. J.,*2008, **14**, 5313–5328.
98. K. L. Klotz, L. M. Slominski, M. E. Riemer, J. A. Phillips, J. A. Halfen, *Inorg. Chem.,*2009, **48**, 801–803.
99. J. J. Scepaniak, J. A. Young, R. P. Bontchev, J. M. Smith, *Angew. Chem. Int. Ed.*,2009, **48**, 3158–3160.
100. P. Leeladee, G. N. L. Jameson, M. A. Siegler, D. Kumar, S. P. de Visser, D. P. Goldberg, *Inorg. Chem.*, 2013, **52**, 4668–4682.
101. M. J. Zdilla, M. M. Abu-Omar, *J. Am. Chem. Soc.*, 2006, **128**, 16971-16979.
102. S. Kundu, E. Miceli, E. Farquhar, F. F. Pfaff, U. Kuhlmann, P. Hildebrandt, B. Braun, C. Greco, K. Ray, *J. Am. Chem. Soc.,*2012, **134**,14710−14713.
103. J. W. W. Chang, P. W. H. Chan, *Angew. Chem. Int. Ed.,*2008, **47**, 1138–1140.
104. E. T. Hennessy, T. A. Betley, *Science,*2013, **340**, 591–595.
105. A. K. Vardhaman, P. Barman, S. Kumar, C. V. Sastri, D. Kumar and S. P. de visser, *Angew. Chem. Int. Ed.,*2013, **52**, 12288-12292.

CHAPTER-II

Materials and Methods

2.1 Introduction

In this Chapter, a listing of all the materials employed at different stages of the investigation and procedures for purification of the utilized chemicals and solvents are given. Also given here are preparations of the various precursor materials and a brief description of the physicochemical techniques employed in this study.

2.2 Experimental Section

2.2.1 Materials

All chemicals obtained from Aldrich Chemical Co. were the best available purity and were used without further purification unless otherwise indicated. Solvents were dried according to published procedures and distilled under argon prior to use.[1] Tetrabutylammonium halides (TBAX) used as substrates are hydroscopic in nature. These are purified before use. Typically TBAX were dissolved suitable solvents (5mL/gr) at 80ºC and stirred. This hot solution was added to non-polar solvents (ex. Diethyl ether or hexane) and allowed to cool (5 ^{o}C). After several days, shiny white crystalline TBAX salts crystallized which were dried over P_2O_5. Purified TBAX were stored in schlenk tubes to avoid moisture contamination.

The deuterated substrate fluorene-d_2, was prepared by taking fluorene (2 gr, 12 mmol) in DMSO-d_6 (3 mL) along with NaH (0.577 gr, 24 mmol) under an inert atmosphere. The deep red solution was stirred at room temperature for 8 h, and the reaction was quenched with D_2O (5 mL. The crude product was filtered and washed with copious amounts of H_2O and dried in vacuum. ^{1}H-NMR confirmed >99% deuteration.[2] All other compounds used in this thesis were prepared as per reported procedures in good to moderate yields.

2.2.2 Preparation of Oxidants

Iodosylbenzene (PhIO) was prepared according to literature procedure.[3] In a typical preparation finely ground iodosobenzene diacetate (3.21 g, 1 mmole) is placed in 250 mL beaker. To it was added of 3 N NaOH (150 ml) solutions slowly over a period of 15-minutes time with vigorous stirring. Now thoroughly mix the lumps for additional 45 minutes with glass rod and spatula. Water (100 mL) was now added to the reaction mixture under vigorous stirring to precipitate crude solid iodosobenzene which was then collected on Buchner funnel. The wet solid was triturated with copious amount of water and finally with $CHCl_3$ to remove any un-reacted starting material. The dried PhIO was stored in cool and dark place.

[N-(*p*-tolylsulfonyl)-imino)]phenyliodinane (PhINTs) was prepared according to literature procedure.[4] In a typical preparation finely ground iodosobenzene diacetate (3.21 g, 1.0 mmol) was added to the stirred mixture of *p*-toluenesulonamide (1.71 g, 1.0 mmol) and potassium hydroxide (1.4 g, 0.025 mmol) in HPLC grade methanol (40 mL), keeping the temperature below 10 ºC during the addition. The resulting clear yellow solution was stirred for three hours at room temperature and then poured into distilled water (250 mL). Over a period of 12 hours a yellow precipitate formed and this was then filtered, washed with distilled water and dried at room temperature in a vacuum desiccator. Recrystallized from methanol to give crystalline PhINTs which was stored in cool and dark place

2.2.3 Synthesis of N, N-bis(2-pyridylmethyl)-N-bis(2-pyridyl) methylamine (N4Py) [5]

The desired Ligand N4Py was prepared in a three step synthesis process. In the first step, di(2-pyridly) ketone was converted to di(2-pyridly) ketoxime. Typically a mixure of di(2-pyridly) ketone (5.0 g, 0.027 mmol), and hydroxylamine hydrochloride (4.17 g, 0.06 mmol) were dissolved in 10 mL ethanol in a 100 mL round bottom flask which contains NaOH (4 g in 20 mL H_2O) and 20 mL of water and refluxed for 2 hours. Excess of ethanol was then removed under vacuum and the resultant solution was diluted to 1 L with ice cold water. To it was added HCl (drop wise) to adjust the resultant pH ~ 7. Pinkish white precipitate of di(2-pyridly) ketoxime was filtered and dried in vacuum desiccator.

In the second step, di(2-pyridly) ketoxime was reduced to bis(2-pyridyl)methylamine using Zn dust. The di(2-pyridly) ketoxime obtained from step 1 was dissolved in ethanol (100 mL) in a three neck round bottom flask. Hydrazine hydrate (60 mL) and Zn dust (in excess) were added in consecutive steps over a period of 6 hours. The resultant solution was refluxed overnight and filtered to remove Zn dust. The filterate was evaporated to near dryness under vacuum and then diluted in ice NaOH solution (4 N in 250 mL). Extraction with CH_2Cl_2 yielded bis(2-pyridyl)methylamine

In the final step, Picolyl chloride hydrochloride (6.8 g. 41.5 mmol) was added to an aqueous solution of NaOH (4 N, 20 mL) at 0°C. After stirring for 10 min, this solution was added to bis(2-pyridyl)methylamine (4.1 3 g. 20.75

mmol) and another portion of aqueous NaOH (4 N, 20 mL). This solutlon was allowed to stir for 72 h at 25 ℃. and then concentrated $HClO_4$, was added to precipitate a yellow solid, which was recrystallized from hot water. Treatment of this perchlorate salt with NaOH (4 N, 20 mL) solution and extraction with dichloromethane yielded the free amine of N4Py.

2.2.4 Synthesis of N-benzyl-N, N', N'-tris(2-pyridylmethyl)ethane-1,2-diamine (Bn-Tpen) [6]

A solution of N-benzylethylenediamine (2.0 g, 13.3 mmol) in CH_2Cl_2 (20 mL) was added to a solution of 2-(chloromethyl) pyridine hydrochloride (6.55 g, 40 mmol) in water (20 mL). NaOH (3.2 g, 80 mmol) in water (10 mL) was added in small portions over 5 days, keeping the reaction under an N_2 atmosphere. The reaction mixture was extracted with methylene chloride (3 × 25 mL). The combined organic phases were dried over MgSO4 and evaporated to dryness to yield a white solid. It was purified by extraction in a Soxhlet apparatus using low boiling petroleum.

2.2.5 Preparation of $[Fe^{II}(N4Py)(CH_3CN)](CF_3SO_3)_2$ (1) [5]

$Fe^{II}(CF_3SO_3)_2$. $2CH_3CN$ (0.124 g, 0.284 mmol) dissolved in CH_3CN (1.5 mL) was added drop wise to a solution of N4Py (0.1 g, 0.284 mmol) in ethyl acetate (5 mL). An orange-red precipitate was formed within 15 minutes. The reaction was allowed to stir further for 45 minutes. Excess of solvent was removed and washed thoroughly with ethyl acetate and dried. Recrystallization from acetonitrile-diethyl ether mixture gives dark red crystals of $[Fe^{II}(N4Py)(CH_3CN)](CF_3SO_3)_2$.

2.2.6 Preparation of $[Fe^{II}(Bn\text{-}Tpen)(CH_3CN)](CF_3SO_3)_2$ (2) [6]

A suspension of $Fe^{II}(CF_3SO_3)_2$. $2CH_3CN$ (0.436 g, 1 mmol) in CH_2Cl_2 (1.5 mL) was added drop wise to a solution of Bn-Tpen (0.423 g, 1 mmol) in CH_2Cl_2 (3 mL). The resultant yellow-red solution was allowed to stir for overnight at room temperature. The final solution was concentrated to half its original volume under vaccum and layered with di-ethylether to yield yellow crystals of $[Fe^{II}(Bn\text{-}Tpen)(CH_3CN)](CF_3SO_3)_2$.

2.3 Physical methods

UV-vis absorption spectra were recorded on a Hewlett Packard 8453 spectrophotometer equipped with either constant temperature circulating water bath or a liquid nitrogen cryostat (Unisoku) with a temperature controller. Electrospray ionization mass spectra (ESI-MS) were recorded on a Waters (Micromass MS Technologies) Q-TOF Premier mass spectrometer by infusing samples directly into the source at 15 μL/min using a syringe pump. The spray voltage was set at 2 kV and the capillary temperature at 80 °C. All electrochemical measurements were carried out under Ar atmosphere using a CH Instruments (CHI1120B) electrochemical analyzer. Cyclic voltammetric measurements were carried out in deaerated CH_3CN containing iron complexes (1 mM) and tetrabutylammonium hexafluorophosphate ($TBAPF_6$, 0.1 M) as a supporting electrolyte at 298 K. A conventional three-electrode cell was used with a platinum disk (surface area of 0.3 mm^2) as working electrode and a platinum wire as a counter electrode. The platinum working electrode were routinely polished with polishing alumina suspension and rinsed with acetone and acetonitrile before use.The measured potentials were recorded with respect to an Ag/Ag^+ (0.01 M) reference electrode and reported versus a $Fc^{+/0}$ (Fc = Ferrocene)

couple. The cyclic voltamograms were run at a scan rate of 100 mV s^{-1} Gas chromatographic analyses (product analysis) were performed on Bruker Gas chromatograph (Model: 450-GC) equipped with a FID detector using 30 m x 0.32 mm CP-Sil 5CB column.

2.4 Spectral Characterization of Iron(II) Complexes

The iron(II) complexes used this study were well characterized by ESI-MS and UV-vis spectroscopic techniques. The analysis $[Fe^{II}(N4Py)CH_3CN](CF_3SO_3)_2$ (**1**) and $[Fe^{II}(Bn\text{-}Tpen)\ CF_3SO_3](CF_3SO_3)$ (**2**) by high-resolution ESI-MS gave convincing initial evidence for their formulation as iron(II)complexes. These complexes gave ESI-MS peak at *m/z* = 572.07 and 628.13 corresponding to $[Fe^{II}(N4Py)CF_3SO_3]^+$ and $[Fe^{II}(Bn\text{-}Tpen)CF_3SO_3]^+$ respectively with an isotope pattern that matches the theoretically expected distribution, Figure 2.1. The UV-vis spectral profiles showed the characteristic LMCT band at 450 nm and 350 nm for $[Fe^{II}(N4Py)CH_3CN](CF_3SO_3)_2$ and $[Fe^{II}(Bn\text{-}Tpen)CF_3SO_3](CF_3SO_3)$ respectively.

2.5 Generation of High-Valent Intermediates

High-valent iron intermediates, iron(III)-hydroperoxo and iron(IV)-oxo intermediates were generated in-situ from 1mM solution of the respective iron(II) complexes. The iron(III)-hydroperoxo complexes $[Fe^{III}(OOH)N4Py](CF_3SO_3)_2$ (**1a**) and $[Fe^{III}(OOH)Bn\text{-}Tpen](CF_3SO_3)_2$ (**2a**) were generated on addition of 10 equiv. of H_2O_2 to iron(II) complexes in methanolic solution at 273 K.[7] Iron(IV)-oxo complexes $[Fe(O)(N4Py)]^{2+}$ (**1b**) and $[Fe(O)(Bn\text{-}Tpen)]^{2+}$ (**2b**) compounds were generated vigorous stirring with excess solid PhIO at room temperature, and remaining unreacted PhIO can be removed by 0.2 μm syringe filters following of iron(IV)-oxo complexes.[8] These **1b** and **2b** were stable at room temperature, and

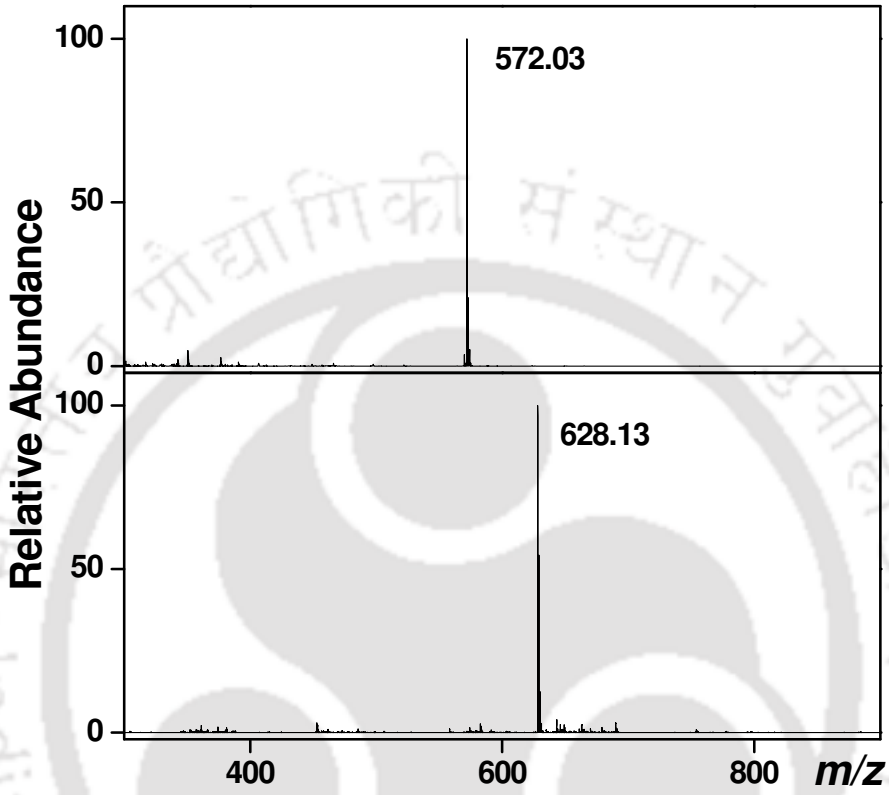

Figure 2.1 **ESI-MS spectra of $[Fe^{II}(N4Py)CH_3CN](CF_3SO_3)_2$ and $[Fe^{II}(Bn\text{-}Tpen)CF_3SO_3](CF_3SO_3)$. Mass peaks at *m/z* of 572.03 was assigned to $\{[Fe^{II}(N4Py)]CF_3SO_3\}^+$ and 628.13 was assigned to $\{[Fe^{II}(Bn\text{-}Tpen)]CF_3SO_3\}^+$.**

half-lives of of ~60 hours and ~6 hours respectively, in acetonitrile at 25 °C. Iron(IV)-imido complex **1c** was generated in an acetonitrile solution *in situ* using 1.5 equiv. of PhINTs as tosylimido donor using procedures reported before.[9] The relatively higher stability of the intermediates aided the ease of spectral characterization by ESI-MS and UV-vis spectroscopy.

2.6 Spectral Characterization of High-Valent Iron Complexes

2.6.1 ESI-MS Analysis

High-resolution ESI-MS analysis of complexes **1a** and **2a** gave convincing initial evidence for their formulation as iron(III)-hydroperoxo intermediates. The ESI-MS spectra gave *m/z* values at 605.13 which is corresponding to $\{[Fe^{III}(OOH)N4Py](CF_3SO_3)\}^+$ (Figure 2.2a) and *m/z* = 661.13 for $\{[Fe^{III}(OOH)Bn\text{-}Tpen](CF_3SO_3)\}^+$ (Figure 2.3a) with an isotope pattern that matches the theoretically expected distribution. The ESI-MS of iron(IV)-oxo complexes **1b** gave a major peak at *m/z*=587.91 corresponding to $\{[Fe^{IV}(O)N4Py](CF_3SO_3)\}^+$ (Figure 2.2b) and for $[Fe^{IV}(O)(Bn\text{-}Tpen)]^{2+}$ gave a major peak at *m/z*= 644.09 corresponding to $\{[Fe^{IV}(O)Bn\text{-}Tpen](CF_3SO_3)\}^+$ (Figure 2.3b) with an isotope pattern that matches the theoretically expected distribution. The electron spray ionization mass spectrum of **1c** gave a major peak at *m/z* = 741.07 corresponding to $\{[Fe^{IV}(NTs)N4Py](CF_3SO_3)\}^+$ (Figure 2.4) with an isotope pattern that matches the theoretically expected distribution. The reported ESI-MS values and the spectral profile matches well with the literature reports.

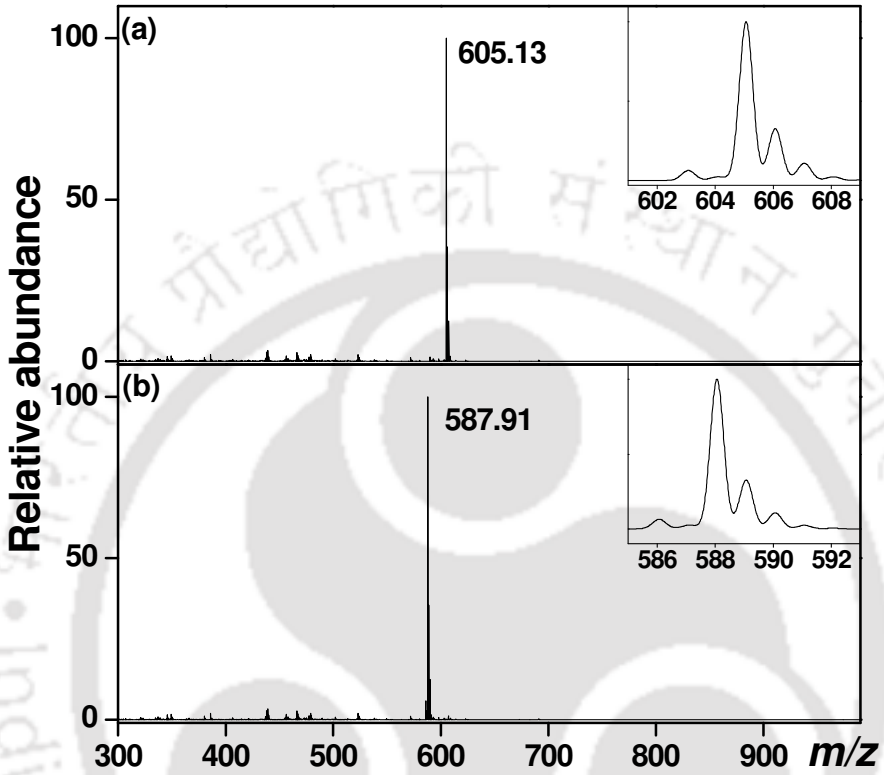

Figure 2.2 **ESI-MS spectra of (a) $[[Fe^{III}(OOH)N4Py](CF_3SO_3)_2$ and (b) $[[Fe^{IV}(O)N4Py](CF_3SO_3)_2$. Mass peaks at *m/z* of 605.13 was assigned to $\{[Fe^{III}(OOH)(N4Py)]CF_3SO_3\}^+$ and 587.91 was assigned to $\{[Fe^{IV}(O)(N4Py)]CF_3SO_3\}^+$. Insets show the isotopic distribution in the region of *m/z*.**

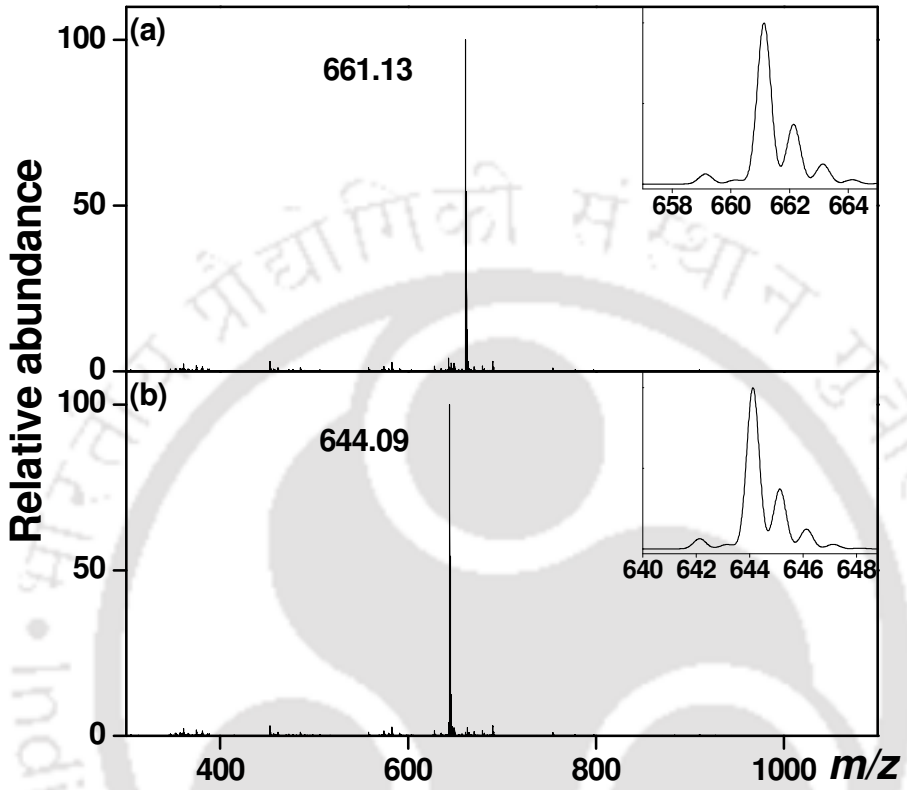

Figure 2.3 **ESI-MS spectra of (a) $[[Fe^{III}(OOH)Bn\text{-}Tpen](CF_3SO_3)_2$ and (b) $[[Fe^{IV}(O)Bn\text{-}Tpen](OTf)_2$. Mass peaks at *m/z* of 661.13 was assigned to $\{[Fe^{III}(OOH)(Bn\text{-}Tpen)]CF_3SO_3\}^+$ and 644.09 was assigned to $\{[Fe^{IV}(O)(Bn\text{-}Tpen)]CF_3SO_3\}^+$. Insets show the isotopic distribution in the region of *m/z*.**

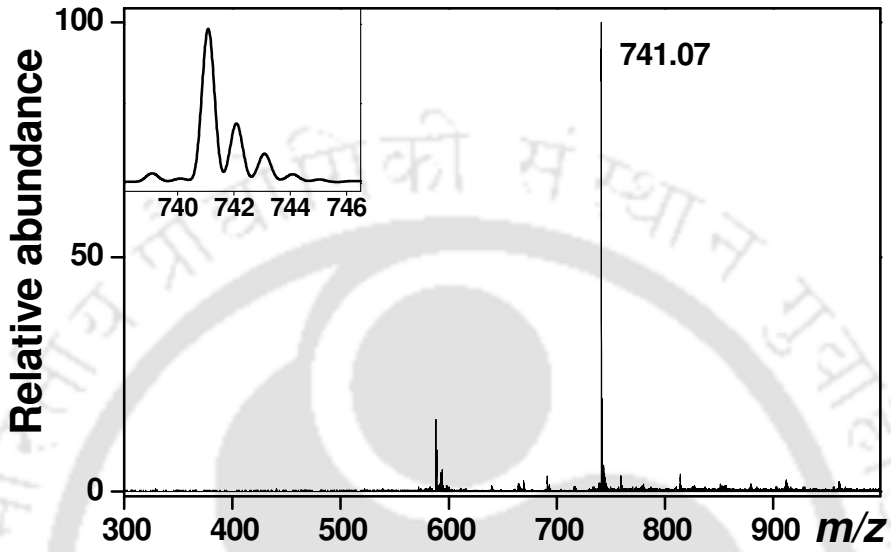

Figure 2.4 **ESI-MS spectra of $[[Fe^{IV}(NTs)N4Py](CF_3SO_3)_2$. A mass peak at *m/z* of 741.07 is assigned to $\{[Fe^{IV}(NTs)(N4Py)]CF_3SO_3\}^+$, Insets shows the isotopic distribution in the region of *m/z*.**

2.6.2 UV-vis Spectroscopy

The initial identifications of the intermediates prepared were based on their respective signature absorption bands in the visible-NIR region. The iron(III)-hydroperoxo intermediates showed the characteristic LMCT band at 548 nm (ε = 1100 M^{-1} cm^{-1}) and 535 nm (ε =1000 M^{-1} cm^{-1}) for **1a** and **2a** respectively (Figure 2.5 and Figure 2.6). The iron(IV)-oxo intermediates **1b** and **2b** were confirmed on the basis of visible features with low energy bands observed at 695 nm and 735 nm respectively (ε = 400 M^{-1} cm^{-1}), that arises from ligand field transitions characteristic for S = 1 iron(IV) complexes , (Figure 2.5 and Figure 2.6). The identity of iron(IV)-imido complex **1c** was confirmed on the

basis of visible features with an intense LMCT band at 445 nm (ε = 2700 M^{-1} cm^{-1}) and a low energy 660 nm band (ε = 250 M^{-1} cm^{-1}) that arises from ligand field transitions characteristic for *S* = 1 iron(IV)complexes.(Figure 2.7)

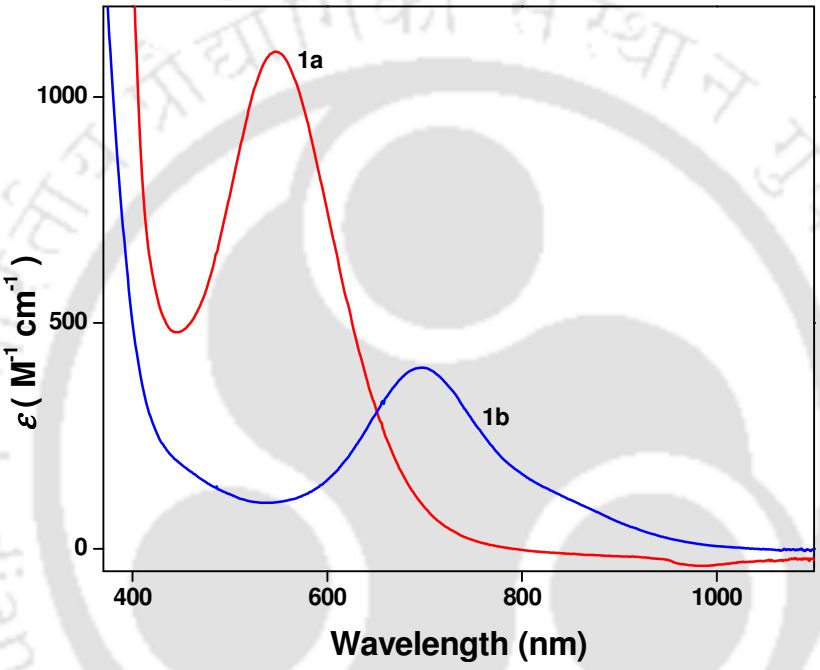

Figure 2.5 **UV-vis spectral profiles of $[Fe^{III}(OOH)N4Py](CF_3SO_3)_2$ (1a) and $[Fe^{IV}(O)N4Py]$ $(CF_3SO_3)_2$ (1b) at 298 K.**

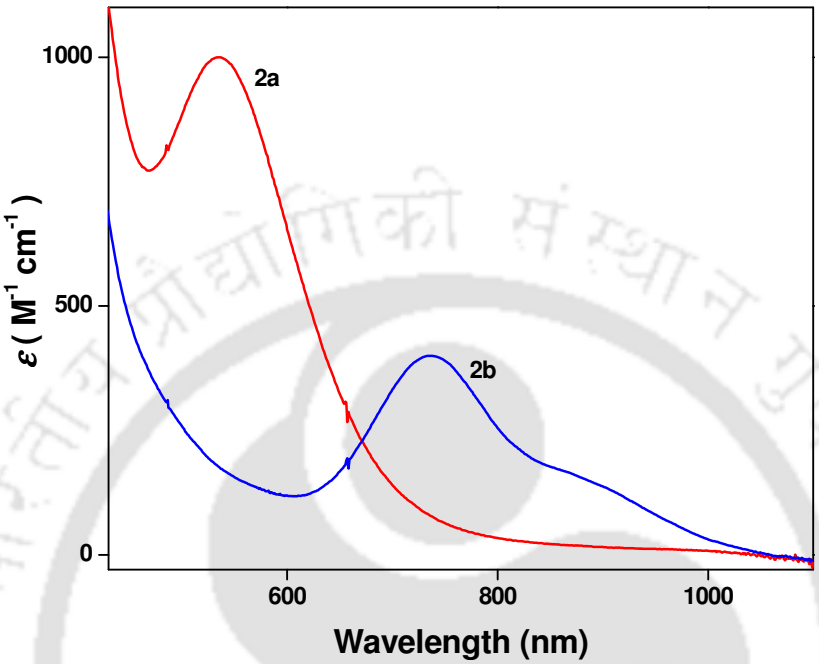

Figure 2.6 **UV-vis spectral profiles of $[Fe^{III}(OOH)Bn\text{-}Tpen](CF_3SO_3)_2$ (2a) and $[Fe^{IV}(O)Bn\text{-}Tpen](CF_3SO_3)_2$ (2b) at 298 K.**

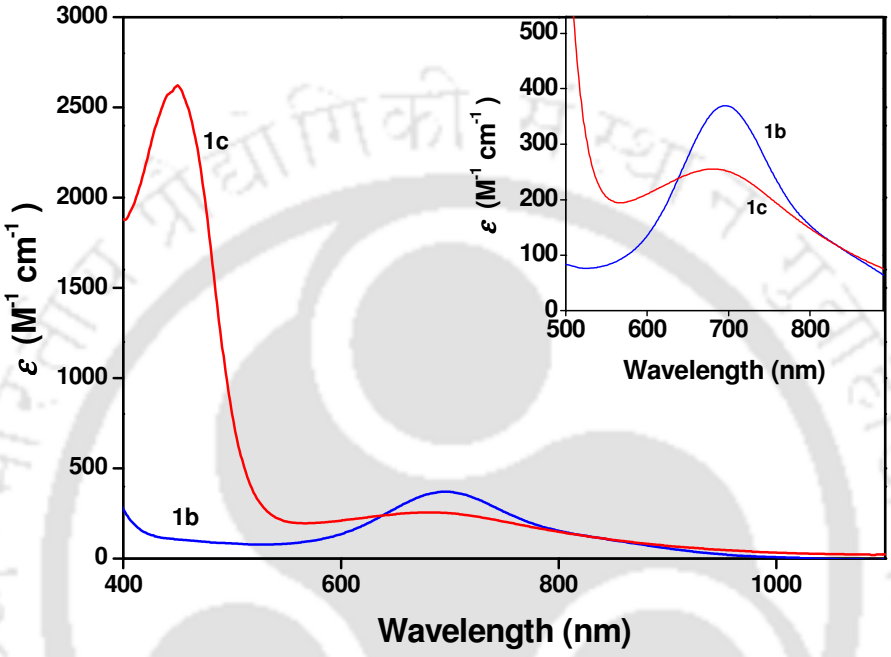

Figure 2.7 **UV-vis spectral profiles of $[Fe^{IV}(O)N4Py](CF_3SO_3)_2$ (1b) and $[[Fe^{IV}(NTs)N4Py](CF_3SO_3)_2$ (1c) at 298 K. The inset displays the low energy region.**

2.7 Kinetic Studies

All kinetic measurements were performed on a Hewlett-Packard 8453A Diode Array spectrophotometer interfaced with an IBM compatible PC and equipped with constant temperature circulating water bath or a liquid nitrogen cryostat (Unisoku) with a temperature controller. Standard 10 mm quartz cuvettes were used for all measurements. The temperature of solutions during experiments was kept to within ± 0.2 ^{o}C. The rates for reactions of all the intermediates in the presence of suitable substrates were measured by monitoring the decrease of their

characterisitic absorption bands under the conditions that the concentrations of substrates were at least five-fold in excess of the catalyst complexes under study. Pseudo-first-order rate constants (k_{obs}) were determined by non-linear least-squares fits of ($A_f - A_t$) to time (t) according to the following equation:

$$[A_f - A_t] = [A_f - A_i] \exp(-k_{obs}*t) \qquad \text{-----} \qquad \text{(equn. 2.1)}$$

Where A_f and A_i are the final and initial absorbance respectively, and A_t is the absorbance measured at time t. Kinetic rate over four half-lives ($t_{1/2}$) were used for the least-squares fitting. Second-order rate constants, k_2, were obtained from linear fit of k_{obs} values to [substrate].

2.8 References

1. Purification of Laboratory Chemicals; W. L. F. Armarego, D. D. Perrin (Eds.); Pergamon Press: Oxford, 1997.
2. C. R. Goldsmith, R. T. Jonas, T. D. P. Stack, *J. Am. Chem. Soc.,* 2001, **124**, 83-96.
3. H. Saltzman, in *Organic Syntheses*, Vol. V (Eds: J. G. Sharefkin); Wiley, New York, **1973**, pp. 658.
4. S. Taylor , J. Gullick , P. McMorn , D. Bethell , P. C. Bulman Page , F. E. Hancock, F. King, G. J. Hutchings., *J. Chem. Soc., Perkin Trans*. 2001, **2**, 1714–1723.
5. M. Lubben, A. Wilkinson, B. Feringa, L. Que Jr, *Angew. Chem. Int. Ed.,* 1995, **34**, 1512-1514.
6. L. Duelund, R. Hazell, C. J. McKenzie, L. P. Nielsen, H. J. Toftlund, *J. Chem. Soc. Dalton Trans.,* 2001, 152-156.
7. A. Hazell, C. J. McKenzie, L. P. Nielsen, S. Schindler, M. Weitzer, *J. Chem. Soc. Dalton Trans.,* 2002, 310-314.
8. J. Kaizer, E. J. Klinker, N. Y. Oh, J.-U. Rohde, W. J. Song, A. Stubna, J. Kim, E. Münck, W. Nam, L. Que, Jr., *J. Am. Chem. Soc*., 2004, **126**, 472-473.
9. E. J. Klinker, T. A. Jackson, M. P. Jensen, A. Stubna, G. Juhász, E. L. Bominaar, E. Münck, L. Que Jr*, Angew. Chem. Int. Ed*. 2006, **45**, 7394–7397.

CHAPTER-III

Non-Heme Ferric Hydroperoxo Intermediates are Efficient Oxidants of Bromide Oxidation

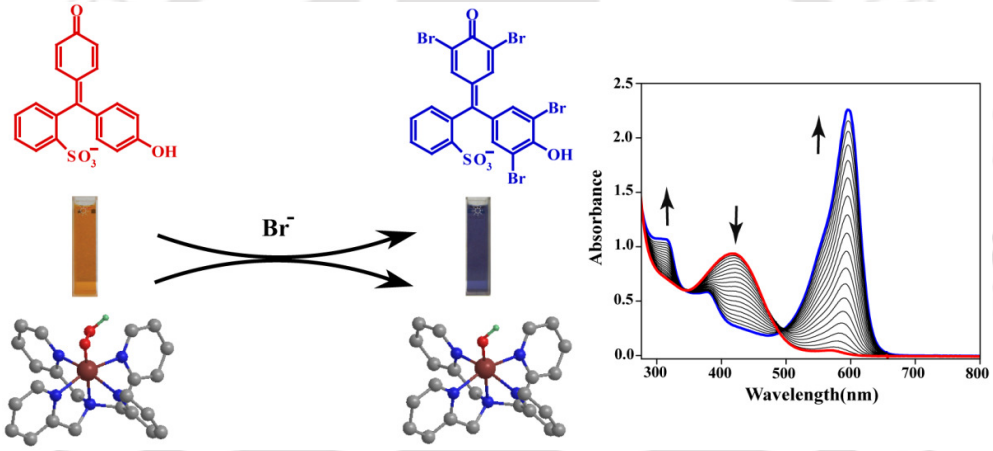

Chem. Commun. 2011, **47**, 11044-11046.

3.1 Introduction

Oxygen atom transfer reactions are vital processes in biosystems and take part in biodegradation, biosynthesis and bioconversion reactions in the body. Many of the enzymes utilize molecular oxygen on an iron center and, for instance, contain the class of cytochrome P450 enzymes (P450s), which is a versatile group of enzymes involved in drug metabolism, hormone biosynthesis and detoxification processes.[1-3] The active species of the P450s is an iron(IV)-oxo heme cation radical (Compound I, Cpd I) and its precursor in the catalytic cycle is the iron(III)-hydroperoxo species (Compound 0, Cpd 0). Cpd I and Cpd 0 have both been characterized with spectroscopic methods and are relatively short-lived.[4-7] Reactivity studies together with supporting computational modeling provided evidence, however, that only Cpd I is an active oxidant of oxygen atom transfer reactions, while Cpd 0 is a sluggish oxidant.[8-10]

In non-heme enzymatic and model systems, iron(III)-hydroperoxo species (Fe^{III}-OOH) have been proposed as a "second electrophilic oxidant" in a variety of oxygenation reactions including alkane hydroxylation and olefin epoxidation reactions. In addition, low-spin iron(III)-hydroperoxo species have been characterized for "activated bleomycin", which is the last detectable intermediate in the reaction cycle of bleomycin and a plausible oxidant responsible for DNA cleavage reaction and the oxygenation of hydrocarbons.

The non-heme iron chemistry of biomimetic systems and enzymes led to the characterization of a number of high-valent iron(IV)-oxo intermediates in electrophilic and nucleophilic oxygenation reactions.[11-15] However, the reactivity patterns of the corresponding non-heme iron(III)-hydroperoxo intermediates are not well understood. The non-heme complexes bearing pentadentate ligands and their corresponding iron(IV)-oxo complexes have been shown to give efficient electrophilic reactivity patterns with substrates including hydrogen atom

abstraction mechanisms.[16-18] The corresponding iron(III)-hydroperoxo intermediates studies by Nam and co-workers were found to be inactive towards the oxidation reactions of thioanisole and cyclohexene.[19] This chapter aims to present a better insights into the reactivity patterns of non-heme iron(III)-hydroperoxo intermediates in electrophilic reaction mechanisms. The results of the investigation in bromide oxidation by $[Fe^{III}(OOH)(N4Py)]^{2+}$ **(1a)** (N4Py = N,N-bis(2-pyridylmethyl)-N-bis(2-pyridyl)-methylamine) and $[Fe^{III}(OOH)(Bn\text{-}Tpen)]^{2+}$ **(2a)** (Bn-Tpen = N-benzyl-N,N′,N′-tris(2-pyridylmethyl)ethane-1,2-diamine) are presented in this chapter. The oxidation rates of the ferric(III)-hydroperoxo intermediates were compared with their respective iron(IV)-oxo complexes viz: $[Fe^{IV}(O)(N4Py)]^{2+}$ **(1b)** and $[Fe^{IV}(O)(Bn\text{-}Tpen)]^{2+}$ **(2b)**.

3.2 Experimental Section

High-valent iron intermediates, iron(III)-hydroperoxo and iron(IV)-oxo intermediates were generated *in-situ* from 1mM solution of the respective iron(II) complexes. The iron(III)-hydroperoxo complexes were generated on addition of 10 equiv.. of H_2O_2 to iron(II) complexes in methanolic solution at 273K. The iron(IV)-oxo complexes were prepared using iodosylbenzene (PhIO) as an oxidant in acetonitrile solution at 298 K. The oxidation reactions of bromide were followed by monitoring the change in absorption spectrum of the intermediates using UV-vis. spectroscopy. The second order rate constants were determined by varying bromide concentration, 10-40 mM for **1a** and **2a** and 100-400 mM for **1b** and **2b**.

3.3 Results and discussions

The iron(II) complexes bearing pentadentate ligands were prepared and characterized as reported earlier.[20-21] The complexes gave ESI-MS peak at *m/z* =

572.03 and 628.13 corresponding to $[Fe^{II}(N4Py)CF_3SO_3]^+$ and $[Fe^{II}(Bn\text{-}Tpen)\ CF_3SO_3]^+$ respectively (Figure 2.1). The low spin iron(III)-hydroperoxo intermediates were prepared in-situ on addition of 10 equiv.. of H_2O_2 at 273 K. These intermediates showed the characteristic LMCT band at 548 nm (ε = 1100 $M^{-1}\,cm^{-1}$) and 535 nm (ε = 1000 $M^{-1}\,cm^{-1}$) for **1a** and **2a** respectively, (Figure 2.5 and Figure 2.6). The ESI-MS spectra gave *m/z* values at 605.13 which is corresponding to $\{[Fe^{III}(OOH)N4Py](OTf)\}^+$ and *m/z* = 661.13 for $\{[Fe^{III}(OOH)Bn\text{-}Tpen](OTf)\}^+$ with an isotope pattern that matches the theoretically expected distribution, (Figure 2.2 and Figure 2.3). The iron(IV)-oxo complexes were prepared by stirring 1.5 equiv.. of PhIO in a CH_3CN solution containing iron(II) complexes at ambient temperature. Iron(IV)-oxo intermediates $[Fe^{IV}(O)N4Py]^{2+}$ **(1b)** and $[Fe^{IV}(O)(Bn\text{-}Tpen)]^{2+}$ **(2b)** yields were confirmed on the basis of visible features with low energy 695 nm and 735 nm respectively (ε = 400 $M^{-1}\ cm^{-1}$), that arises from ligand field transitions characteristic for *S* = 1 iron(IV) complexes (Figure 2.5 and Figure 2.6). The electron spray ionization mass spectra (Figure 2.2 and Figure 2.3) gave a major peak at *m/z* = 587.91 corresponding to $\{[Fe^{IV}(O)N4Py](OTf)\}^+$ and for $[Fe^{IV}(O)(Bn\text{-}Tpen)]^{2+}$ gave a major peak at *m/z* = 644.09 corresponding to $\{[Fe^{IV}(O)Bn\text{-}Tpen](OTf)\}^+$ with an isotope pattern that matches the theoretically expected distribution.

Bromide oxidation reactions were studied upon addition of excess amount of tetrabutylammonium bromide (TBABr) to iron(III)-hydroperoxo and iron(IV)-oxo complexes. The reactions were monitored by the changes in the absoption peak of these intermediates. Addition of 20 equiv.. of TBABr to solution of **1a** at 253 K resulted in a rapid decay (within 300s) of the characteristic 548 nm peak in the UV-vis spectra (Figure 3.1). The dead product of the complex was

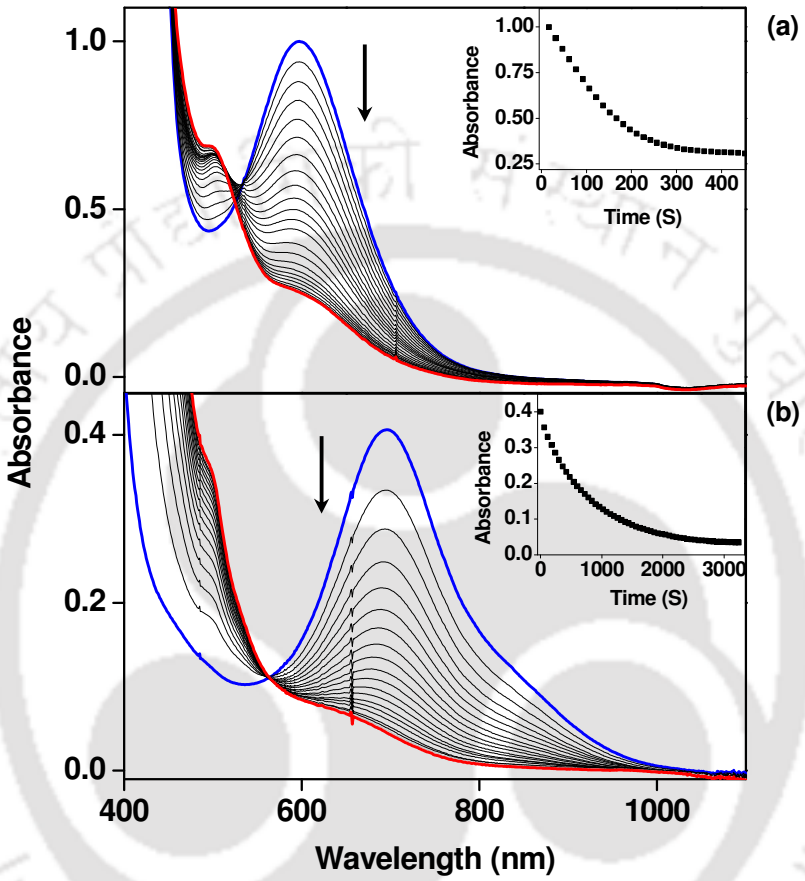

Figure 3.1. **UV-Vis spectral changes of (a) 1a (1 mM) upon addition of 10 equiv. of TBABr at 253 K. Scan interval was 10 s. The inset show the time course of 1a monitored at 548 nm. (b) 1b (1 mM) upon addition of 10 equiv. of TBABr at 298 K. Scan interval was 10 s. The inset displays the time course of 1b monitored at 695 nm.**

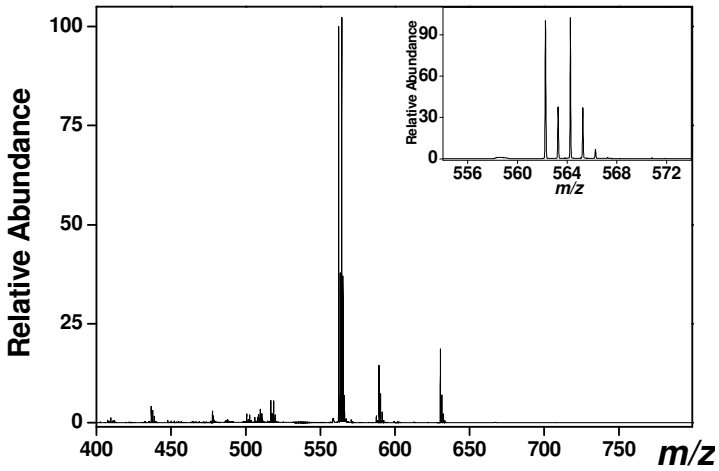

Figure 3.2. **ESI-MS taken after the completion of the reaction of 1b with TBABr in CH_3CN at Room Temperature. A mass peak at *m/z* of 562.27 is assigned to $[Fe^{III}(OH)(N4Py)Br]^+$. Insets show the isotopic distribution in the region of m/z 560–568.**

characterized by ESI-MS which gave a peak at *m/z* = 562.27 corresponding to the formation of $[Fe^{III}(OH)(Br)N4Py]^+$ (Figure 3.2). The second- order rate constant for this reaction was evaluated to be 5.50 x 10^{-1} $M^{-1}s^{-1}$, Table 3.1. The corresponding second-order rate constant for **2a** was evaluated as 2.71 x 10^{-1} $M^{-1}s^{-1}$. This is a very fast reaction and is several orders of magnitude faster than, for instance, the same reaction catalyzed by the corresponding **1b** complexes for which a second order rate constant was evaluated as 6.4 x 10^{-4} M^{-1} s^{-1} using the same experimental conditions (Figure 3.3).Similar trend was also observed when the second order

Table 3.1. Second order rate constants of bromide oxidation by iron(III)-hydroperoxo and iron(IV)-oxo Complexes

Temperature	k_2 (M^{-1} s^{-1})			
	1a	**2a**	**1b**	**2b**
253 K	5.50×10^{-1}	2.71×10^{-1}	6.41×10^{-4}	1.00×10^{-2}
298 K	n.d*	n.d*	1.20×10^{-1}	5.60×10^{-1}

*Not determined

rates were compared for **2b** (k_2=1.00 x 10^{-2} M^{-1} s^{-1}). This implies that the iron(III)-hydroperoxo complex reacts with bromide with rate constants that are about one to three orders of magnitude higher than those found for the iron(IV)-oxo complex.

To highlight the difference in reactivity between **1a** and **1b** with bromide ion, the plot of rate constants of bromide oxidation at different concentrations were shown in Figure 3.3. Here the interesting point should be noted that the order of reactivity for the iron(IV)-oxo complexes was **2b** > **1b**, which is consistent with previous reactivity studies of these oxidants.[16-18] By contrast, the reverse ordering was observed for the iron(III)-hydroperoxo complexes, viz: **1a** > **2a**.

In order to understand the apparent disparity between the reactivity of **1a / 2a** on the one hand versus that of **1b / 2b** on the other hand, as compared to what is known for heme-enzymes and biomimetic analogues, phenol red (phenol sulphonephtalein) colorimetric assays were carried out.[22] Phenol red is commonly used as standard colorimetric assay for haloperoxidase activity. During the course of this reaction, catalysts converts phenol red to bromophenol blue (3,3',5,5'-tetrabromophenol sulphonephthalein) in presence of bromide and hydrogen peroxide.[23] This reaction provides a convenient assay for the detection of

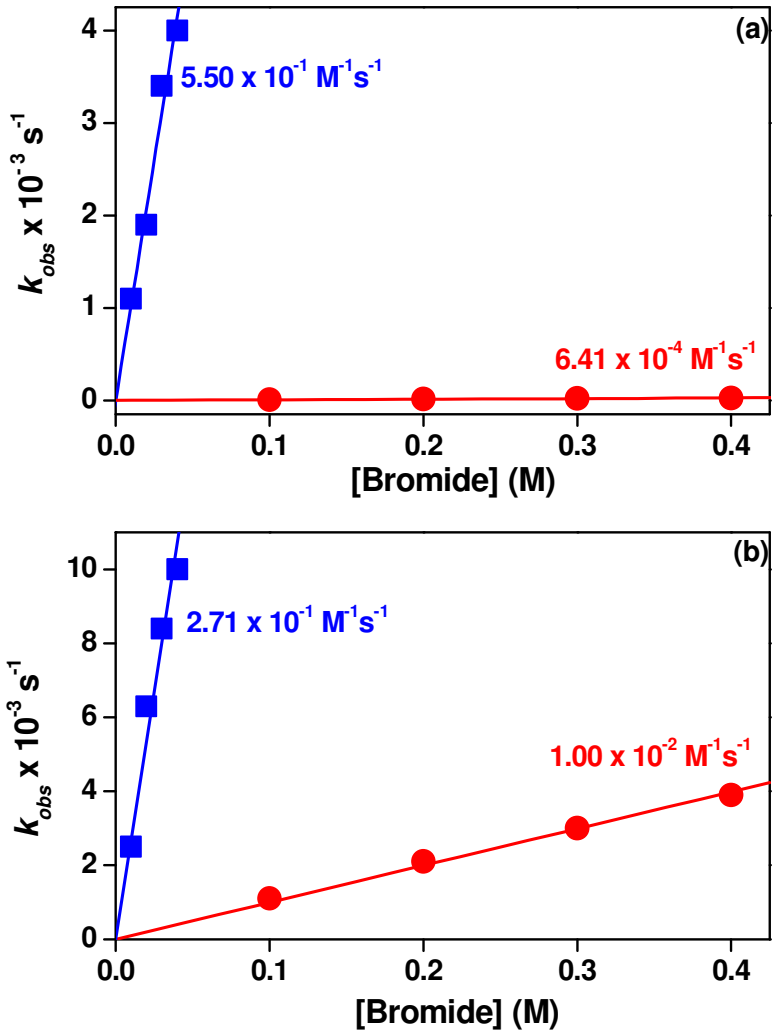

Figure 3.3. **(a) Comparison of second order rate constants as determined in the reactions of 1a (■, Square), and 1b (●, Circle) with TBABr at 253 K. (b) Comparison of second order rate constants as determined in the reactions of 2a(■, Square) and 2b (●, Circle) with TBABr at 253 K.**

bromoperoxidase activity, since the optical absorptions of these two compounds are clearly distinct from each other.[24] However, in the presence of HOBr, Br_2 or Br_3^-, phenol red is easily tetra-brominated to form bromophenol blue. The addition of H_2O_2 to solution containing $[Fe^{II}(N4Py)]^{2+}$ (or $[Fe^{II}(Bn\text{-}Tpen)]^{2+}$) and phenol-red in the presence of excess TBABr resulted in a bathochromic shift in the UV-vis. spectra from 441 nm (ε = 16000 M^{-1} cm^{-1}) (orange-red) to 590 nm (ε = 22000 M^{-1} cm^{-1}) (blue), indicative of the conversion from phenol red to bromophenol blue, scheme.3.1 and Figure 3.4.

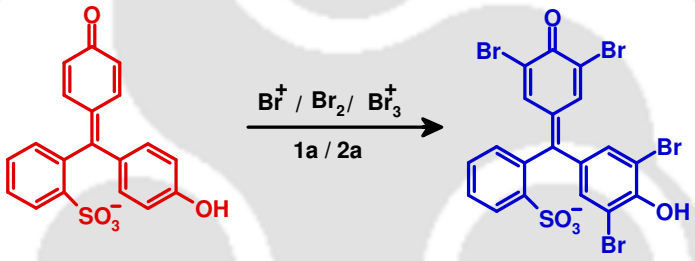

Scheme 3.1. Conversion of Phenol red to Bromophenol blue in the presence of catalysts

Similar results were obtained under inert conditions and thus ruling out over oxidation reaction by dioxygen. The yield of bromophenol blue was estimated as ~ 80% based on the molar absorption coefficient of bromophenol blue and showed a time-dependent absorbance change, arising from the formation of bromophenol blue (inset, Figureure. 3.4). As can be seen from the inset Figureure.3.4, the bromophenol blue initially produced slowly (long lag phase) due to the absence of BrO^-, but after the concentration of BrO^- increases, so does the amount of bromophenol blue. However, when a steady-state concentration of BrO^- is reached, the formation rate of bromophenol blue is equal to the rate of

bromide oxidation by **1a**. The duration of the initial lag decreased with the increasing concentration of the catalyst. The systematic variation of the catalyst concentration and the measurements of the initial rate of bromophenol blue formation were found to be of first-order (Figure. 3.5), which is in agreement with the results given above. The uncatalyzed bromide oxidation by H_2O_2 in the absence of a catalyst was reported to be in the order of 10^{-7} M^{-1} s^{-1}.[25]

These results highlight the fact that iron(III)-hydroperoxo complexes are a better oxidant and their iron(IV)-oxo counterparts and that catalytic bromination

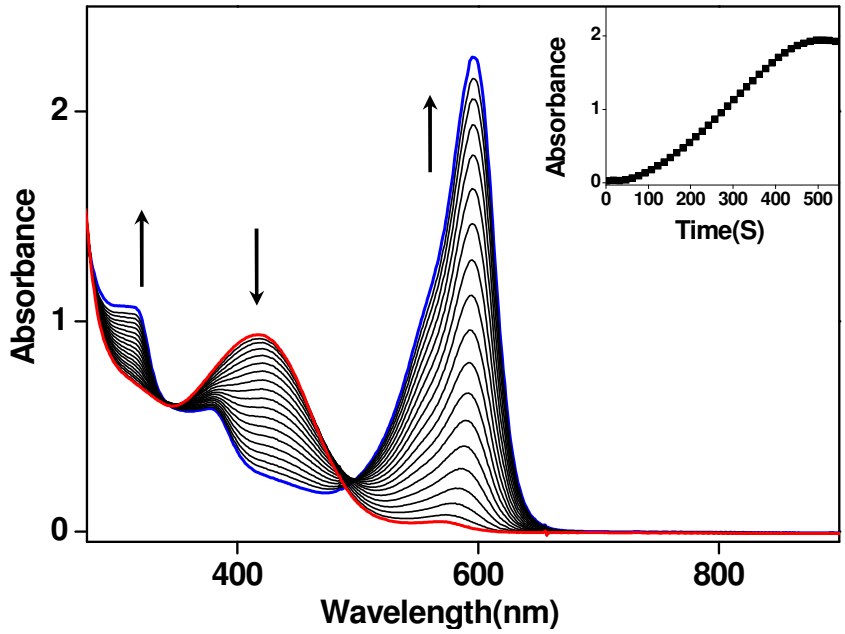

Figure 3.4. **Catalytic conversion of phenol red (62.5 μM) to bromophenol blue in the presence of $[Fe^{II}(N4Py)]^{2+}$ (0.1 mM) and TBABr (80 mM) upon addition of H_2O_2 (10 mM). The inset shows the time course of formation of bromophenol blue monitored at 590 nm.**

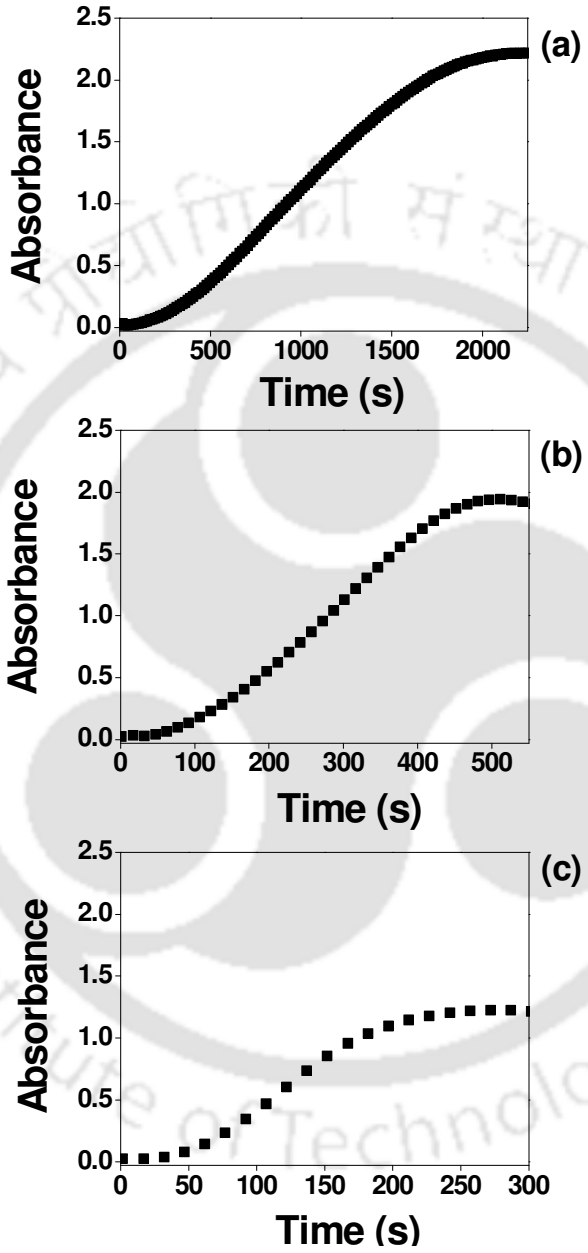

Figure 3.5. **Time course for the of bromophenol blue in the presence of (a) 0.05 mM, (b) 0.10 mM and (c) 0.15 mM of $[Fe^{II}(N4Py)]^{2+}$, TBABr (80 mM), phenol red (62.5 μM) upon addition of H_2O_2(10 mM) at Room Temperature.**

of phenol red were not observed with the latter. The density functional calculation of both iron(III)-hydroperoxo and iron(IV)-oxo complexes carried out in collaboration have also supported the experimental observation.[26] The origin of the high reactivity of non-heme iron(III)-hydroperoxo complexes were traced to the orbital occupation. Further, oxidative potential of the iron(III)-hydroperoxo species, (BDE_{O-H}) were assessed using the reaction equ 3.1. The calculated BDE_{O-H} values from **1a** were found to be 91.1 kcal mol^{-1}, while that from **2a** to be 85.6 kcal mol^{-1}. The larger BDE_{O-H} values correspond to faster rates.

$$[Fe^{III}(OOH)N4Py]^{2+} + H^{\bullet} \longrightarrow [Fe^{IV}(O)N4Py]^{2+} + H_2O \text{ -------- (equ 3.1)}$$

3.4 Conclusion

In conclusion, this chapter presents bromide oxidation by high-valent non-heme iron intermediates. The results demonstrate that iron(III)-hydroperoxo species were more reactive towards bromide oxidation than their corresponding iron(IV)-oxo intermediates. The order of reactivity for iron(III)-hydroperoxo complexes were **1a** > **2a**, whereas the trends observed in iron(IV)-oxo intermediates were **2b** > **1b**. These reactivity variation trends were assessed on the basis of BDE_{OH} reaction energies of isolated intermediates using DFT calculations. The chapter provides the first experimental evidence that non-heme iron(III)-hydroperoxo species are potential oxidants for electrophilic reactions. The results also demonstrate that non-heme iron(III)-hydroperoxo complexes were fundamentally different from heme iron(III)-hydroperoxo species.[26] Subsequent to our report, Nam and co-workers have also demostrated the electrophilic oxidation of thioanisole by a non-heme iron(III)-hydroperoxo complexes bearing tetramethyl cyclam ligand.[27,28]

3.5 References

1. M. Sono, M. P. Roach, E. D. Coulter, J. H. Dawson, *Chem.Rev.,* 1996, **96**, 2841-2888.
2. J. T. Groves, *Proc. Natl. Acad. Sci. U. S. A.,* 2003, **100**, 3569-3579.
3. *Cytochrome P450*: *Structure, Mechanism and Biochemistry,* ed. P. R. Ortiz de Montellano, 3rd edn, Kluwer Academic/Plenum Publ., New York, 2005.
4. R. Davydov, T. M. Makris, V. Kofman, D. E. Werst,S. G. Sligar, B. M. Hoffman, *J. Am. Chem. Soc.,* 2001,**123**, 1403-1415.
5. P. J. Mak, I. G. Denisov, D. Victoria,T. M. Makris, T. Deng, S. G. Sligar, J. R. Kincaid, *J. Am. Chem. Soc.,* 2007, **129**, 6382-6283.
6. J.-G. Liu, T. Ohta, S. Yamaguchi,T. Ogura, S. Sakamoto, Y. Maeda, Y. Naruta, *Angew. Chem., Int. Ed.,* 2009, **48**, 9262-9267.
7. J. Rittle, M. T. Green, *Science,* 2010, **330**, 933-937.
8. F. Ogliaro, S. P. de Visser, S. Cohen, P. K. Sharma, S. Shaik, *J. Am. Chem. Soc.,* 2002, **124**, 2806-2817.
9. S. Shaik, H. Hirao, D. Kumar, *Nat. Prod. Rep.,* 2007, **24**, 533-552.
10. S. P. de Visser, J. S. Valentine, W. Nam, *Angew. Chem., Int. Ed.,* 2010, **49**, 2099-2101.
11. M. Costas, M. P. Mehn, M. P. Jensen, L. Que Jr, *Chem.Rev.,* 2004, **104**, 939-986.
12. M. M. Abu-Omar, A. Loaiza, N. Hontzeas, *Chem. Rev.,* 2005, **105**, 2227-2252.
13. P. C. A. Bruijnincx, G. van Koten, R. J. M. Klein Gebbink, *Chem.Soc. Rev.,* 2008, **37**, 2716-2744.
14. L. Que Jr, *Acc. Chem. Res.,* 2007, **40**, 493-500.
15. W. Nam, *Acc. Chem. Res.,* 2007, **40**, 522-531.

16. J. Kaizer, E. J. Klinker, N. Y. Oh, J.-U. Rohde, W. J. Song,A. Stubna, J. Kim, E. Mu¨nck, W. Nam, L. Que Jr, *J. Am.Chem. Soc.,* 2004, **126**, 472-473.
17. D. Kumar, H. Hirao, L. Que Jr., S. Shaik, *J. Am. Chem. Soc.,* 2005, **127**, 8026-8027.
18. C. V. Sastri, K. Oh, Y. J. Lee, M. S. Seo, W. Shin, W. Nam, *Angew. Chem., Int. Ed.,* 2006, **45**, 3992-3995.
19. M. J. Park, J. Lee, Y. Suh, J. Kim, W. Nam, *J. Am. Chem. Soc.,*2006, **128**, 2630-2634.
20. M. Lubben, A. Meetsma, E. C. Wilkinson, B. Feringa, L. Que, Jr., *Angew. Chem. Int. Ed. Engl.*, 1995, **34**, 1512-1514.
21. L. Duelund, R. Hazell, C. J. McKenzie, L. P. Nielsen, H. Toftlund*, J. Chem. Soc., Dalton Trans.,* 2001, 152-156.
22. D. Lahaye, J. T. Groves, *J. Inorg. Biochem.,* 2007, **101**, 1786-1797.
23. E. de Boer, H. Plat, M. G. M. Tromp, R. Wever, M. C. R. Franssen, H. C. van der Plas, E. M. Meijer, H. E. Schoemaker, *Biotechnol. Bioeng.,* 1987, **30**, 607-610.
24. Phenol red is commonly used as a standard assay for haloperoxidase activity, see e.g. J. V. Walker, M. Morey, H. Carlssom, A. Davidson,G. D. Stucky, A. Butler, *J. Am. Chem. Soc.,* 1997, **119**, 6921-6922.
25. M. S. Reynolds, S. J. Morandi, J. W. Raebiger, S. P. Melican, E. Smith, *Inorg. Chem.,* 1994, **33**, 4977-4984.
26. A. K. Vardhaman, P. Barman, S. Kumar, C. V. Sastri, D. Kumar, S. P. de visser. *Chem. Commun.,* 2013, **49**, 10926-10928.
27. J. Cho, S. Jeon, S. A.Wilson, L. V. Liu, E. A. Kang, J. J. Braymer, M. H. Lim, B. Hedman,K. O. Hodgson, J. S. Valentine, E, I. Solomon, W. Nam, *Nature*, 2011, **478**, 502-505.

28. Y. M. Kim, K. –B. Cho, B. Wang, C. Li, S. Shaik, W. Nam. *J. Am. Chem. Soc.,* 2013, **135**, 8838–8841.

CHAPTER-IV

Mechanistic Insight into Halide Oxidation by Non-Heme Iron Complexes. Haloperoxidase versus Halogenase Activity

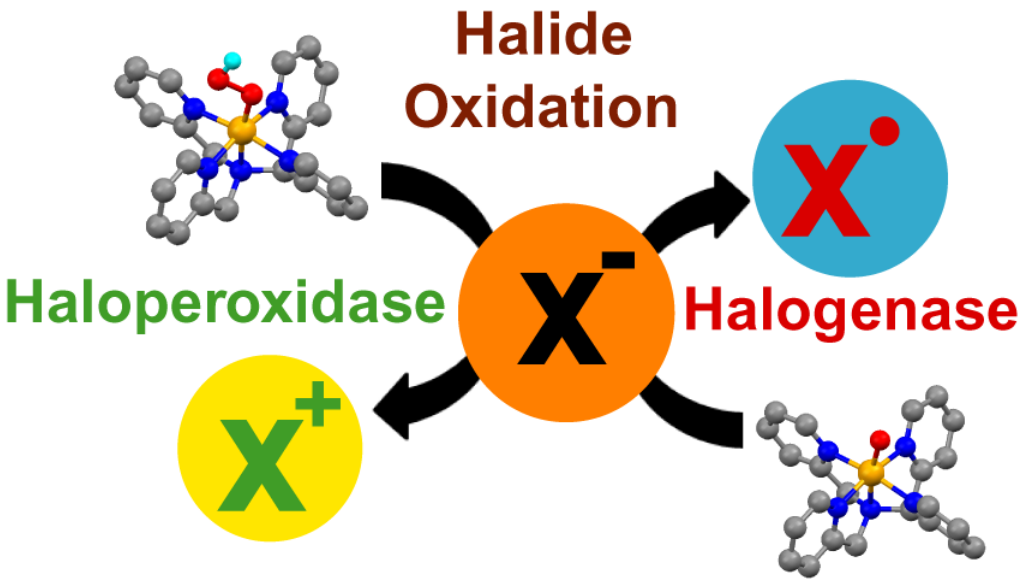

Chem. Commun., 2013, **49**, 10926-10928.

4.1 Introduction

Halogens are an abundant component of the Earth`s bio-sphere, so it is of little surprise that nature produces a profuse number of organo halogens.[1] Nature has developed an exquisite array of methods to introduce halogen atoms into organic compounds.[2] In nature, halogenation is strategy used to increase the biological activity of secondary metabolites, compounds that are often effective as drugs. However halides are not particularly reactive unless they are activated, typically by oxidation.[3]

Iron catalyzed biological halogenation occurs with heme haloperoxidases and the recently discovered and characterized α-ketoglutarate dependent non heme halogenases (α-ketoglutarate).[4-7] Haloperoxidases are a class of enzymes that catalyse the oxidation of halide ions with subsequent halogenation of organic substrates as shown in below equation. These processes, which play a major role in global organohalogen production, are thought to be important components of the chemical defense of organisms that produce them. In addition, these halogenated natural products are of pharmacologiacal interst due to their antifungal, antibacterial, antineoplastiic, antiviral and anti-inflammatory activities. For the catalysis of halogenation reactions, haloperoxidases require hydrogen peroxide (H_2O_2) and halide ions (Cl^-, Br^- and I^- but not F^-).

$$RH + X^- + H^+ + H_2O_2 \xrightarrow{\text{Haloperoxidase}} RX + 2H_2O \qquad \text{----- (equn. 4.1)}$$

(RH = substrate, X = Cl^-, Br^- and I^- but not F^-)

The formation of a carbon-halogen bond is rare in biology, but surprisingly a large variety of natural product biosynthesis reactions involve the halogenation of aromatic and aliphatic carbon centres, for instance, in the biosynthesis of several antibiotics.[8,9] Halogenating enzymes are divided into H_2O_2 required haloperoxidases (heme systems) and oxygen dependent halogenases (non-heme systems).[10-13] The first halogenating enzyme to be discovered was chloroperoxidase from *Caldariomyces fumago*, which produces the chlorinated product caldariomycin.[14] Since then other heme containing haloperoxidases have been discovered that utilize chloride, bromide and iodide ions and catalyse the formation of a carbon-halogen bond in substrates.[15-17] While haloperoxidases catalyse electrophilic halogenation (X^+) reactions, the non-heme iron halogenases, by contrast, generally react via a radical process ($X^\bullet$).

The catalytic halogenation of organic substrates by biomimetic models were reported for a number of complexes that are likely to form a high-valent metal-oxo intermediate.[18-22] In non-heme iron chemistry, although several catalytic halogenation reactions were reported, no detailed mechanistic pathway has been proposed yet.[23-26] However, the reactivity of non-heme iron(III)-hydroperoxo intermediates as effective electrophilic oxidants in substrate halogenation has been reported, and it was found that iron(III)-hydroperoxo under certain conditions is more catalytically active than iron(IV)-oxo.[27,28] To gain insight into the mechanistic pathways by non-heme iron(III)-hydroperoxo intermediates in electrophilic reactions, this chapter explores the halide oxidation reactions (X^- = F^-, Cl^-, Br^- and I^-) by $[Fe^{III}(OOH)(N4Py)]^{2+}$ (**1a**) and $[Fe^{III}(OOH)(Bn\text{-}Tpen)]^{2+}$ (**2a**) and compare the kinetics with the corresponding iron(IV)-oxo complexes, viz: $[Fe^{IV}(O)(N4Py)]^{2+}$ (**1b**) and $[Fe^{IV}(O)(Bn\text{-}Tpen)]^{2+}$ (**2b**) [N4Py = N,N-bis(2-pyridylmethyl)-N-bis(2-pyridyl)-methylamine, Bn-Tpen = N-benzyl-N,N′,N′-tris(2-pyridylmethyl)ethane-1,2-diamine].

4.2 Experimental Section

High-valent iron intermediates, iron(III)-hydroperoxo and iron(IV)-oxo intermediates were generated *in-situ* from 1mM solution of the respective iron(II) complexes. The iron(III)-hydroperoxo complexes were generated on addition of 10 equiv. of H_2O_2 to iron(II) complexes in methanolic solution at 273K. The iron(IV)-oxo complexes were prepared using iodosylbenzene (PhIO) as an oxidant in acetonitrile solution at 298K. The oxidation reactions of halides were followed by monitoring the change in absorption spectrum of the intermediates using UV-vis. spectroscopy. The second order rate constants were determined by varying the concentration of halides

4.3 Results and discussions

The iron(II) complexes bearing pentadentate ligands were prepared and characterized as reported earlier.[29,30] The complexes gave ESI-MS peak at *m/z* = 572.03 and 628.13 corresponding to $[Fe^{II}(N4Py)CF_3SO_3]^+$ and $[Fe^{II}(Bn\text{-}Tpen)\ CF_3SO_3]^+$ respectively (Figure 2.1). The low spin iron(III) hydroperoxo intermediates were prepared in-situ on addition of 10 equiv. of H_2O_2 at 273 K. These intermediates showed the characteristic LMCT band at 548 nm (ε = 1100 $M^{-1}cm^{-1}$) and 535 nm (ε =1000 $M^{-1}cm^{-1}$) for **1a** and **2a** respectively, (Figure 2.5 and Figure 2.6). The ESI-MS spectra gave *m/z* values at 605.13 which corresponds to $\{[Fe^{III}(OOH)N4Py](OTf)\}^+$ and *m/z* = 661.13 for $\{[Fe^{III}(OOH)Bn\text{-}Tpen](OTf)\}^+$ with an isotope pattern that matches the theoretically expected distribution, (Figure 2.2 and Figure 2.3). The iron(IV)-oxo complexes were prepared by stirring 1.5 equiv. of PhIO in a CH_3CN solution containing iron(II) complexes at ambient temperature. The iron(IV)-oxo

intermediates $[Fe^{IV}(O)N4Py]^{2+}$ **(1b)** and $[Fe^{IV}(O)(Bn\text{-}Tpen)]^{2+}$ **(2b)** were confirmed on the basis of visible features with low energy 695 nm and 735 nm respectively (ε = 400 M^{-1} cm^{-1}), that arises from ligand field transitions characteristic for S = 1 iron(IV) complexes (Figure 2.5 and Figure 2.6). The electron spray ionization mass spectra (Figure 2.2 and Figure 2.3) gave a major peak at *m/z* = 587.91 corresponding to $\{[Fe^{IV}(O)N4Py](OTf)\}^{+}$ and for $[Fe^{IV}(O)(Bn\text{-}Tpen)]^{2+}$ gave a major peak at *m/z* = 644.09 corresponding to $\{[Fe^{IV}(O)Bn\text{-}Tpen](OTf)\}^{+}$ with an isotope pattern that matches the theoretically expected distribution.

Addition of tetrabutylammonium halides (TBAX; X = Cl^-, Br^-, I^-) to added to **1a** at 253 K led to decay of the characteristic 548 nm peak in the UV-vis spectra. The second order rate constants extracted from these experiments (Figure. 4.1, Table 4.1) showed a difference of as large as a factor of 6, and the reactivity decreased in the order of $I^- > Br^- > Cl^-$. Surprisingly, the observed trend does not correlate with the electron affinities of these halides. Moreover, when TBA-F was added to **1a** no oxidation reaction of F^- was observed, which may be due to the fact that H_2O_2 lacks the thermodynamic potential to oxidize fluoride.[31,32]

In order to compare the reactivities of the iron(III)-hydroperoxo with iron(IV)-oxo in halide oxidation, generated **1b** and **2b** in CH_3CN using a procedure as reported previously.[31,33] Addition of halides to **1b** under the same conditions as **1a** enabled us to evaluate the second order rate constants: **1b** reacted with halides (Cl^-, Br^-) with much lower rate constants than **1a**, *however, a reversal of the trend was observed in the presence of* I^-. In fact, for iodide oxidation, **1b** was found to react about six times faster than **1a**. This reversal in

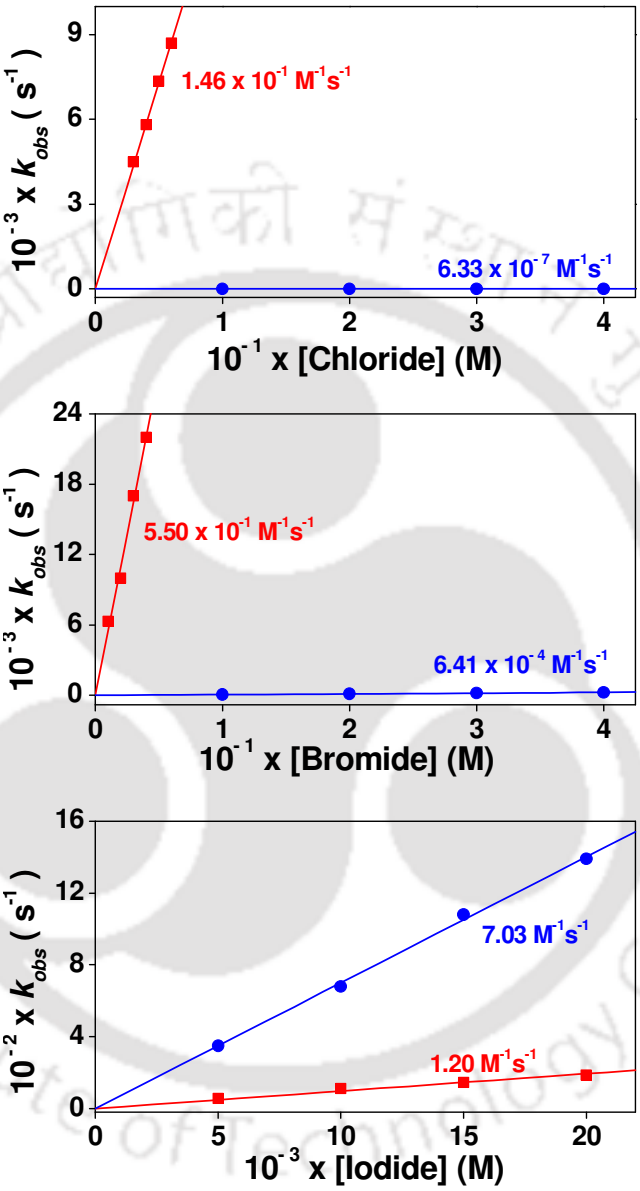

Figure 4.1. **Comparison of the second order rate constants for halide oxidation by 1a (■, Square) and 1b (●, Circle) in the presence of (a) TBACl, (b) TBABr and (c) TBAI at 253K.**

Table 4.1. Second order rate constants for the oxidation of halides

X^-	k_2 ($M^{-1} s^{-1}$)			
	1a	**1b**	**2b**	**2b**
Cl^-	1.46×10^{-1}	6.33×10^{-7}	4.00×10^{-2}	6.00×10^{-5}
Br^-	5.50×10^{-1}	6.41×10^{-4}	2.70×10^{-1}	1.00×10^{-2}
I^-	1.20	7.03	8.01×10^{-1}	19.01

trend may be attributed to the steric factor influenced by the bulky I^- group upon approach of **1a**. Additionally, the reactivity of **1b** was found to be sensitive to the one electron oxidation potential of halides thus demonstrating that the reactivity of non-heme iron(IV)-oxo complexes can be significantly affected by the identity of substrates. The difference in the reactivity between **1a** and **1b** was in the order of ~10^3 in the oxidation reaction of Br^- and increased to ~10^5 for Cl^-. A similar trend was observed when the halide oxidation reactions of **2a** and **2b** were compared (Figure 4.2).

To quantify the difference in the oxidation pathway for iron(III)-hydroperoxo and iron(IV)-oxo intermediates, a plot of the second order rate constants {log(k_2)} against the one electron oxidation potential (E^0_{ox}) of these halides were constructed. A linear correlation was observed with a slope of –0.88 and –6.62 for **1a** and **1b** respectively, Figure 4.3. Similar slopes were obtained for **2a** (–1.23) and **2b** (–5.16), (Figure 4.4). Such large negative values of slopes from a plot of log(k_2) versus one electron oxidation potential implicates a rate determining electron transfer step in the reaction from halides to oxidant, i.e. **1b** (and **2b**), rather than a group transfer.[34] The ease of a plausible electron transfer from I^- to iron(IV)-oxo can now account for the higher oxidation rates observed.

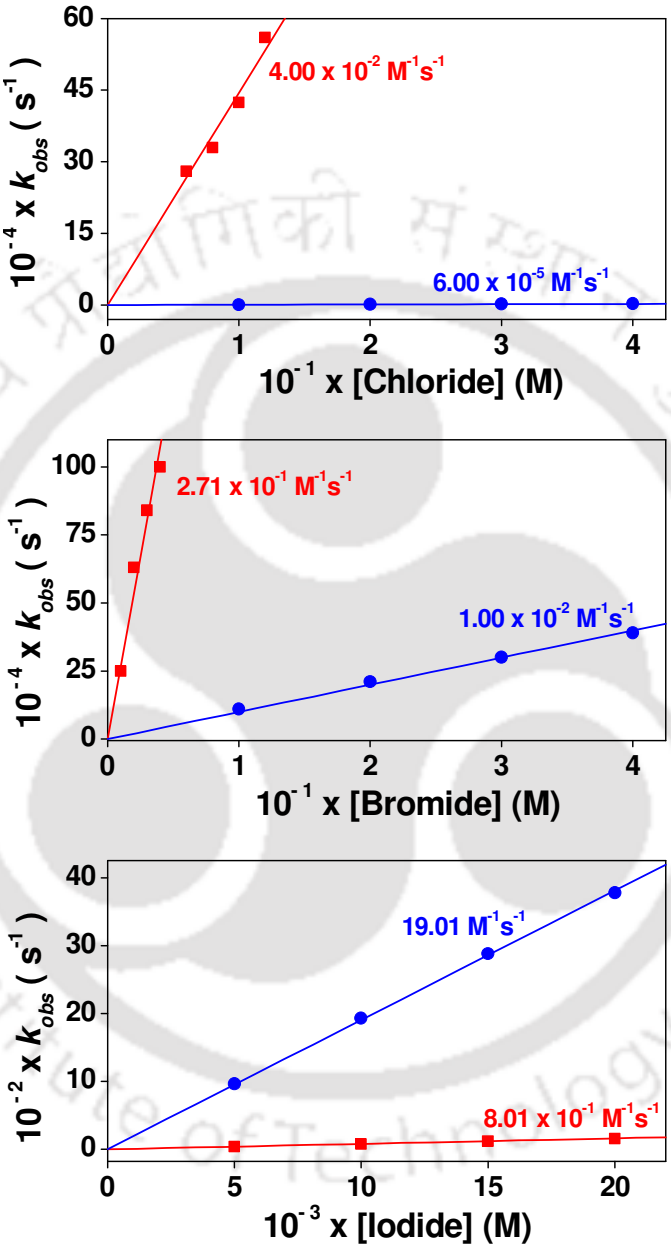

Figure 4.2. **Comparision of second order rate constants for halide oxidation by 2a (■, Square) and 2b (●, Circle) in the presence of (a) TBACl, (b) TBABr and (c) TBAI at 253K.**

Table 4.2. Second order rate constants determined reactions of (1 mM solution) in the presence of halides at 253 K

Halides	E^0_{ox} vs. SCE (V)	Intermediates							
		1a		1b		2a		2b	
		k_2 ($M^{-1}s^{-1}$)	log(k_2)	k_2 ($M^{-1}s^{-1}$)	log(k_2)	k_2 ($M^{-1}s^{-1}$)	log(k_2)	k_2 ($M^{-1}s^{-1}$)	log(k_2)
I^-	0.61	1.20	0.08	7.03	0.84	8.01×10^{-1}	-0.09	19.01	1.28
Br^-	1.11	5.50×10^{-1}	-0.26	6.41×10^{-4}	-3.19	2.71×10^{-1}	-0.57	1.00×10^{-2}	-2.00
Cl^-	1.67	1.46×10^{-1}	-0.85	6.33×10^{-7}	-6.20	4.00×10^{-2}	-1.40	6.00×10^{-5}	-4.22

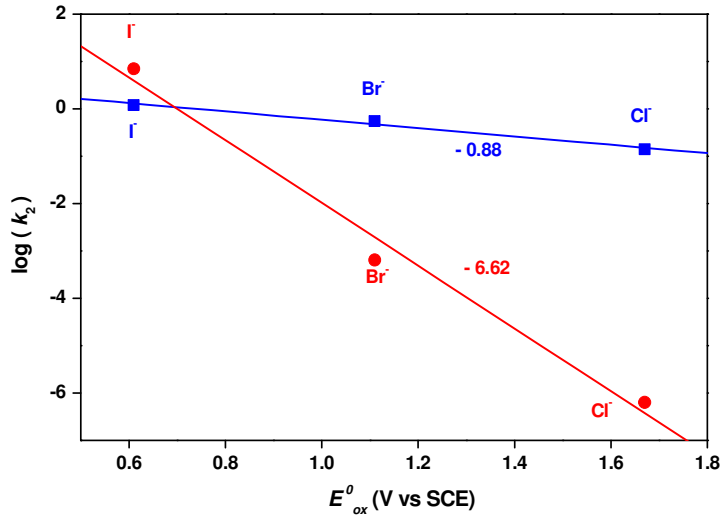

Figure 4.3. Plot of log(k_2) against the one-electron oxidation potentials (E^0_{ox}) of halides of 1a (■, Square) and 1b (●, Circle) at 253 K.

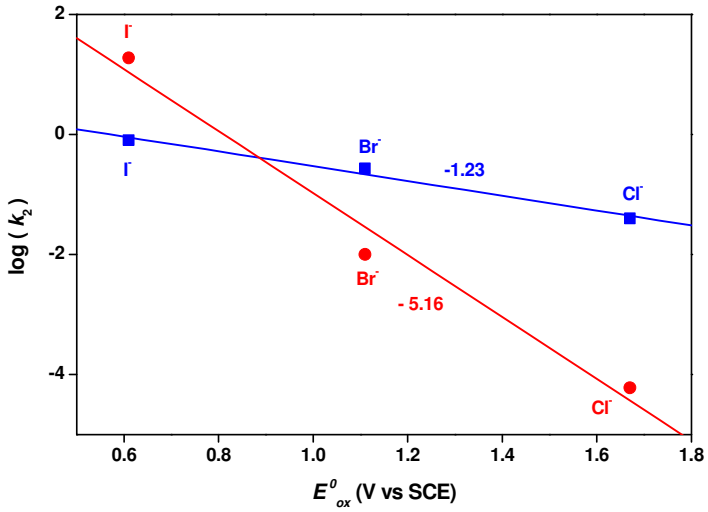

Figure 4.4. Plot of log(k_2) against the one-electron oxidation potentials (E^0_{ox}) of halides against the rate constant of halide oxidation by 2a (■, Square) and 2b (●, Circle) at 253 K.

The difference in reaction mechanism for the oxidation of halides for iron(IV)-oxo as compared to iron(III)-hydroperoxo complexes can be attributed to the interactions of the negatively charged substrate with the electrophilic iron centre.

Further evidence of the mechanistic insights was obtained from the catalytic oxidation of anisole by **1a** and **1b** in the presence of TBACl. These two chlorinating species yield different products with anisole. The oxidation of chloride involves either a one-electron oxidation ($Cl^- \rightarrow Cl^{\bullet} + e^-$) to form chloride radical or an overall two electron oxidation ($Cl^- \rightarrow Cl^+ + 2e^-$) to give the chloronium ion. Chlorination by **1a** gave only monochlorinated product (*para* and *ortho* isomers). In stark contrast, the chlorination reaction of anisole by **1b** gave a mixture of mono- and di-substituted chlorinated products, Scheme. 4.1. The isomer distribution and product ratios indicate that the chlorinating agent in the presence of **1a** is Cl^+. The formation of di-substituted anisole and phenoxymethyl chloride is characteristic of free radical chlorination of anisole in the presence of **1b**.[35]

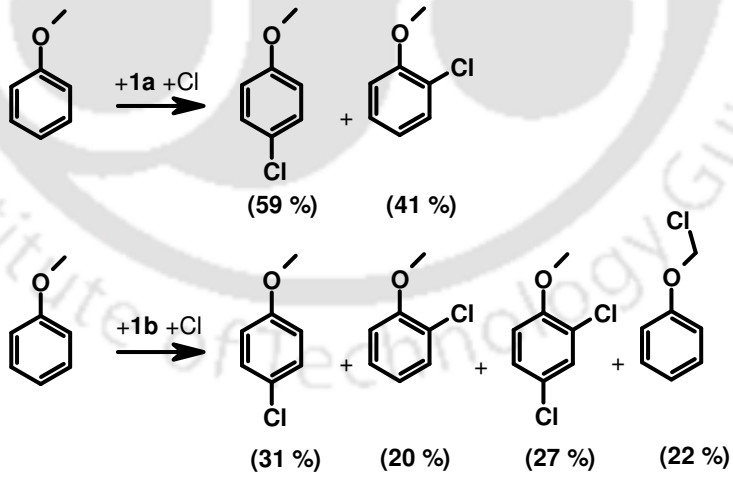

Scheme 4.1. Products observed from the reaction of anisole with 1a and 1b in the presence of TBACl at 298 K.

Further to prove the Myeloperoxidase like activity by non-heme iron(III) hydroperoxo complexes, competitive experiments were performed in the oxidation reaction of 1,2-phenylenediamine (OPD) reactions which is generally used as a standard assay for peroxidase like activity. The OPD undergoes oxidation reactions in the presence of catalyst and H_2O_2 to form the dimeric product 2,3-diaminophenazine (DAP) (Figure 4.5), which is dependent on concentration of catalyst. The competitive oxidation reactions of OPD were carried out in the presence of excess of (~ 100 equiv.) of halides. A significant quenching of OPD oxidation was observed. The extent of quenching was proportional to the pKa of hypohalous acids (HOX) formed during the course of the reaction. When halides were replaced by N_3^-, a complete quenching of the

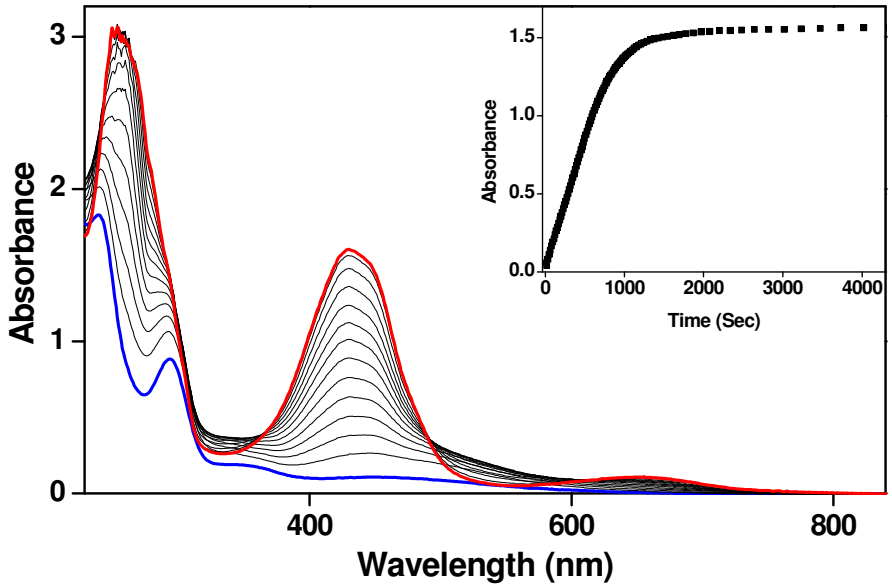

Figure 4.5. UV-vis spectral changes of 1a (1 mM) upon addition of 10 equiv. H_2O_2 OPD at 273 K. Scan intervals were 10 s. The inset shows the time course of DAP monitored at 420 nm.

DAP formation was observed. It is known that N_3^- is a classical inhibitor for Myeloperoxidase.

The density functional theory (DFT) calculation of halide oxidation with both iron(III)-hydroperoxo and iron(IV)-oxo complexes carried out in collaboration have also supported the experimental observation.[36] The DFT calculations also substantiate the experimental evidence of electron transfer processes in electrophilic reaction mechanisms which are dependent on the nature of the oxidant. The electron affinity differences of **1a** versus **1b** were believed to determine the electrophilic reaction rates with halides. The calculated electron affinities for **1a** and **1b** of $\Delta E+ZPE+E_{solv}$ were 102.6 and 108.7 kcal mol^{-1}, respectively. Thus, the larger electron affinity of the iron(IV)-oxo as compared to the iron(III)-hydroperoxo species will enable a much quicker and efficient electron transfer by the iron(IV)-oxo complexes. These computational results are also in perfect agreement with the plot in Figure 4.1 that shows a correlation of the reaction rate with the electron oxidation potential.

4.4 Conclusion

In conclusion, this chapter presents a comparative study of the reactivity of non-heme iron(III)-hydroperoxo versus iron(IV)-oxo in halide oxidation reactions. A detailed analysis of the plausible difference in the reaction pathway of iron(III)-hydroperoxo complexes in comparison with iron(IV)-oxo complexes were presented. The results demonstrate a difference in the reaction pathway for the two reactions, whereby iron(IV)-oxo reacts via a one-electron transfer and iron(III)-hydroperoxo by group transfer.

4.5 References

1. G. W. Gribble, *J. Am. Chem. Soc*., 2004, **92**, 342-349.
2. J. M. Winter, B. S. Moore, *J. Biol. Chem.,* 2009, **284**, 18577-18581.
3. A. Butler, M. Sandy, *Nature,* 2009, **460**, 848-854.
4. F. H. Vaillancourt, E. Yeh, D. A. Vosburg, S. Garneau-Tsodikova, C. T. Walsh, *Chem. Rev*., 2006, **106**, 3364-3378.
5. F. H. Vaillancourt, E. Yeh, D. A. Vosburg, S. E. O`Conner, C. T. Walsh, *Nature*, 2005, **436**, 1191-1194.
6. L. C. Blasiak, F. H. Vaillancourt, C. T. Walsh, C. L. Drewman, *Nature*. 2006, **440**, 368- 371.
7. F. H. Vaillancourt, J. Yin, C. T. Walsh, *Proc. Natl. Acad. Sci. U.S.A*. 2005, **102**, 10111-10116.
8. G. W. Gribble, *J. Chem. Educ*., 2004, **81**, 1441-1449.
9. A. Butler, M. Sandy, *Nature*, 2009,**460**, 848-854.
10. F. H. Vaillancourt, E. Yeh, D. A. Vosburg, S. Garneau-Tsodikova, C. T. Walsh, *Chem. Rev*., 2006, **106**, 3364-3378.
11. K. H. Van Peé, C. Dong, S. Flecks, J. Naismith, E. P. Patallo, T. Wage, *Adv. Appl. Microbiol*., 2006, **59**, 127-157.
12. J. L. Anderson, S. K. Chapman, *Mol. Biosyst*., 2006, **2**, 350-357.
13. D. G. Fujimori, C. T. Walsh, *Curr. Opin. Chem. Biol*. 2007, **11**, 553-560.
14. L. P. Hager, D. R. Morris, F. S. Brown, H. Eberwein, *J. Biol. Chem*., 1966, **241**, 1769-1777.
15. J. A. Manthey, L. P. Hager, *Biochemistry*, 1989, **28**, 3052-3057.
16. J. A. Manthey, L. P. Hager, *J. Biol. Chem*., 1985, 260, **260**, 9654-9659.
17. M. P. Roach, Y. P. Chen, S. A. Woodin, D. E. Lincoln, C. R. Lovell, J. H. Dawson, *Biochemistry*, 1997, **36**, 2197-2202.
18. P. Comba, S. Wunderlich, *Chem. Eur. J.* 2010, **16**, 7293-7299.

19. W. Liu, J. T. Groves, *J. Am. Chem. Soc*., 2010, **132**, 12847-12849.
20. W. Liu, X. Huang, M.-J. Cheng, R. J. Nielsen,W. A. Goddard III, J. T. Groves, *Science,* 2012, **337**, 1322-1325.
21. A. Bakac, C. Shi, O. Pestovsky, *Inorg. Chem.* 2004, **43**, 5416-5421.
22. P. Galloni, M. Mancini, B. Floris, V. Conte, *Dalton Trans.,* 2013, **42**, 11963-11970.
23. G. K. Cook, J. M. Mayer, *J. Am. Chem. Soc*., 1994, **116**, 1855-1868.
24. J. M. Mayer, *Acc. Chem. Res*., 1998, **31**, 441-450.
25. T. Kojima, R. A. Leising, S. Yan, L. Que, Jr., *J. Am. Chem. Soc*., 1993, **115**, 11328-11335
26. A. Podgoršek, M. Zupan, J. Iskra, *Angew. Chem. Int. Ed*., 2009, **48**, 8424-8450.
27. A. K. Vardhaman, C. V. Sastri, D. Kumar, S. P. de Visser, *Chem. Commun*., 2011, **47**, 11044-11046.
28. J. Cho, S. Jeon, S. A.Wilson, L. V. Liu, E. A. Kang, J. J. Braymer, M. H. Lim, B. Hedman, K. O. Hodgson, J. S. Valentine, E. I. Solomon, W. Nam, *Nature*, 2011, **478**, 502-505.
29. M. Lubben, A. Meetsma, E. C. Wilkinson, B. Feringa, L. Que, Jr., *Angew. Chem. Int. Ed. Engl.,*1995, ***34***, 1512–1515.
30. L. Duelund, R. Hazell, C. J. McKenzie, L. P. Nielsen, H. J. Toftlund, *J. Chem. Soc. Dalton Trans.,* 2001, 152-156.
31. O. Nashiru , D. L. Zechel, D. Stoll ,T. Mohammadzadeh, R. A. J. Warren, S. G. Withers, *Angew. Chem. Int. Ed*., 2001, **40**, 417-420.
32. D. L. Zechel, S. P. Reid, O. Nashiru, C. Mayer, D. Stoll, D. L. Jakeman, R. A. J. Warren, S. G. Withers, *J. Am. Chem. Soc*., 2001, **123**, 4350-4351.

33. J. Kaizer, E. J. Klinker, N. Y. Oh, J.-U. Rohde, W. J. Song, A. Stubna, J. Kim, E. Münck, W. Nam, L. Que Jr., *J. Am. Chem. Soc.*, 2004, **126**, 472-473.

34. Y. Goto, T. Matsui, S.-I. Ozaki, Y. Watanabe , S. Fukuzumi, *J. Am. Chem. Soc*., 1999, **121**, 9497-9502.

35. F. S. Brown, L. P. Hager, *J. Am. Chem. Soc*., 1967, **89**, 719-720.

36. A. K. Vardhaman, P. Barman, S. Kumar, C. V. Sastri, D. Kumar, S. P. de visser. *Chem. Commun.,* 2013, **49**, 10926-10928.

CHAPTER-V

Comparison of the Reactivity of Non-Heme Iron(IV)-oxo versus Iron(IV)-imido Complexes

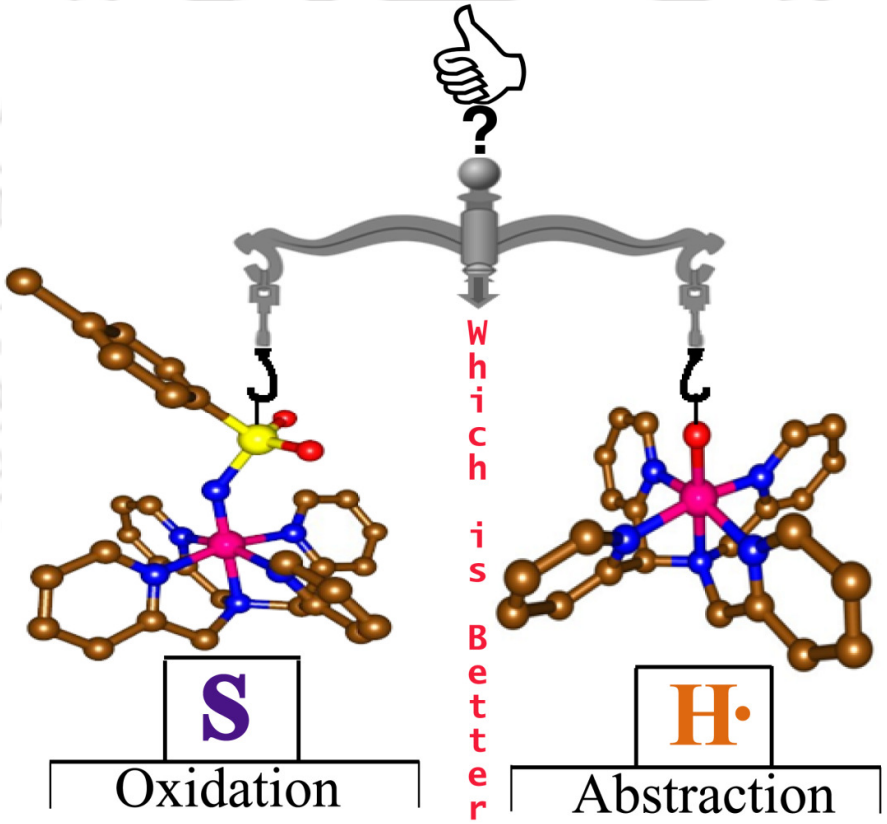

Angew. Chem. Int. Ed., 2013, 52, 12288-12292.

5.1 Introduction

High-valent heme and non-heme iron(IV)-oxo complexes play key roles in biology as catalytic intermediates in enzymes, where they catalyze vital biotransformations for human health including detoxification processes in the liver, as well as the biosynthesis of hormones.[1-11] Mono- and dioxygenases bind and utilize molecular oxygen on an iron center and form a catalytically active iron(IV)-oxo species that transfers the oxygen atom to substrate. Technically, using a nitrogen donor one should be able to synthesize the analogous iron(IV)-imido and/or iron(V)-nitrido complexes. Although these complexes are rare in nature, evidence exists of substrate aziridination by cytochrome P450 enzymes that presumably takes place via a high-valent iron(IV)-nitrido or iron(IV)-imido complex.[12-14] Several iron-porphyrin models with nitrene or imido ligands have been synthesized and their reactivity patterns implicated efficient aziridination of olefins.[15-19]

By contrast to iron(IV)-oxo complexes, which have been extensively studied over the years, only few studies have been reported on its closely related iron(V)-nitrido species ($Fe^{V}\equiv N$) or the iron(IV)-imido ($Fe^{IV}=NR$) species. In principle, these high-valent metal-nitrido/imido complexes should have strong oxidative power and capable to catalyze isolobal amination reactions. During the past decade, the chemistry of metal-catalyzed aziridination of alkenes and aminidation of aliphatic C–H bonds using iminoiodane reagents have been studied by several groups.[20-27] In recent years, the putative metal-nitrogen multiple bonded species have been isolated and spectroscopically characterized, which led to significant progress on the understanding of its fundamental chemical properties.[20-24,28-35] However, details on its potential as nitrogen atom transfer agent are lacking and little knowledge exists in its relative reactivity with respect to the well-known iron(IV)-oxo species.[35]

In non heme iron chemistry, the aromatic amination of ligands by an iron-nitrido complex was reported by several groups,[24,36,37] and recently, the spectroscopic characterization of the iron(IV)-tosylimido (tosylimido^{2-} = NTs) complex with pentadentate N4Py ligand (N4Py = *N*,*N*-bis(2-pyridylmethyl)-*N*-bis(2-pyridyl) methylamine), $[Fe^{IV}(NTs)(N4Py)]^{2+}$, was described.[38] As this species was shown to have a relatively long lifetime, it makes it highly suitable for reactivity studies, especially since the iron(IV)-oxo analogue can be studied in tandem. This chapter discusses in depth the reactivity of $[Fe^{IV}(NTs)(N4Py)]^{2+}$ (**1c**) and $[Fe^{IV}(O)(N4Py)]^{2+}$ (**1b**) towards S-oxidation and C-H activation. Attempts have been made to gain insights to the similarities and differences in the reaction pathway of the two intermediates.

5.2 Experimental Section

High-valent iron intermediates iron(IV)-oxo intermediate and iron(IV)-imido were generated in-situ from 1mM solution of the respective iron(II) complexes. The iron(IV)-oxo complex **1b** was prepared using 1.5 equiv. of iodosylbenzene (PhIO) as an oxidant in acetonitrile solution at 298 K. The iron(IV)-imido complex **1c** was generated in an acetonitrile solution *in situ* using 1.5 equiv. of PhINTs as tosylimido donor using procedures reported before.[38,39]. The oxidation reactions of thioanisole and C-H bonds were followed by monitoring the change in absorption spectrum of the intermediates using UV-vis. spectroscopy. The second order rate constants were determined by varying the concentration of thioanisole (10-80 mM), Xanthene (5-20 mM), 9,10-Dihydroanthracene (DHA) (5-20 mM), 1,4-Cyclohexadiene (CHD) (10-40 mM), fluorene (20-100 mM) and triphenylmethane (50 mM) for **1b** and **1c**.

5.3 Results and discussions

The $[Fe(N4Py)CH_3CN)](CF_3SO_3)_2$ (**1**) was prepared and characterized as reported earlier.[40] The complex gave ESI-MS peak at *m/z* = 572.03 corresponding to $[Fe^{II}(N4Py)CF_3SO_3]^+$ (Figure 2.1). Complexes **1c** and **1b** were generated in an acetonitrile solution *in situ* using either PhINTs as tosylimido donor or PhIO as oxygen atom donor using procedures reported before.[38,39] The iron(IV)-oxo intermediate **1b** was confirmed on the basis of visible features with low energy 695 nm (ε = 400 M^{-1} cm^{-1}), that arises from ligand field transitions characteristic for *S* = 1 iron(IV) complexes (Figure 2.5). The electron spray ionization mass spectra (Figure 2.2) gave a major peak at *m/z* = 587.91 corresponding to $\{[Fe^{IV}(O)N4Py](OTf)\}^+$ with an isotope pattern that matches the theoretically expected distribution. The identity of iron(IV)-imido complex **1c** was confirmed on the basis of visible features with an intense LMCT band at 445 nm (ε = 2700 M^{-1} cm^{-1}) and a low energy 660 nm band (ε = 250 M^{-1} cm^{-1}) that arises from ligand field transitions characteristic for *S* = 1 iron(IV) complexes (Figure 2.7). The electron spray ionization mass spectrum (Figure 2.4) gave a major peak at *m/z* = 741.07 corresponding to $\{[Fe^{IV}(NTs)N4Py](OTf)\}^+$ with an isotope pattern that matches the theoretically expected distribution.

The addition of thioanisole to the solution of **1c** at 273 K, led to the decay of the characteristic peak at 660 nm in the UV-vis. spectrum concomitant with the appearance of its iron(II) precursor (λ_{max} = 450 nm) with an isosbestic point at 516 nm (Figure 5.1). Aminidation of thioanisole to *N*-*p*-tosylmethylphenyl sulfilimine was obtained in ~85% yield, and a second order rate constant for this reaction was evaluated of 0.260 M^{-1} s^{-1}.[41] By contrast, the second order rate constant for **1b** determined under the same reaction conditions was found to be

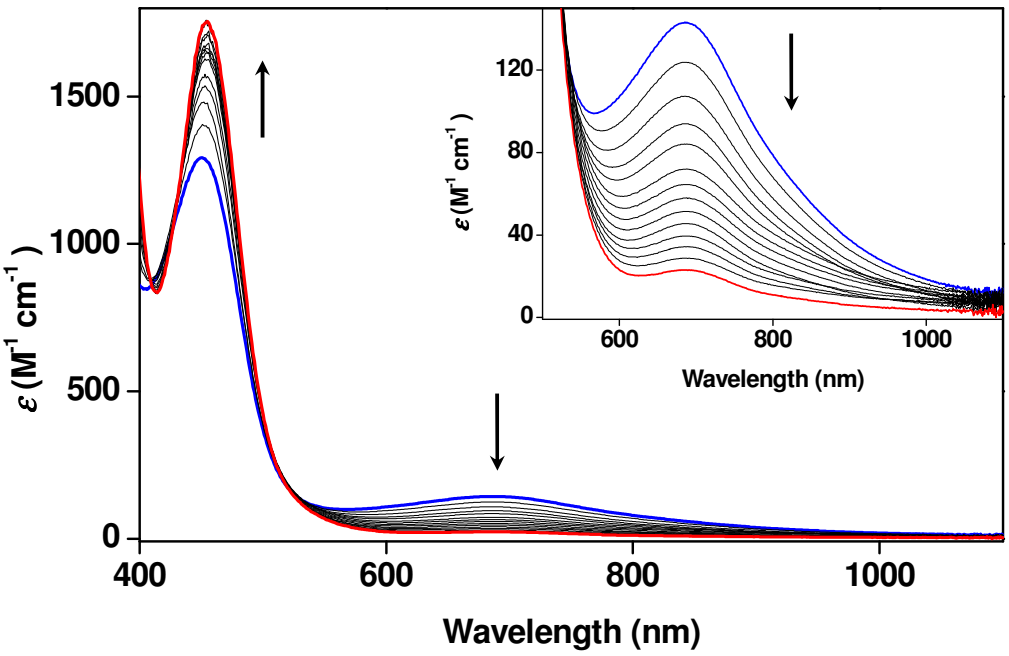

Figure 5.1. **UV-vis. spectral changes of 1c (0.5 mM, blue line) upon the addition of thioanisole (40 equiv diluted in 50 µL of CH_3CN) in CH_3CN at 273 K . Inset shows decay profile of 660 nm band at a scan interval of 30 s.**

0.050 M^{-1} s^{-1} only (Figure 5.2a). It appears, therefore, that the $[Fe^{IV}(NTs)(N4Py)]^{2+}$ complex *reacts with thioanisole with rate constants that are about five times higher* than those found for the $[Fe^{IV}(O)(N4Py)]^{2+}$ complex.

The pseudo-first-order rate constants were then determined for the reaction of **1c** and **1b** with various *p*-substituted thioanisoles. From a direct comparison of the k_{obs} values for the reactions of **1c** and **1b** with different *para*-substituted thioanisoles, it is evident that the reactivity of **1c** is more sensitive than that of **1b** to substitution at the *para* position of the thioanisole substrate.

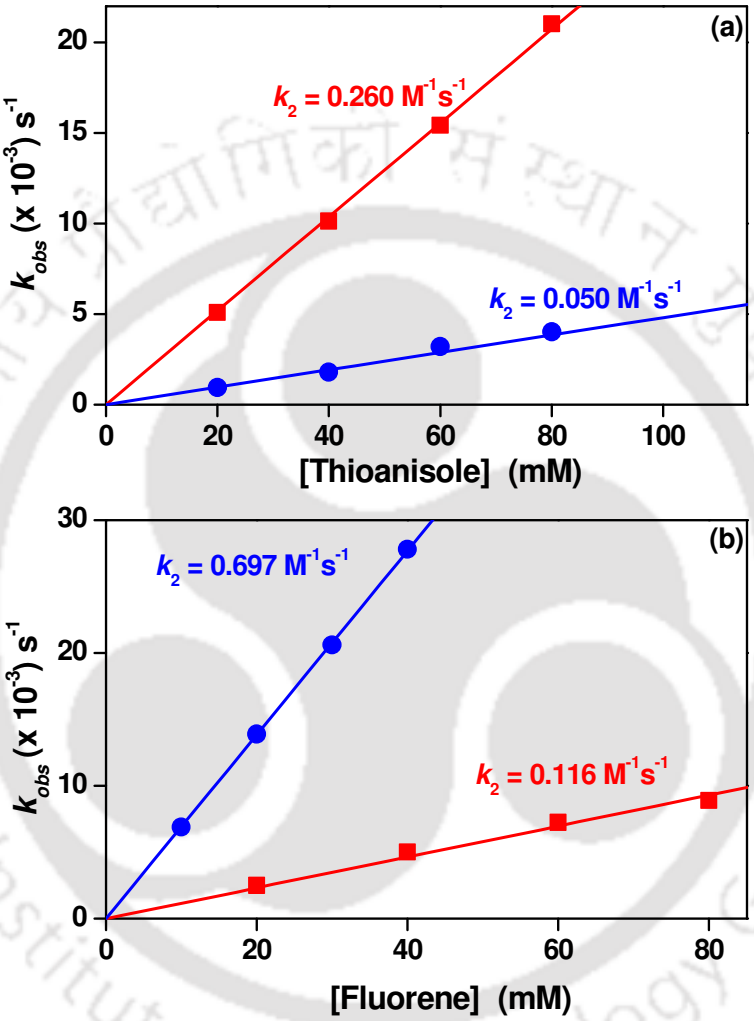

Figure 5.2. Second-order rate constants determined in the reactions of 1 mM $[Fe^{IV}(NTs)(N4Py)]^{2+}$ 1c (■, Square) and $[Fe^{IV}(O)(N4Py)]^{2+}$ 1b (●, Circle) in CH_3CN solution against various concentrations of: a) thioanisole at 273 K, b) fluorene at 298 K.

Hammett plots were created, for a quantitative examination of the substituent effect on the reaction rates. For **1b**, a linear correlation with σ was found with a ρ = –0.90. By contrast, when a similar plot was made for **1c**, non-linearity was observed with ρ = –3.36 (Figure 5.3), which is likely as a result of additional stabilization of positive charge in the transition state by electron donating groups in the *para*-position of thioanisole and thus enhanced the overall rate of oxidation.

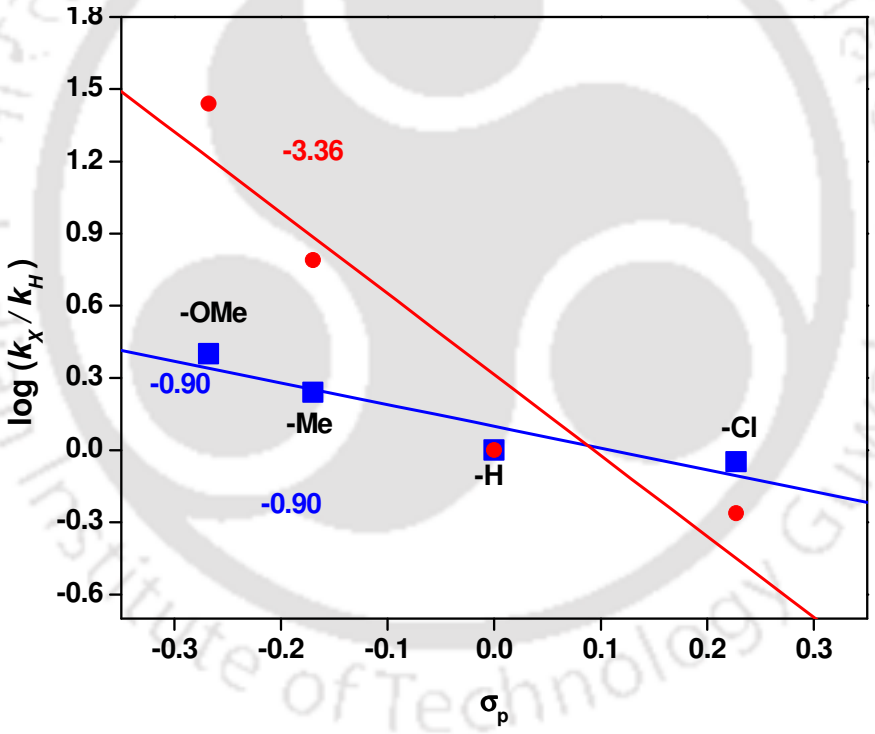

Figure 5.3. Plot of log(k_X/k_H) against σ_p of *para*-X-thioanisole of $[Fe^{IV}(O)(N4Py)]^{2+}$(■, Square) and $[Fe^{IV}(NTs)(N4Py)]^{2+}$ (●, Circle) at 273 K.

Table 5.1. Pseudo first order rate constants determined reactions of 1c and 1b (1 mM solution) in the presence of *para* substituted thioanisols at 273 K in CH_3CN

Substituent of *para*-X-Thioanisole	E^0_{ox} vs. SCE (V)[42]	σ_p [43]	σ_p^+ [43]	Intermediates			
				1c		1b	
				k_{obs} (s^{-1}) ($\times 10^{-3}$)	$\log(k_{rel})$	k_{obs} (s^{-1}) ($\times 10^{-3}$)	$\log(k_{rel})$
CH_3O-	1.13	-0.268	-0.778	140.19(3)	1.44	2.39(1)	0.40
CH_3-	1.24	-0.170	-0.311	31.38(1)	0.79	1.65(2)	0.24
H-	1.34	0.0	0.0	5.09(2)	0.00	0.95(1)	0.00
Cl-	1.37	0.227	0.114	2.78(2)	-0.26	0.85(3)	-0.05

In order to accommodate the additional stabilization of the positive charge in transition state, new Hammett plots were now made using σ^+ values leading to ρ values of –1.92 and –0.52, respectively, for **1c** and **1b** (Figure 5.4). This difference is slopes quantitatively reflect that **1c** is more sensitive to electronic effects of the *para*-substituents than **1b**. Further, the plot of $\log(k_X/k_H)$ values against the E^0_{ox} of sulfides, gave a linear correlation with a slope of –7.1 and –1.92 for **1c** and **1b**, respectively (Figure 5.5). Such a large negative slope obtained from these plots implicates a rate determining electron transfer from sulfides to **1c** rather than a grouptransfer.[44, 45]

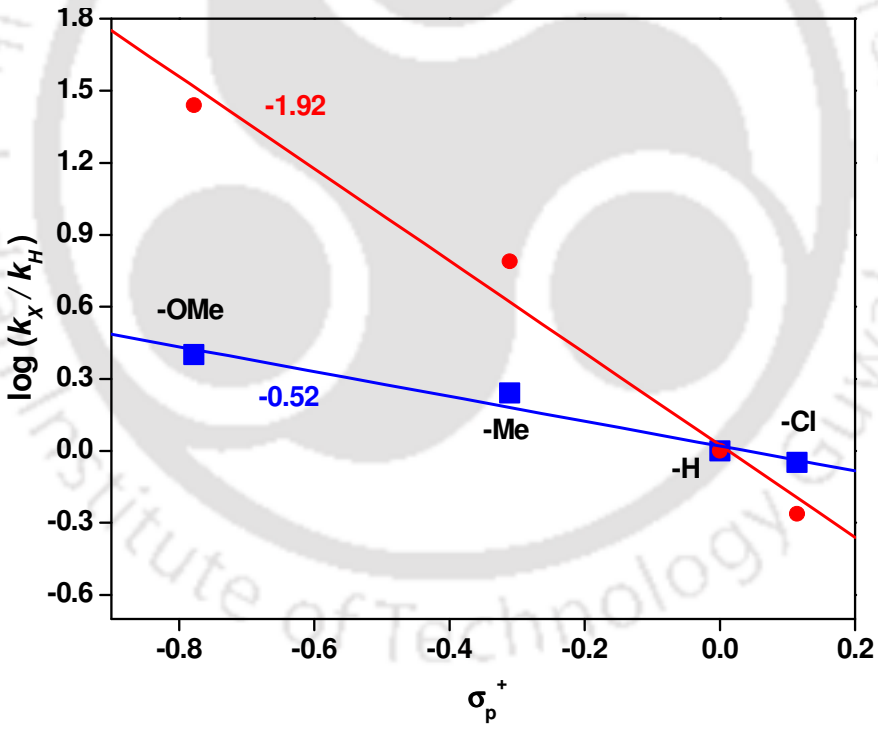

Figure 5.4. Plot of $\log(k_X/k_H)$ against σ_p^+ of *para*-X-thioanisole of $[Fe^{IV}(O)(N4Py)]^{2+}$(■, Square) and $[Fe^{IV}(NTs)(N4Py)]^{2+}$(●, Circle) at 273 K.

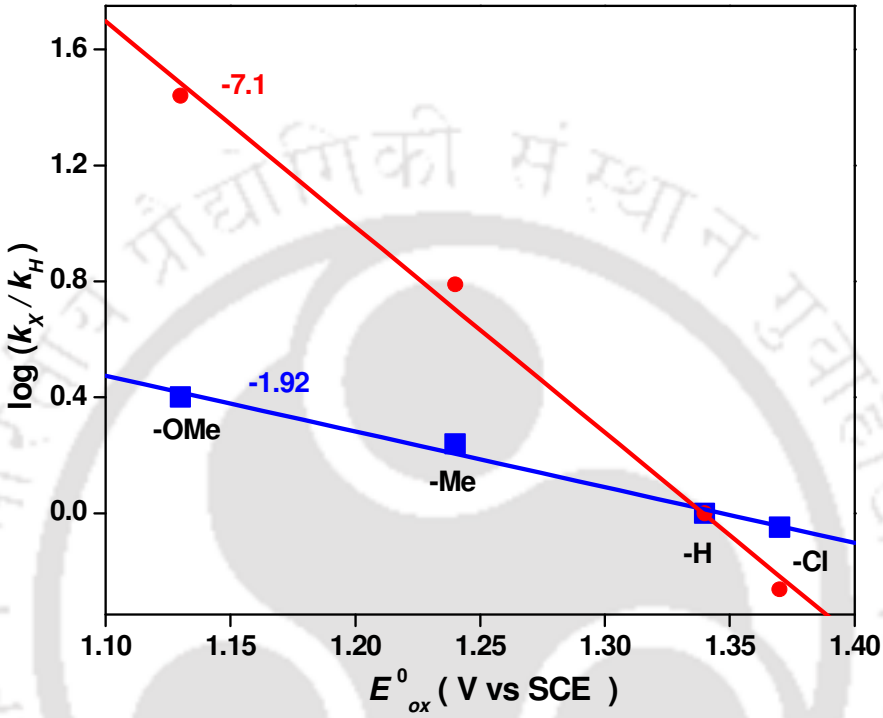

Figure 5.5. Plot of log(k_X/k_H) against the one-electron oxidation potentials (E^0_{ox}) of *para*-X-thioanisole of $[Fe^{IV}(O)(N4Py)]^{2+}$(■, Square) and $[Fe^{IV}(NTs)(N4Py)]^{2+}$(●, Circle) at 273 K.

Considering the high reactivity of **1c** over **1b** in the oxidation of thioanisole, we then evaluated the hydrogen atom transfer (HAT) capability of **1c**. It has been shown that the rate constant of HAT reactions often correlates with the strength of the C–H bond that is broken, i.e. BDE_{C-H} or bond dissociation energy.[45-49] Therefore, studied the rates of HAT between **1c** and substrates with a range of BDE_{C-H} values: xanthene (BDE_{C-H}=75.5), DHA (BDE_{C-H} =77.0 kcal mol^{-1}), CHD (BDE_{C-H} = 78.0 kcal mol^{-1}), fluorene (BDE_{C-H}= 80.0 kcal mol^{-1}) and triphenylmethane (BDE_{C-H} = 81 kcal mol^{-1}). Indeed a plot of

the logarithm of the rate constant of HAT by **1c** versus the BDE_{C-H} value of the substrate gave a linear correlation, Figure 5.6. However, when excess triphenylmethane was added to a solution of **1c** at 298 K, no change in 660 nm absorption band was observed, despite observable reactivity with fluorene, which has a comparable BDE_{C-H}.[39] Most probably the difference in reactivity between these two substrates with closely related BDE_{C-H} values is due to stereochemical clashes of **1c** with the approaching substrate. This is particularly important for substrates with bulky groups adjacent to the hydrogen abstraction center such as triphenylmethane

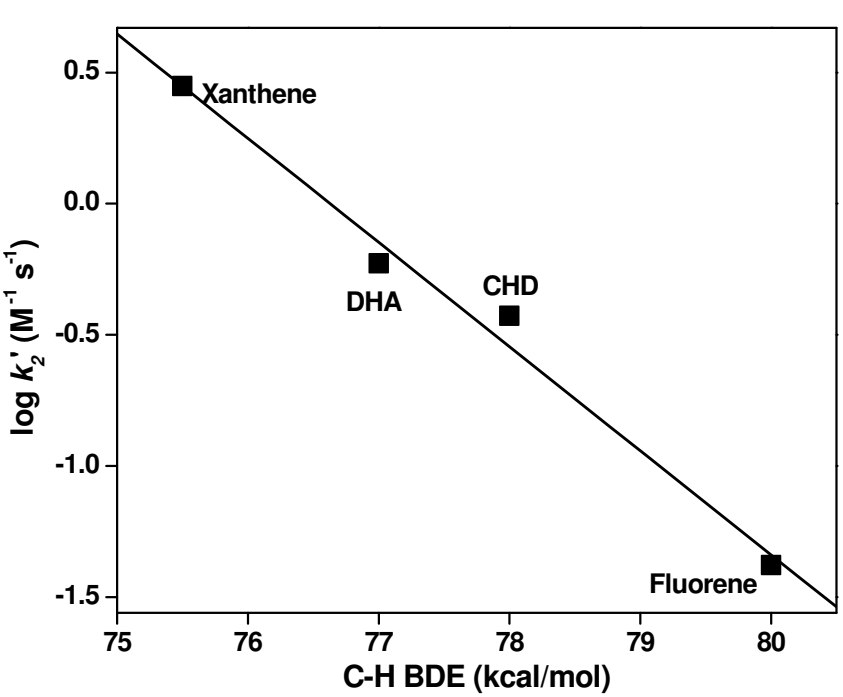

Figure 5.6. Correlation of the second order rate constants (determined at 288 K) for HAT by $[Fe^{IV}(NTs)(N4Py)]^{2+}$ (1c) with BDE_{C-H} of substrates.

.

Subsequently, we compared the relative activity in HAT processes of **1c** and **1b** using fluorene as the substrate (Table 5.2). The reaction of **1c** and **1b** follows pseudo-first-order kinetics and second-order rate constants were determined for each system, Figure 5.2b. At 298 K, complex **1c** decayed with a second order rate constant of 0.116 M^{-1} s^{-1} to form 9H,9′H-[9,9′]bifluorenyl (9,9′-bifluorene) product in ~32% yield as a product yield based. These results indicate that **1c** effectively acts as one-electron oxidizing agent in HAT reactions, whereby the 32% yield of 9,9′-bifluorene reflects the conversion of ~64% of iron(IV)imido complex in two one electron oxidation steps by fluorene. By comparison, complex **1b** decays with a k_2 = 0.697 M^{-1} s^{-1} to form fluorenone as the dominant product.[50] The observed slower rate (~6 times) of **1c** relative to **1b** for C–H bond activation is opposite to that observed for thioanisole oxidation (vide supra). This observation indicates that iron(IV)-tosylimido complex is a less effective oxidant than iron(IV)-oxo for hydrogen atom abstraction reactions.

Further evidence of a rate determining HAT reaction comes from kinetic isotope effect (KIE) studies of **1b** with fluorene (KIE = 30). Such large KIE values exceed the semi-classical limit and suggest strong tunnelling behaviour in the reaction mechanism. On the other hand, the reaction of deuterated fluorene with **1c** gave a KIE = 7 only, although it is still regarded as a HAT mechanism (Figure 5.7).

Table 5.2. Second order rate constants of sulfoxidation of thioanisole and hydrogen atom abstraction of fluorene by 1b and 1c.

Temperature	Substrate	(k_2) M^{-1} s^{-1}	
		1b	**1c**
273 K	Thioanisole	0.050	0.697
298 K	Fluorene (KIE)	0.697 (30)	0.116 (7)

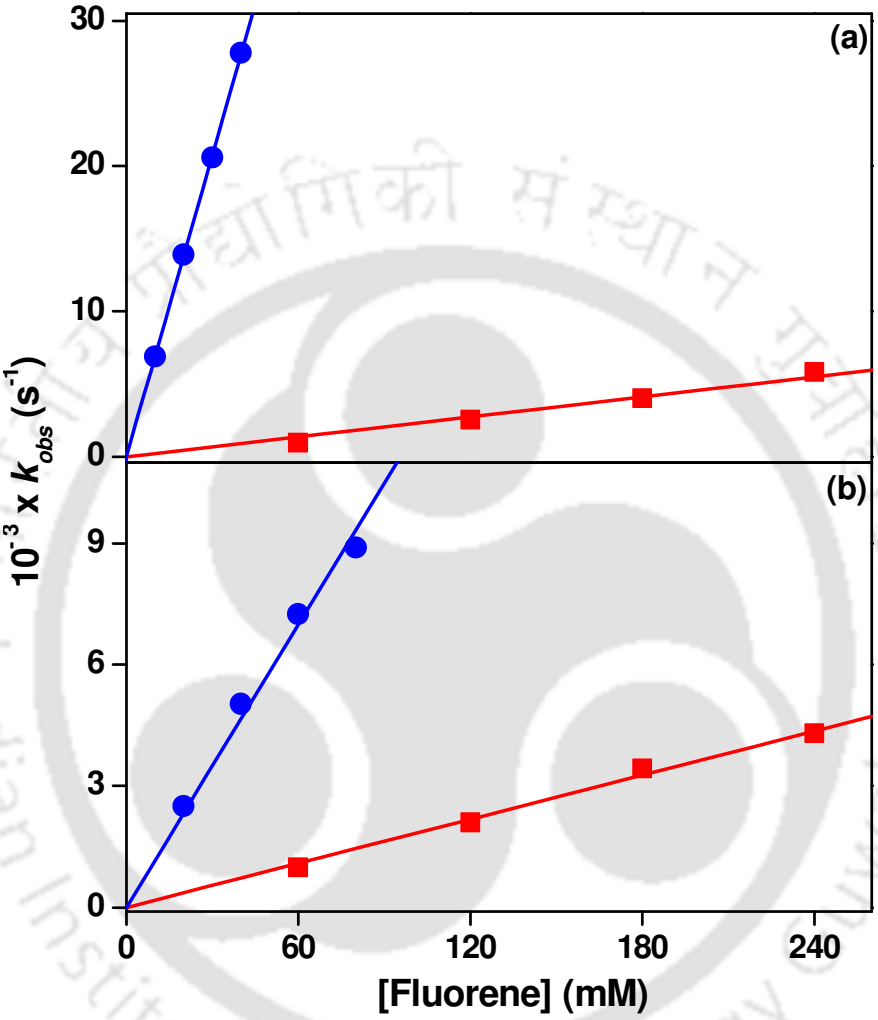

Figure 5.7. Second order rate constants determined in the reactions of fluorene (●, Circle) and fluorene-d_2 (■, Square) against 1 mM of (a) $[Fe^{IV}(O)(N4Py)]^{2+}$ and (b) $[Fe^{IV}(NTs)(N4Py)]^{2+}$ at 298K.

The density functional theory (DFT) calculation of both iron(IV)-imido and iron(IV)-oxo complexes carried out in collaboration have also supported the experimental observation.[51] According to DFT studies substrate sulfoxidation by either **1c** or **1b** appears to be concerted through a single rate-determining transition state, actually there are some critical differences between the two sulfoxidation processes. By contrast, the electron transfer processes from substrate to iron(IV)-oxo happen at a much later timescale, and electron affinities of **1c** and **1b**, which gave values of 120.5 and 94.6 kcal mol^{-1}, respectively. Therefore, **1c** is more electrophilic than **1b**.

Whereas, in C-H activation in **1c** this alignment is not possible to approach the substrate, because of stereochemical constraints of the NTs group with the approaching substrate and hence a more sideways approach is essential. As a consequence, the quintet spin barriers have gone up in energy and in the case of HAT from CHD. These studies support the experimental observation mentioned above that **1b** will be better in catalysing HAT reaction mechanisms due to lesser stereochemical interactions between substrate and oxidant as compared to **1c**. Hydrogen atom abstraction is accompanied by the breaking of the C–H bond of the substrate and the formation of an O/N–H bond with the oxidant. It has been shown that hydrogen atom abstraction barriers tend to correlate with the BDE_{C-H} bond of the substrate as well as the BDE_{O-H} bond of the oxidant.[45-49,52-54] The calculated values of BDE_{N-H} = 94.4 kcal mol^{-1} and BDE_{O-H} = 96.7 kcal mol^{-1} for **1c** and **1b**, respectively which implies that **1b** and **1c** should be similarly good oxidants of HAT reactions.Instead, differences in HAT catalysis are most likely originated by stereochemical repulsions of the approaching substrate with the oxidant. Consequently, the attack of substrate on **1c** will be more stereochemically constraint than in **1b** and hence generally higher barriers for HAT reactions.

5.4 Conclusion

In summary, this chapter present here the first comparative study on the reactivity patterns of nonheme iron(IV)-oxo versus iron(IV)-imido complexes. The observed difference in the reactivity for S-oxidation reactions were accounted for on the basis of difference in electron affinity of the oxidants. Owing to the larger electron affinity of the oxidant iron(IV)–imido was a better oxidant of sulfoxidation reactions than iron(IV)–oxo. By contrast, these trends were reversed for stepwise one-electron transfer reactions, such as hydrogen atom abstraction reactions where stereochemical interactions upon substrate approach determine the relative rate constants. The mechanistic pathway for S-oxidation reactions for iron(IV)-oxo and iron(IV)-imido were different. The former proceed via oxygen atom transfer while in the latter case electron transfer is the rate limiting step.

5.5 References

1. M. Sono, M. P. Roach, E. D. Coulter, J. H. Dawson, *Chem. Rev*. 1996, **96**, 2841–2888.
2. J. T. Groves, *Proc. Natl. Acad. Sci. USA*.2003, **100**, 3569–3574.
3. P. R. Ortiz de Montellano, Ed. *Cytochrome P450: Structure, Mechanism and Biochemistry*. 3rd ed.; Kluwer Academic/Plenum Publishers, New York, 2004.
4. K. M. Kadish, K. M. Smith, R. Guilard, Eds. *Handbook of Porphyrin Science*; World Scientific Publishing Co.: New Jersey, 2010.
5. S. P. de Visser and D. Kumar (Eds.) *Iron-containing enzymes: Versatile catalysts of hydroxylation reactions in nature*. RSC Publishing, Cambridge, 2011.
6. M. Costas, M. P. Mehn, M. P. Jensen, L. Que Jr., *Chem. Rev*. 2004, **104**, 939–986.
7. S. V. Kryatov, E. V. Rybak-Akimova, S. Schindler, *Chem. Rev*. 2005, **105**, 2175–2226.
8. M. M. Abu-Omar, A. Loaiza, N. Hontzeas, *Chem. Rev*. 2005, **105**, 2227–2252.
9. R. van Eldik, *Coord. Chem. Rev*. 2007, **251**, 1649–1662.
10. P. C. A. Bruijnincx, G. van Koten, R. J. M. Klein Gebbink, *Chem. Soc. Rev*., 2008, **37**, 2716–2744.
11. A. R. McDonald, L. Que Jr, *Coord. Chem. Rev*., 2013, **257**, 414–428.
12. R. E. White, M. B. McCarthy, *J. Am. Chem. Soc*., 1984, **106**, 4922–4926.
13. E. W. Svastis, J. H. Dawson, R. Breslow, S. H.Gellman, *J. Am. Chem. Soc*., 1985, **107**, 6427–6428.
14. J. Hohenberger, K. Ray, K. Meyer, *Nature Comm*., 2012, **3**, 1–13.

15. D. Mansuy, P. Battioni, J.-P. Mahy, *J. Am. Chem. Soc*. 1982, **104**, 4487–4489.
16. J.-P. Mahy, P. Battioni, D. Mansuy, J. Fisher, R. Weiss, J. Mispelter, I. Morgenstern-Badarau, P. Gans, *J. Am. Chem. Soc*. 1984, **106**, 1699–1706.
17. J.-P. Mahy, P. Nattioni, D. Mansuy, *J. Am. Chem. Soc*. 1986, **108**, 1079–1080.
18. C.-M. Che, C.-Y. Zhou, E. L.-M. Wong, *Top. Organomet. Chem.*2011, **33**, 111–138.
19. T. W.-S. Chow, G.-Q. Chen, Y. Liu, C.-Y. Zhou, C.-M. Che, *Pure Appl. Chem*. 2012, **84**, 1685–1704.
20. J. F. Berry, E. Bill, E. Bothe, S. DeBeer George, B. Mienert, F. Neese, K. Wieghardt, *Science*2006, **312**, 1937–1941.
21. P. Comba, C. Lang, C. Lopez de Laorden, A. Muruganatham, G. Rajaraman, H. Wadepohl, M. Zajaczkowski, *Chem. Eur. J*. 2008, **14**, 5313–5328.
22. K. L. Klotz, L. M. Slominski, M. E. Riemer, J. A. Phillips, J. A. Halfen, *Inorg. Chem.*2009, **48**, 801–803.
23. J. J. Scepaniak, J. A. Young, R. P. Bontchev, J. M. Smith, *Angew. Chem. Int. Ed*. 2009, **48**, 3158–3160.
24. P. Leeladee, G. N. L. Jameson, M. A. Siegler, D. Kumar, S. P. de Visser, D. P. Goldberg, *Inorg. Chem*. 2013, **52**, 4668–4682.
25. M. J. Zdilla, M. M. Abu-Omar, *J. Am. Chem. Soc*. 2006, **128**, 16971-16979.
26. S. Kundu, E. Miceli, E. Farquhar, F. F. Pfaff, U. Kuhlmann, P. Hildebrandt, B. Braun, C. Greco, K. Ray, *J. Am. Chem. Soc.* 2012, **134**,14710−14713.

27. J. W. W. Chang, P. W. H. Chan, *Angew. Chem. Int. Ed.* 2008, **47**, 1138–1140.
28. T. Petrenko, S. DeBeer George, N. Aliaga-Alcalde, E. Bill, B. Mienert, Y. Xiao, Y. S. Guo, W. Sturhahn, S. P. Cramer, K. Wieghardt, F. Neese, *J. Am. Chem. Soc*. 2007, **129**, 11053–11060.
29. R. E. Cowly, N. A. Eckert, S. Vaddadi, T. M. Figureg, T. R. Cundari, P. L. Holland, *J. Am. Chem. Soc*. 2011, **133**, 9796–9811.
30. M. P. Mehn, J. C. Peters, *J. Inorg. Biochem*. 2006, **100**, 634–643.
31. C. M. Thomas, N. P. Mankad, J. C. Peters, *J. Am. Chem. Soc*. 2006, **128**, 4956–4957.
32. I. Neito, F. Ding, R. P. Bontchev, H. Wang, J. M. Smith *J. Am. Chem. Soc*. 2008, **130**, 2716–2717.
33. E. R. King, E. T. Hennessy, T. A. Betley, *J. Am. Chem. Soc*. 2011, **133**, 4917–4923.
34. Y. Liu, X. Guan, E. L. –M. Wong, P. Liu, J. –S. Huang, C.-M. Che, *J. Am. Chem. Soc*. 2013, **135**, 7194–7204.
35. E. T. Hennessy, T. A. Betley, *Science* 2013, **340**, 591–595.
36. M. P. Jensen, M. P. Mehn, L. Que Jr, *Angew. Chem. Int. Ed.*2003, **42**, 4357–4360.
37. H. S. Soo, M. T. Sougrati, F. Grandjean, G. J. Long, C. J. Chang, *Inorg. Chim. Acta.* 2011, **369**, 82–96.
38. E. J. Klinker, T. A. Jackson, M. P. Jensen, A. Stubna, G. Juhász, E. L. Bominaar, E. Münck, L. Que Jr*, Angew. Chem. Int. Ed*. 2006, **45**, 7394–7397.
39. J. Kaizer, E. J. Klinker, N. Y. Oh, J.-U. Rohde, W. J. Song, A. Stubna, J. Kim, E. Münck, W. Nam, L. Que, Jr., *J. Am. Chem. Soc*. 2004, **126**, 472–473.

40. M. Lubben, A. Meetsma, E. C. Wilkinson, B. Feringa, L. Que, Jr., *Angew. Chem. Int. Ed. Engl.,***1995**, *34*, 1512–1515.
41. Small amounts (<15%) of methylphenylsulfoxide products were detected and are likely due to hydrolysis of sulfilimine.
42. Y. Goto, T. Matsui, S.-I. Ozaki, Y. Watanabe , S. Fukuzumi, *J. Am. Chem. Soc.* 1999, **121**, 9497–9502.
43. H. C. Brown, Y. Okamoto, *J. Am. Chem. Soc.,* 1958, **80**, 4979–4987
44. J. Park, Y. Morimoto, Y.-M. Lee, W. Nam, S. Fukuzumi, *J. Am. Chem. Soc.* 2011, **133**, 5236–5239.
45. L. E. Friedrich, *J. Org. Chem*. 1983, **48**, 3851–3852.
46. F. G. Bordwell, J.-P. Cheng, *J. Am. Chem. Soc*. 1991, **113**, 1736–1743.
47. C. V. Sastri, J. Lee, K. Oh, Y. J. Lee, J. Lee, T. A. Jackson, K, Ray, H. Hirao, W. Shin, J. A. Halfen, J. Kim, L. Que Jr, S. Shaik, W. Nam, *Proc. Natl. Acad. Sci. U.S.A*. 2007, **104**, 19181–19186.
48. J. J. Warren, T. A. Tronic, J. M. Mayer, *Chem. Rev*. 2010, **110**, 6961–7001.
49. K. A. Prokop, S. P. de Visser, D. P. Goldberg, *Angew. Chem. Int. Ed*. 2010, **49**, 5091–5095.
50. J. R. Bryant, J. M. Mayer, *J. Am. Chem. Soc*. 2003, **125**, 10351–10361.
51. A. K. Vardhaman, P. Barman, S. Kumar, C. V. Sastri, D. Kumar, S. P. de visser. *Angew. Chem. Int. Ed.,* **2013**, *52*, 12288-12292.
52. J. M. Mayer, *Acc. Chem. Res*. **1998**, *31*, 441–450.
53. J. Yoon, S. A. Wilson, Y. K. Jang, M. S. Seo, K. Nehru, B. Hedman, K. O. Hodgson, E. Bill, E. I. Solomon, W. Nam, *Angew. Chem. Int. Ed*. **2009**, *48*, 1257–1260.
54. D. E. Lansky, D. P. Goldberg, *Inorg. Chem*. **2006**, *45*, 5119–5125.

CHAPTER-VI

Oxidation of Dibenzothiophene by Mononuclear Non-Heme Iron Complexes

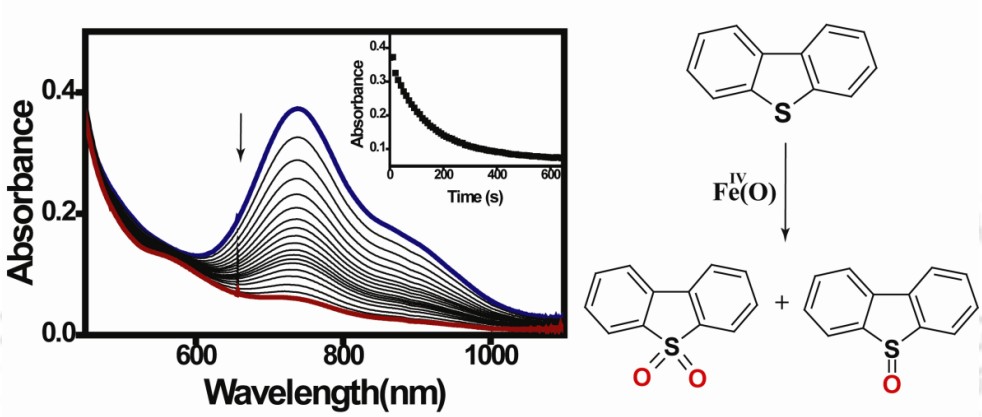

Indian J. Chem., Sect A., **2011**, *50A*, 427-431.

6.1 Introduction

Sulphur is a natural constituent of hydrocarbon fuels, such as coal and crude oil. The presence of sulphur in these fuels causes poisoning of catalysts; corrosion of surfaces, and air pollution.[1] Consequently, sulphur-containing compounds must be removed from coal in order to attain high energy values and satisfactory environmental standards. The conventional process of sulphur removal in fuels is known as hydrodesulphurization (HDS). Oxidative desulphurization (ODS) provides a deep desulphurization process alternative to traditional HDS, because it can be conducted in liquid phase under mild conditions.[2,3] In oxidation, the divalent sulphur of dibenzothiophenes (DBTs), which are the most unreactive sulphur compounds during HDS, can be oxidized by the electrophilic addition reaction of oxygen atoms to the hexavalent of sulfones. The oxy-desulfurization process involves S-oxidation mainly by hydrogen peroxide and either using a homogeneous catalyst, such as acetic acid, formic acid or using different heterogeneous catalysts.[4-13] This chemical process involves the removal of organic sulphur from coal via oxidation of dibenzothiphene to its S-oxide and then to its S-dioxide (sulfone) (Scheme 6.1).

Dibenzothiophene (DBT) are a widely accepted model compound for organic sulphur in coal.[1, 14] This substance possesses low reactivity since the

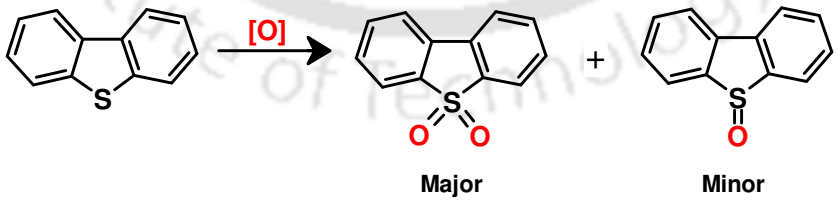

Scheme 6.1. Oxidation reaction of dibenzothiophene

electron density is delocalized by benzene rings; hence, it is difficult to transform by chemical methods. Metallo-peroxidases are also known to participate in the oxidative metabolism of organosulfur compounds. The oxygenation of benzyl methyl sulfide, thioanisole, and thiobenzamide to the respective sulfoxides has been found to be catalyzed by chloroperoxidase, lactoperoxidase, and horseradish peroxidase.[15-19] It has been demonstrated that non-heme iron(IV)-oxo complexes are capable of oxygenating various organic substrates such as PPh_3, sulphides, olefins and alkanes.[20-28] This chapter deals the exploring the reactivity of such intermediates to oxidize DBT to the corresponding S-oxide and/or sulfone. The rationale behind this transformation is as follows: oxidation of dibenzothiophene should improve its solubility in water, thereby facilitating the subsequent aqueous extraction from coal; and oxidized species of dibenzothiophene are more amenable to the subsequent biological or chemical degradation than the parent compound. In this chapter biomimetic approach for the oxidation of dibenzothiophene by mononuclear non-heme iron(IV)-oxo complexes $[Fe^{IV}(O)(N4Py)]^{2+}$ **(1b)** and $[Fe^{IV}(O)(Bn\text{-}Tpen)]^{2+}$ **(2b)** bearing penta-dentate ligands, (N4Py = N,N-bis(2-pyridylmethyl)-N-bis(2-pyridyl)methylamine) (Bn-Tpen = N-benzyl-N,N',N'-tris(2-pyridylmethyl)ethane-1,2-diamine). The detailed kinetic and thermodynamic parameters for DBT oxidation have been evaluated and compared with those of simple sulphur oxidation (thioanisole).

6.2 Experimental Section

High-valent iron intermediates iron(IV)-oxo intermediates were generated *in-situ* from 1mM solution of the respective iron(II) complexes. The iron(IV)-oxo complexes were prepared using iodosylbenzene (PhIO) as an oxidant in acetonitrile solution at 298 K. The oxidation reactions of DBT and thioanisole were followed by monitoring the change in absorption spectrum of the

intermediates using UV-vis. spectroscopy. The second order rate constants were determined by varying the concentration of DBT.

6.3 Results and discussions

The iron(II) complexes bearing pentadentate ligands were prepared and characterized as reported earlier.[29-30] The complexes gave ESI-MS peak at *m/z* = 572.03 and 628.13 corresponding to $[Fe^{II}(N4Py)CF_3SO_3]^+$ and $[Fe^{II}(Bn\text{-}Tpen)\ CF_3SO_3]^+$ respectively (Figure 2.1). The iron(IV)-oxo complexes were prepared by stirring 1.5 equiv. of PhIO in a CH_3CN solution containing iron(II) complexes at room temperature. The iron(IV)-oxo intermediates **1b** and **2b** were confirmed on the basis of visible features with low energy 695 nm and 735 nm respectively (ε = 400 M^{-1} cm^{-1}), that arises from ligand field transitions characteristic for *S* = 1 iron(IV) complexes (Figure 2.5 and Figure 2.6). The electron spray ionization mass spectra of **1b** (Figure 2.2b) gave a major peak at *m/z* = 587.91 corresponding to $\{[Fe^{IV}(O)N4Py](OTf)\}^+$ and for **2b** (Figure 2.3b) gave a major peak at *m/z*= 644.09 corresponding to $\{[Fe^{IV}(O)Bn\text{-}Tpen](OTf)\}^+$ with an isotope pattern that matches the theoretically expected distribution.

The addition of DBT to a solution of **1b** and **2b** in CH_3CN at 25 ^oC afforded changes in the absorption spectra with a *pseudo*-first-order decay of the signature iron(IV)-oxo low energy 735 nm band that arises from ligand field transitions characteristic for *S* = 1 iron(IV) complexes (Figure 6.1).

The *pseudo*-first-order fitting of the kinetic data, monitored at 695 nm (**1b**) and 735 nm (**2b**), yielded the k_{obs} value of 1.27×10^{-3} s^{-1} (400 mM of DBT) and 1.67×10^{-3} s^{-1} (10 mM of DBT) respectively. The product analysis of the final reaction mixture with HPLC, LC-MS, GC, and GC-MS revealed that dibenzothiophene sulfone was produced predominantly. Under the identical

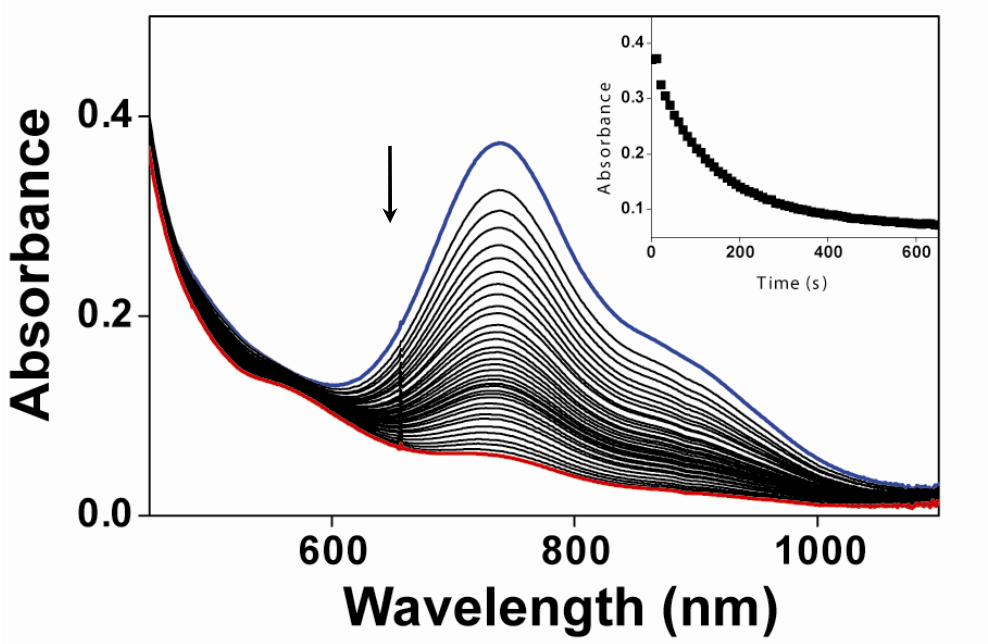

Figure 6.1. **UV-vis spectral change of 2b (1mM) upon addition of 80 equiv. DBT at 298K. Scan interval: 15 s (first scan was 15 s after the addition of thioanisole). Inset shows time course of the decay of 2b monitored at 735 nm.**

conditions, only trace amounts of products were formed in the absence of the iron complexes. Similar results were obtained when H_2O_2 was used as an oxidant to generate iron(IV)-oxo complexes. The analysis of the decomposed product of the intermediates in the presence of the substrate showed the presence of $[Fe^{II}(L)]^{2+}$ (L = N4Py or Bn-Tpen), indicating the recovery of active catalyst. The *pseudo*-first-order rate constants increased proportionally with the DBT concentration, from which the second-order rate constants were determined as 1.5 x 10^{-1} $M^{-1}s^{-1}$ and 3.2 x 10^{-3} $M^{-1}s^{-1}$ for **1b** and **2b** respectively (Figure 6.2a). It was of interest to compare the reactivity of iron(IV)-oxo complexes with thioanisole.Under similar conditions, the intermediates **1b** and **2b** react with thioansiole almost instantaneously and hence the rate constants couldnot be evaluated. The

evaluation of the second-order rate constants for thioanisole oxidation at 263K yielded the values 1.48 x 10^{-2} $M^{-1}s^{-1}$ and 3.4 x 10^{-1} $M^{-1}s^{-1}$ for **1b** and **2b** respectively (Table 6.1, Figure 6.2b).

Table 6.1. Second order rate constant of the reaction of oxo-iron(IV) complexes (1 mM) with substrate in CH_3CN.

Temperature	Substrate	$k_2(M^{-1}s^{-1})$	
		1b	**2b**
263 K	Thioanisole	1.48 x 10^{-2}	3.4 x 10^{-1}
298 K	Dibenzothiphene	3.2 x 10^{-3}	1.5 x 10^{-1}

The reaction mechanism of oxidation in thioanisole is known to proceed via "oxygen atom transfer".[31-32] The ease of oxidation of thioanisole over DBT clearly indicate the influence of delocalized electron density by benzene rings on DBT in comparison with thioanisole. The first-order rate constants for the oxidative desulphurization of DBT and S-oxidation of thioanisole by **1b** and **2b** at variable temperature were determined to calculate activation parameters.

The *pseudo*-first-order rate constants were obtained at variable temperatures in the presence of 30 equiv. of the substrate. The comparison of the activation barrier for the DBT reactions in comparison with that for thioanisole reaction reveal the significant variation in the reaction enthalpy ($\Delta H^{\#}$), but a comparable ($\Delta S^{\#}$) entropy values (Table 6.2, Figure 6.3). An enthalpy difference of 12 kJ/mol (for **2b**) and 11 kJ/mol (for **1b**) were observed for the oxidation of DBT and thioanisole. The $\Delta H^{\#}$ values thus obtained from the Eyring plots, when used in Arrhenius equation gave the rate constants which are in agreement with

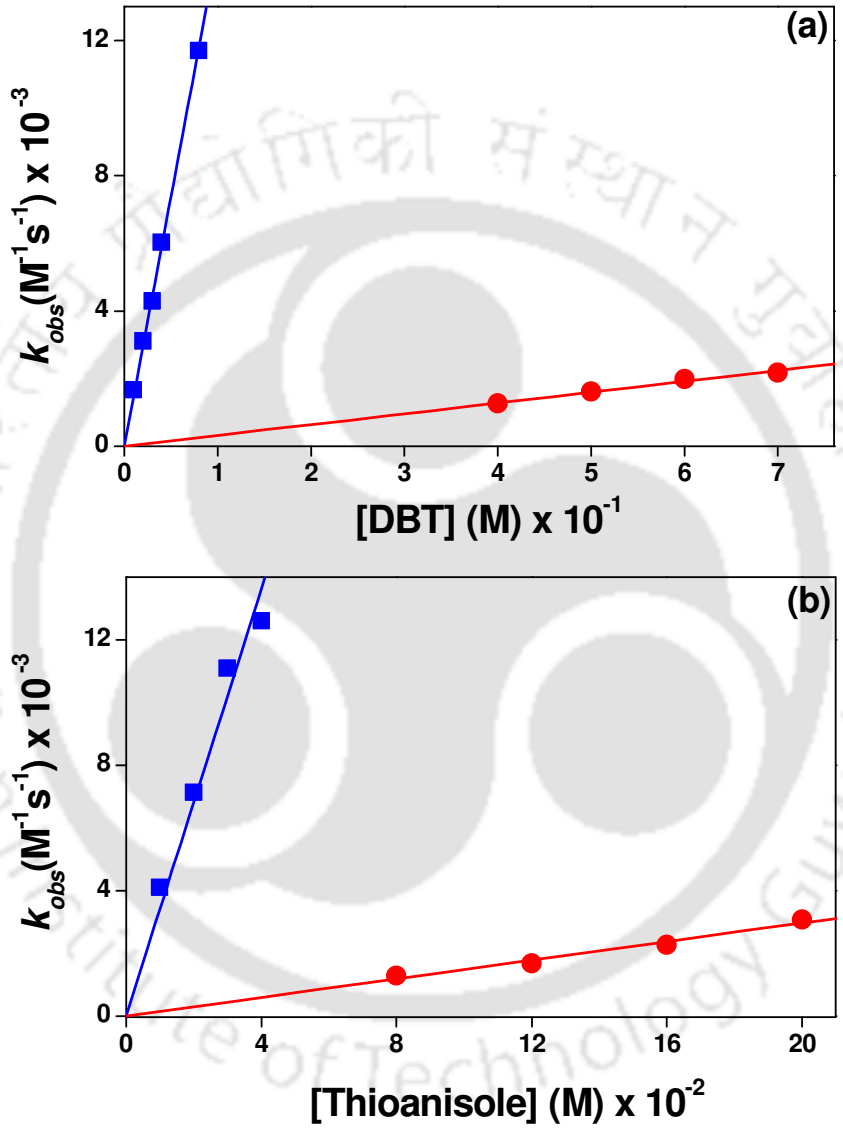

Figure 6.2. **Plots of k_{obs} against substrate concentration for the reactions of 1b (●, circle) and 2b (■, square) (a) DBT at 298K and (b) Thioanisole at 263K**

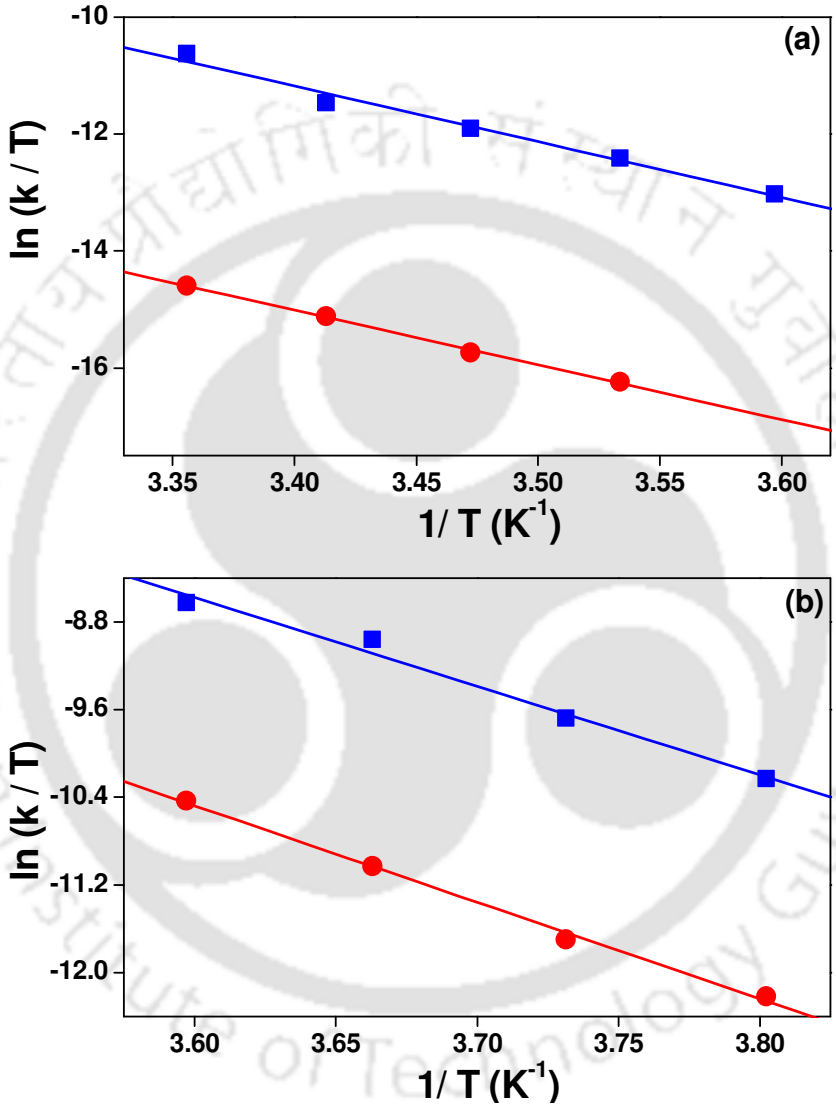

Figure 6.3. Determination of activation parameters for the oxidation of (a) DBT and (b) thioanisole in CH_3CN with 1b (●, Circle) and 2b (■, Square).

Table 6.2. Activation parameters for the oxidation of DBT and thioanisole in CH_3CN.

Iron(IV)-oxo	Dibenzothiphene		Thioanisole	
	$\Delta H^{\#}$ (kJ/mol)	$\Delta S^{\#}$ (J/mol)	$\Delta H^{\#}$ (kJ/mol)	$\Delta S^{\#}$ (J/mol)
1b	84.21	-21.40	73.24	-20.99
2b	79.15	-18.12	67.32	-26.52

the experimental second order rate constants observed in the oxidation reactions of thioanisole and DBT. The comparable $\Delta S^{\#}$
indicates the similar mechanistic pathway; significantly varying $\Delta H^{\#}$ values for the reactions highlight the role of extended electron delocalization by the benzene rings in DBT for S-oxidation vide infra. The higher oxidizing power of **2b** than that of **1b**, is due to the more electron deficient character of 2b. Such similar results were obtained for the oxidation of other organic substrates by such high-valent oxo-iron(IV) complexes.[24,33]

6.3 Conclusion

In this chapter the oxidation of DBT by mononuclear non-heme iron(IV)-oxo complexes were described. The S-oxidation reaction rates of DBT have been compared with that of thioanaisole to highlight the challenges present for the oxidation of deactivated sulphur. Present evidence also highlights the use of environmentally benign oxidant like H_2O_2 with appropriate non-heme catalysts as a feasible technique for deep desulfurization of commercial fuels. It should be stressed that DBT and some similar sulphur compounds present in fuel can be effectively removed, after oxidation, using ethanol. Efforts are currently underway to design more effective catalysts for DBT oxidation by tuning the ligand architecture.

6.4 References

1. *Fuel Science and Technology Handbook,* J. G. Speight, ed. M. Dekker, New York, 1990.
2. I. V. Babich, J. A. Moulijn, *Fuel,* 2003, **82**, 607-631.
3. C. Song, X. Ma, *Appl. Catal. B*., 2003, **41**, 207-238.
4. F. Al-Shahrani, T. Xiao, S. A. Llewellyn, S. Barri, Z. Jiang, H. Shi, G. Martinie, M. L. H. Green, *Appl. Catal. B.,*2007, **73**, 311-316.
5. Y. Shiraishi, K. Tachibana, T. Hirai, I. Komasawa, *Ind. Eng. Chem. Res*.,2002, **41**, 4362-4375.
6. L. F. Ramı´rez-Verduzco, E. Murrieta-Guevara, J. L.García-Gutiérrez,R. S. Martín-Castañón, M. C. Martínez-Guerrero, M. C. Montiel-Pacheco, R. Mata-Díaz, *Pet.Sci. Technol*., 2004, **22**, 129-139.
7. M. F. Ali, A. Al-Malki, S. Ahmed, *Fuel Process. Technol*., 2009, **90**, 536-544.
8. A. M. Dehkordi, Z.Kiaei, Sobati, *Fuel Process. Technol*., 2009, **90**, 435-445.
9. M. Te, C. Fairbridge, Z. Ring, *Appl. Catal. A.,* 2001, **219**, 267-280.
10. L. F. Ramı´rez-Verduzco, E. Torres-Garcı´a, R. Go´mez-Quintana, V. Gonza´lez-Pen˜a, F. Murrieta-Guevara, *Catal. Today,* 2004, **98**, 289-294.
11. J. T. Sampanthar, H. Xiao, J. Dou, T. Y. Nah, X. Rong, W. P. Kwan, *Appl. Catal. B,* 2006, **63**, 85-93.
12. X. Jiang, H. Li, W. Zhu, L. He, H. Shu, J. Lu, *Fuel,* 2009, **88**, 431-436.
13. L. C. Caero E. Herna´ndez, F. Pedraza, F. Murrieta, *Catal. Today.* 2005, **107-108**, 564-569.
14. J. J. Kilbane, *Trends Biotechnol*., 1989, **7**, 97-101.
15. U. Perez, H. B. Dunford, *Biochim. Biophys. Acta.,* 1990, **1038**, 98-104.
16. U. Perez, H. B. Dunford, *Biochemistry*, 1990, **29**, 2757-2763.

17. D. R. Doedge, N. M. Cooray, M. E. Brewster, *Biochemistry*, 1991, **30**, 8960-8964.
18. S. Colonna, N. Gaggero, A. Manfredi, L. Casella, M. Gullotti, G. Carrea, P. Pasta, *Biochemistry,* 1990, **29**, 10465-10468.
19. S. Kobayashi, M. Nakano, T. Kimura, A. P. Schaap, *Biochemistry*, 1987, **26**, 5019-5022.
20. J. -U. Rohde, J. -H. In, M. H. Lim, W. W. Brennessel, M. R. Bukowski, A. Stubna, E. Münck, W. Nam, L.Que Jr, *Science,* 2003, **299**, 1037-1039.
21. S. O. Kim, C. V. Sastri, M. S. Seo, J. Kim, W. Nam, *J. Am. Chem. Soc*. 2005, **127**, 4178-4179.
22. C. V. Sastri, M. J. Park, T. Ohta, T. A. Jackson, A. Stubna, M. S. Seo, J. Lee, J. Kim, T. Kitagawa, E. Münck, L. Que Jr., W. Nam, *J. Am. Chem. Soc*., 2005, **127**, 12494-12495.
23. M. Martinho, F. Banse, J. -F. Bartoli, T. A. Mattioli, P. Battioni, O. Horner, S. Bourcier, J. -J. Girerd, *Inorg. Chem*., 2005, **44**, 9592-9596.
24. C. V. Sastri, M. S. Seo, M. J. Park, K. M. Kim, W. Nam, *Chem. Commun*., **2005**, 1405-1407.
25. M. H. Lim, J. -U. Rohde, A. Stubna, M. R. Bukowski, M. Costas, R. Y. N. Ho, E. Münck, W. Nam, L. Que Jr, *Proc. Natl. Acad. Sci.U. S. A.,* 2003, **100**, 3665-3670.
26. V. Ball, M. -F. Charlot, F. Banse, J. -J. Girerd, T. A. Mattioli, E. Bill, J. -F. Bartoli, P. Battioni, D. Mansuy, *Eur. J. Inorg. Chem*., 2004, 301-308.
27. J. -U. Rohde, L. Que Jr, *Angew. Chem. Int. Ed*., 2005, **44**, 2255-2258.
28. M. R. Bukowski, K. D. Koehntop, A. Stubna, E. L. Bominaar, J. A. Halfen, E. Münck, W. Nam, L. Que Jr, *Science,* 2005, **310**, 1000-1002.
29. M. Lubben, A. Meetsma, E. C. Wilkinson, B. Feringa, L. Que Jr, *Angew. Chem. Int. Ed.,* 1995, **34**, 1512-1514.

30. L. Duelund, R. Hazell, C. J. McKenzie, L. P. Nielsen, H. Toftlund, *J. Chem. Soc., Dalton Trans.,* 2001, 152-156.
31. M. Taki,S. Itoh, S. Fukuzumi*, J. Am. Chem. Soc*., 2002, **124**, 998-1002.
32. Y. Goto, T. Matsui, S. –I. Ozaki, Y. Watanabe, S. Fukuzumi, *J. Am. Chem. Soc*., 1999,**121**, 9497-9502.
33. N. Y. Oh, Y. Suh, M. J. Park, M. S. Seo, J. Kim, W. Nam, *Angew. Chem*., 2005, **117**, 4307-4311.